Cover Page

The handle http://hdl.handle.net/1887/47913 holds various files of this Leiden University dissertation

Author: Jansen, D.T.S.L.
Title: Functional aspects of the adaptive immune system in arthritis
Issue Date: 2017-03-08

Functional aspects of the adaptive immune system in arthritis

Diahann Talia Satirah Ludovica Jansen

Functional aspects of the adaptive immune system in arthritis

PROEFSCHRIFT

ter verkrijging van
de graad van Doctor aan de Universiteit Leiden,
op gezag van Rector Magnificus prof.mr. C.J.J.M. Stolker,
volgens besluit van het College voor Promoties
te verdedigen op woensdag 8 maart 2017
klokke 15:00 uur

door

Diahann Talia Satirah Ludovica Jansen
geboren te Rotterdam
in 1986

PROMOTOREN

Prof.dr. R.E.M. Toes

Prof.dr. T.W.J. Huizinga

LEDEN PROMOTIECOMMISSIE

Prof.dr. C. van Kooten

Prof.dr. M.J. Jager

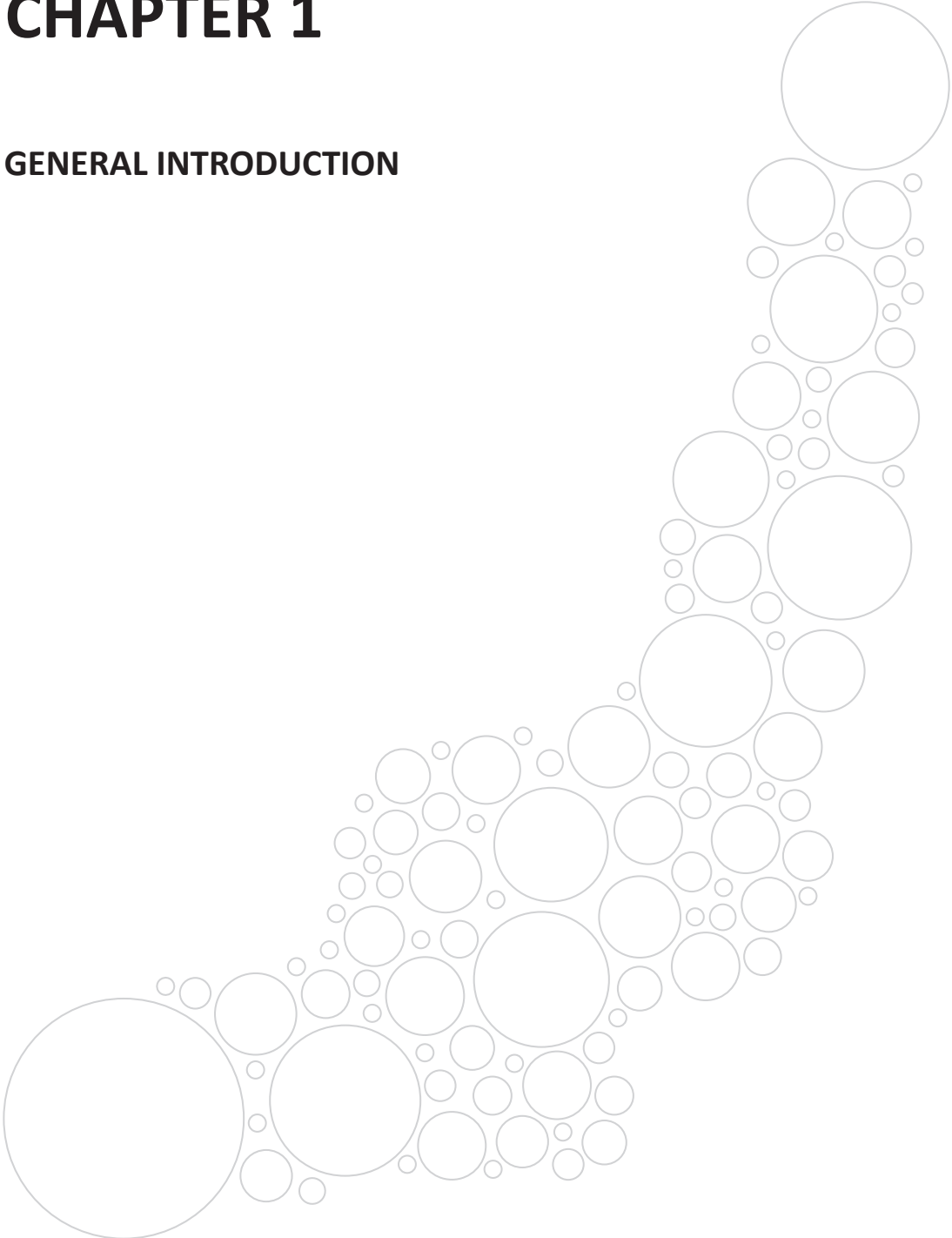Prof.dr. A.M.H. Boots (UMCG/Universiteit Groningen)

Dr. J.H.W. Leusen (UMCU/Universiteit Utrecht)

TABLE OF CONTENTS

CHAPTER 1

GENERAL INTRODUCTION

1

ADAPTIVE IMMUNE SYSTEM

The main purpose of the immune system is to protect the human body from invasion by microorganisms that cause disease including bacteria, viruses, fungi and parasites. The immune system consists of two parts to assure this protection: the innate and the adaptive immune system. The innate immune system provides the first line of defense against an invading pathogen reacting fast but nonspecific. The adaptive immune system reacts slower, but is highly specific and generates memory resulting in a fast and specific immune response upon a second infection with the same pathogen. The adaptive immune system includes humoral responses and cell-mediated responses provided by T cell and B cells. Both cell types express T or B cell receptors, which are highly specific receptors recognizing a wide variety of antigens providing protection to a very large diversity of pathogens[1].

T cells

T cells can be divided in two types with distinct effector mechanisms. CD8+ T cells recognize processed intracellular antigens presented by human leukocyte antigens (HLA) class I molecules and subsequently kill infected cells. CD4+ T cells recognize peptides from an extracellular source presented by HLA class II molecules expressed by antigen presenting cells (APCs). In addition to the recognition of their cognate antigen and HLA molecule, T cells need costimulation to be activated. APCs express, amongst a range of other costimulatory molecules, CD80 and CD86 on their surface, which binds to CD28 expressed by the T cell providing the second signal needed for activation (Figure 1)[1]. As a third signal the APCs produce cytokines directing the differentiation into the different T helper subsets. The main effector function of CD4+ T cells is production of cytokines that help the activity of other immune cells. CD4+ T cells are important in the activation and growth of CD8+ T cells, attract other immune cells to the site of infection or inflammation and suppress immune responses. They are also essential for the activation of B cells as B cells need binding of their CD40 to CD40L on the T cell and the cytokines produced by the T cell to be able to perform antibody class switching and differentiate into highly effective antibody producing cells (plasma cells)[2-4].

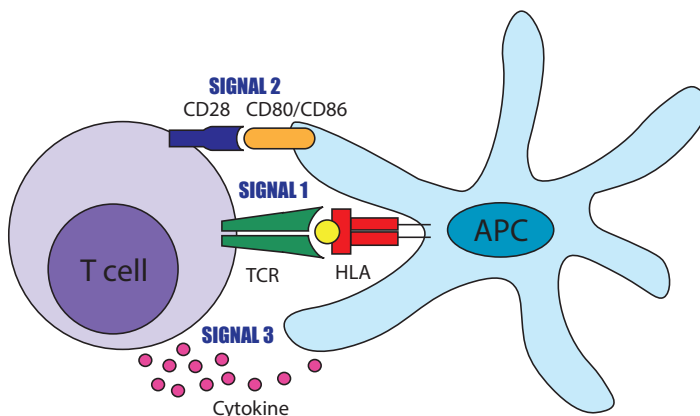**Figure 1. The three APC-derived signals required for T cell activation.** Signal 1 is the antigen-specific signal mediated by the TCR on the T cell recognizing processed peptides from pathogens presented by HLA class II molecules. Signal 2 is the co-stimulatory signal provided by CD28 binding to CD80 or CD86. Signal 3 is the polarizing signal that is mediated by soluble factors like cytokines.

CD4+ T helper subsets

CD4+ T cells can be divided in several T helper subsets based on their cytokine profile and function (Table 1)[5]. T helper 1 cells (Th1) produce IFNγ, IL-2 and TNF and are involved in the elimination of intracellular viral and bacterial pathogens. IFNγ is essential for activation of phagocytes including macrophages resulting in enhanced phagocytosis and pathogen clearance[6]. T helper 2 cells (Th2) are essential for the clearance of extracellular pathogens and produce IL-4, IL-5 and IL-13. T helper 17 cells (Th17) are responsible for the immune response against extracellular bacteria and fungi and produce IL-17, IL-21 and IL-22 as their main effector cytokines. T follicular helper cells (Tfh) are the T cells that mediate humoral immunity by providing help to an antigen-primed B cell, which subsequently differentiates into an Ig-producing plasma cell[4,7].

In addition to T cell subsets that are pro-inflammatory, there are anti-inflammatory T cell as well. Regulatory T cells (Tregs) suppress the immune response after clearance of the pathogen, thereby protecting from tissue damage due to the inflammatory response. They are also responsible for the maintenance of immunologic tolerance against self and foreign antigens[4,7].

Table 1. CD4+ T helper subsets

CD4+ subset	Signature cytokines	Transcription factors	Function
Th1	IFNγ, TNF, IL-2	T-bet	Intracellular pathogens
Th2	IL-4, IL-5, IL-13	GATA3	Extracellular pathogens
Th17	IL-17, IL-21, IL-22	RORγt	Extracellular bacteria and fungi
Tfh	IL-6, IL-21	Bcl6	Help to B cells
Treg	IL-10, TGFβ	Foxp3	Suppress immune response

T and B cell selection

Due to the strong potency of T and B cells to elicit a specific immune response, it is of utmost importance to prevent their activation in response to self-antigens. The specificity of T and B cell receptors is generated by random gene rearrangements and amino acid insertions creating T cell receptors and antibodies directed against antigens the host has never encountered, which is a powerful tool in the defense against evolving pathogens. However, the random rearrangements can also lead to the recognition of an antigen derived from the host itself by chance. Therefore, B cells are selected in the bone marrow by negative selection and only B cells that do not recognize self-antigens are allowed to enter the periphery. B cells that do recognize self-antigen die and are thereby eliminated from the B cell repertoire. T cell selection occurs in the thymus and is more stringent than B cell selection. T cells are first selected on their recognition of HLA molecules (positive selection), subsequently, they are selected on the recognition of self-antigens (negative selection) to generate a peripheral T cell repertoire recognizing self-HLA molecules, but not self-antigens[1]. Nonetheless, this selection

1

is not absolute and self-reactive T cells can escape to the periphery causing inflammation and autoimmune disease[8].

RHEUMATOID ARTHRITIS

Rheumatoid arthritis (RA) is a systemic inflammatory autoimmune disease characterized by synovial inflammation leading to cartilage and bone destruction[9,10]. In developed countries, 0.5-1% of the adults are affected with this disease and the disease is three times more frequent in women compared to men[9,11]. Prevalence rises with age resulting in an average age of onset of 55 years. The bone destruction and deformities resulting from the inflammation in the joints lead to progressive disability and a large disease burden. The cause of RA is unknown, however, important studies on the drivers of the inflammatory process have resulted in the development of therapeutics that greatly enhanced the quality of life of RA patients. Despite novel therapeutics and identification of important pathways, little is known about the initiation of RA.

ACPA

One of the characteristics of RA is the presence of autoantibodies such as rheumatoid factor (RF), anti-citrullinated protein antibodies (ACPA) and the recently identified anti-carbamylated protein antibodies[12]. ACPA can be detected in 50-70% of the RA patients and is highly specific for RA[13-15]. Therefore, ACPA status was included in the new 2010 classification criteria for RA in addition to RF levels (that were already included in the 1987 criteria)[16,17]. Intriguingly, ACPA-positive RA patients present with more severe joint destruction and disease progression compared to ACPA-negative patients and therefore ACPA-status can be used as a predictive biomarker[18-20]. Since ACPA-positive disease is also associated with different genetic and environmental risk factors than ACPA-negative disease, it is believed that they are two separate diseases with different underlying pathophysiological mechanisms, but with a similar clinical profile at first diagnosis[21-23]. ACPA recognize the non-classical amino acid citrulline[24], which is a non-encoded amino acid that is generated by the conversion of the positively charged amino acid arginine to the uncharged citrulline by protein-arginine deiminase enzymes (PADI)[25]. This post-translational modification occurs during a variety of biological processes including inflammation. ACPA can recognize a diversity of citrullinated peptides and proteins, including citrullinated fibrinogen[26], citrullinated vimentin[27], citrullinated type II collagen[28], citrullinated α-enolase[29] and can be crossreactive[30]. ACPA can already be detected in the serum of patients up to 10 years before clinical symptoms develop[31,32], however, the titers are low and the peptide reactivity is restricted[33]. A spread of peptides recognized by ACPA (epitope spreading) and an increase in titers is observed as the individual approaches disease onset[33,34]. This 'maturation' of the ACPA response also includes an increase in isotype-usage[35] and the number of ACPA isotypes has been described to predict radiographic damage[36]. Different isotypes can activate different immune effector mechanisms, like stimulation of osteoclast precursors and osteoclastogenesis[37], formation

of immune complexes and activation of inflammatory cells through Fcγ receptors[38] and complement activation[39], which suggest involvement of ACPA in the inflammatory response using multiple effector pathways.

Risk factors

Over the years, several risk factors for the development of RA have been identified. Twin studies have estimated the relative contribution of genetic factors to be around 50% and the rest is determined by environment and chance[40,41]. The biggest environmental risk factor is cigarette smoking, however, only for autoantibody-positive RA patients carrying the high-risk HLA-DR alleles[42-45]. The most important genetic risk factor for autoantibody-positive RA is the HLA class II locus. HLA class II molecules consist of two chains, an alpha and a beta chain, and are encoded by the HLA-DRA1 gene and the HLA-DRB1 gene respectively. The site of interaction between these two chains forms the peptide-binding groove in which peptides are presented. The HLA-DR genes are in linkage disequilibrium with the genes encoding HLA-DQ, another classical HLA class II molecule, and these genes are inherited together in haplotypes. In 1976, it was described for the first time that the presence of HLA-DRB1*04 strongly predisposes to RA[46]. Subsequent studies reported that several HLA-DR alleles are associated with RA leading to the postulation of the shared epitope (SE) hypothesis[47]. This hypothesis is based on the fact that all HLA-DR alleles that predispose to RA share a similar amino acid sequence (shared epitope) at position 70-74 of the HLA-DRB1 molecule (QRRAA, QKRAA or RRRAA). These positions are located in the peptide-binging groove of the HLA molecule and are therefore potentially involved in peptide binding and T cell recognition[47]. Further investigation led to the conclusion that the SE alleles were specifically associated with and therefore predispose to ACPA-positive RA, but not to ACPA-negative disease[48]. Reports on the ability of SE HLA molecules to bind and present citrullinated peptides showed a possible association between ACPA and the SE alleles[49,50]. Recently, the association between ACPA-positive RA and the HLA-DRB1 variants has been refined using a statistical approach[51]. The amino acids at position 11 and 13 of the HLA-DRB1 chain were identified with the strongest association alongside position 71 and 74, which are all part of the peptide-binding groove. However, because these positions show the most variation in the HLA class II locus, it is conceivable that position 11 and 13, rather than being involved in the presentation of arthritogenic peptides, associate best with RA because they tag the susceptible haplotype the best (i.e. higher p-value). Because of the strong linkage between HLA-DR and HLA-DQ it is difficult to identify which molecule is responsible for the association with RA. Therefore, it is possible that the HLA-DQ genes are involved in the association as well[23].

In addition to predisposition to RA, several other HLA-DRB1 alleles are associated with protection against RA. Protection against ACPA-positive disease is most strongly associated with HLA-DRB1*1301 and this allele is also protective in the presence of SE alleles[52]. Protection can also be transferred from a mother with a protective allele to a child without a protective allele, suggesting that protection is an active and dominant process[53].

The HLA class II locus is not the only genetic risk factor associated with ACPA-positive disease. Genes involved in nuclear factor κB (NF-κB)-dependent signalling, for example *TRAF1-C5* and *c-REL*, and genes involved in T cell activation, e.g. *PTPN22* and *CTLA4*, are also identified as risk alleles as is *PADI* [54,55].

THERAPY FOR RA

Unfortunately, there is no cure for RA, however, current treatment strategies are very effective in controlling the inflammation. They are aimed at remission or sustained low disease activity, also known as treat to target[9]. RA patients are usually first treated with disease-modifying antirheumatic drugs (DMARDs), a group of drugs that reduce joint swelling and pain, limit progressive joint damage and improve function by incompletely understood mechanisms. The most frequently used DMARD is methotrexate and is thought to work through inhibition of adenosine metabolism and T cell activation[56,57]. Sulfasalazine, leflunomide and hydroxychloroquine are also DMARDs and can be used as monotherapy. However, clinical trials have shown that the combination of methotrexate, sulfasalazine and hydroxychloroquine is more effective than monotherapy[58,59]. In addition to conventional DMARDs, biological DMARDs have been developed that target specific molecules and pathways in the pathogenesis of RA. If a patient does not respond adequately to conventional DMARDs, the treatment regimen can be changed to a biological DMARD. The first biological agents that were developed and approved as treatment for RA were TNF inhibitors (infliximab, etanercept, adalimumab)[60,61]. Subsequent studies indicated that the different monoclonal antibodies against TNF were most effective when combined with methotrexate[62,63]. After the success of TNF blockade several other biological drugs were developed. Anakinra blocks IL-1 signalling by inhibiting binding of IL-1 to its receptor, however, it was not as effective as TNF blockade[64]. Tocilizumab, a monoclonal antibody directed against the IL-6 receptor, is efficient in reducing both inflammation and erosion[65,66]. Drugs specifically targeting T and B cells have been developed as well. Rituximab is a monoclonal antibody that binds to CD20 expressed by B cells and depletes them from the circulation[67]. This drug is very effective in autoantibody positive RA patients. Abatacept is thought to target T cells by inhibiting T cell costimulation. Abatacept is a fusion protein of human cytotoxic T lymphocyte associated protein 4 (CTLA-4) and the Fc region of IgG1. It can bind to CD80 and CD86 expressed by APCs and therefore CD28 on the T cell is not able bind to CD80 or CD86 anymore and the T cell cannot receive the costimulation needed for activation (Figure 2). When a patient does not respond to a TNF inhibitor, the regimen can be switched to another TNF inhibitor or to a different biological like Abatacept. Abatacept is effective in RA patients with moderate to severe RA, however, the effectiveness has also been studied in early erosive RA[68-73].

These treatment options are effective in decreasing disease activity, however, they all modulate the immune response in a non-specific approach. New treatments that are currently in development are antigen-specific immunotherapies that target autoantigens.
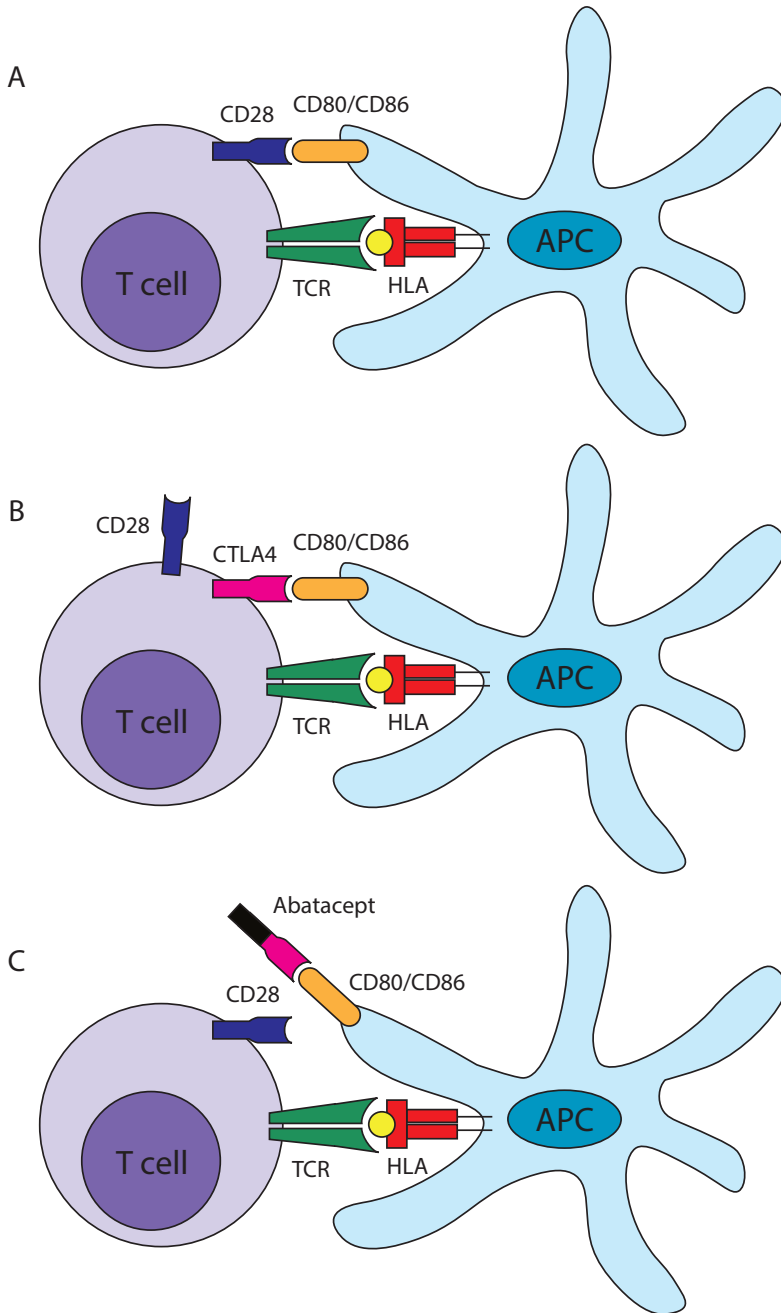
Figure 2. Working mechanism of Abatacept. (A) T cells bind with their TCR to the HLA-peptide complex presented by the APC upon recognition of their cognate antigen. For full activation of the T cell costimulation is provided by the APC through the expression of CD80/CD86, which binds to CD28 expressed by the T cell. (B) CTLA4 expressed by T cells can bind to CD80/CD86 as well providing an inhibitory signal to the T cell. (C) Abatacept is a fusion protein of CTLA4 and the Fc region of IgG1 and binds to CD80/CD86 on the APC, thereby blocking the binding of CD28 to CD80/CD86 and inhibiting costimulation of T cells.

1

SPONDYLOARTHRITIS

Another autoimmune disease with a very strong association with HLA is spondyloarthritis (SpA). Around 80-90% of the SpA patients is positive for HLA-B27 and HLA-B27 positivity is also part of the classification criteria[74,75]. Spondyloarthritis is a group of diseases of which ankylosing spondylitis (AS) is the prototypic and best studied disorder. AS is characterized by inflammation in the sacroiliac joints (SI joints) and vertebrae causing severe back pain. The inflammation can lead to bone formation in the SI joints, decreasing spinal mobility and impairing daily function. In addition to spinal features, peripheral arthritis, enthesitis (inflammation of the site where tendons and ligaments insert into the bone) and extra-articular features like uveitis can be involved in the disease. To diagnose AS, conventional radiographs are used to detect sacroiliitis, however, sacroiliitis is detected at a rather late stage of the disease on radiographs, as they detect only structural damage as a consequence of inflammation and not the inflammation itself. Early detection of AS is important since the new bone formation is irreversible and a sign of advanced disease. Therefore, the new Assessment of SpondyloArthritis International Society (ASAS) classification criteria were developed covering both radiographic axial SpA (AS) and nonradiographic axial SpA, which identifies patients with axial SpA without structural changes in the SI joints[74]. Patients with nonradiographic SpA can either show inflammation of the SI joints on MRI with one SpA feature or they are HLA-B27 positive with two additional SpA features.

To investigate the possibilities to diagnose SpA in the early stages of the disease and start treatment as early as possible to reduce the structural damage the SPondyloArthritis Caught Early (SPACE) study was started. In addition to the use of radiographic techniques such as MRI, the identification of biomarkers could contribute to early diagnosis as well.

THESIS OUTLINE

The general aim of this thesis was to provide a better understanding of the role of the adaptive immune system in the development, treatment and diagnosis of rheumatic diseases. The studies were divided in three parts.

In PART I, we studied the association between HLA class II and RA. As discussed previously, HLA class II is a risk factor for the development of (antibody-positive) RA[48]. However, the molecular basis of this association has been unknown. In **Chapter 2**, we investigated the contribution of predisposing and protective HLA class II molecules in the HLA-RA association. We identified (citrullinated) vinculin as a new autoantigen recognized by ACPA and CD4+ T cells in individuals carrying predisposing HLA molecules. The core sequence recognized by these vinculin reactive CD4+ T cells is present in many microbes and the protective HLA-DRB1*13 molecules. We described crossreactivity between the vinculin- and microbe-derived epitopes, however, these CD4+ T cells were not detected in HLA-DRB1*13-positive donors. This indicates that the epitope derived from the protective HLA molecule induces tolerance in these donors explaining the protective effects associated with HLA-DRB1*13. These results indicate the involvement of pathogen induced CD4+ T cells in the association

between HLA and RA and provide a molecular basis for the contribution of protective and predisposing HLA molecules.

In PART II, we focused on the therapeutic treatment of RA and in particular the biologic DMARD Abatacept. Abatacept is thought to block costimulation of CD4+ T cells by binding to CD80 and CD86 expressed by APCs[73]. In **Chapter 3**, we showed that Abatacept was still effective in the absence of CD4+ T cells in a mouse model of arthritis indicating that there is another mode of action in addition to blockade of costimulation of T cells. In **Chapter 4**, we investigated the effect of Abatacept in a cohort of early RA patients by performing post hoc analysis on the AGREE study (Abatacept trial to Gauge Remission and joint damage progression in methotrexate-naive patients with Early Erosive rheumatoid arthritis)[71]. We focused on patients that were positive for autoantibodies at the start of treatment with methotrexate and Abatacept, but converted to autoantibody negative patients after treatment.

In PART III, we explored the use of the adaptive immune system as a potential biomarker for early diagnosis of spondyloarthritis by investigating IL-17 producing CD4+ T cells in patients with early, active axial spondyloarthritis in **Chapter 5**. In **Chapter 6**, we focused on a different cytokine, IL-27, and its production by CD4+ T cells.

Finally, in **Chapter 7** we discuss the importance and the implications of the results obtained in the different chapters and the future directions towards the ultimate understanding of the role of the adaptive immune system in the development, treatment and diagnosis of RA.

REFERENCES

1.   Parham P. The Immune System. New York: Garland Science; 2005.

2.   Vinuesa CG, Tangye SG, Moser B, Mackay CR. Follicular B helper T cells in antibody responses and autoimmunity. Nat Rev Immunol 2005;5:853-65.

3.   Breitfeld D, Ohl L, Kremmer E, et al. Follicular B helper T cells express CXC chemokine receptor 5, localize to B cell follicles, and support immunoglobulin production. The Journal of experimental medicine 2000;192:1545-52.

4.   Zhu J, Yamane H, Paul WE. Differentiation of effector CD4 T cell populations (*). Annual review of immunology 2010;28:445-89.

5.   Zhu J, Paul WE. CD4 T cells: fates, functions, and faults. Blood 2008;112:1557-69.

6.   Boehm U, Klamp T, Groot M, Howard JC. Cellular responses to interferon-gamma. Annual review of immunology 1997;15:749-95.

7.   Luckheeram RV, Zhou R, Verma AD, Xia B. CD4(+)T cells: differentiation and functions. Clinical & developmental immunology 2012;2012:925135.

8.   Liu GY, Fairchild PJ, Smith RM, Prowle JR, Kioussis D, Wraith DC. Low avidity recognition of self-antigen by T cells permits escape from central tolerance. Immunity 1995;3:407-15.

9.   Scott DL, Wolfe F, Huizinga TW. Rheumatoid arthritis. Lancet (London, England) 2010;376:1094-108.

10.   McInnes IB, Schett G. The pathogenesis of rheumatoid arthritis. The New England journal of medicine 2011;365:2205-19.

11.   Alamanos Y, Drosos AA. Epidemiology of adult rheumatoid arthritis. Autoimmunity reviews 2005;4:130-6.

12.   Shi J, Knevel R, Suwannalai P, et al. Autoantibodies recognizing carbamylated proteins are present in sera of patients with rheumatoid arthritis and predict joint damage. Proceedings of the National Academy of Sciences of the United States of America 2011;108:17372-7.

13.   Nishimura K, Sugiyama D, Kogata Y, et al. Meta-analysis: diagnostic accuracy of anti-cyclic citrullinated peptide antibody and rheumatoid factor for rheumatoid arthritis. Annals of internal medicine 2007;146:797-808.

14.   Schellekens GA, Visser H, de Jong BA, et al. The diagnostic properties of rheumatoid arthritis antibodies recognizing a cyclic citrullinated peptide. Arthritis Rheum 2000;43:155-63.

15.   van Venrooij WJ, van Beers JJ, Pruijn GJ. Anti-CCP Antibody, a Marker for the Early Detection of Rheumatoid Arthritis. Annals of the New York Academy of Sciences 2008;1143:268-85.

16.   Aletaha D, Neogi T, Silman AJ, et al. 2010 Rheumatoid arthritis classification criteria: an American College of Rheumatology/European League Against Rheumatism collaborative initiative. Arthritis Rheum 2010;62:2569-81.

17.   Aletaha D, Neogi T, Silman AJ, et al. 2010 rheumatoid arthritis classification criteria: an American College of Rheumatology/European League Against Rheumatism collaborative initiative. Annals of the rheumatic diseases 2010;69:1580-8.

18.   Kroot EJ, de Jong BA, van Leeuwen MA, et al. The prognostic value of anti-cyclic citrullinated peptide antibody in patients with recent-onset rheumatoid arthritis. Arthritis Rheum 2000;43:1831-5.

19.   van der Helm-van Mil AH, Verpoort KN, Breedveld FC, Toes RE, Huizinga TW. Antibodies to citrullinated proteins and differences in clinical progression of rheumatoid arthritis. Arthritis research & therapy 2005;7:R949-58.

20.   van Gaalen FA, van Aken J, Huizinga TW, et al. Association between HLA class II genes and autoantibodies to cyclic citrullinated peptides (CCPs) influences the severity of rheumatoid arthritis. Arthritis Rheum 2004;50:2113-21.

21.   Verpoort KN, van Gaalen FA, van der Helm-van Mil AH, et al. Association of HLA-DR3 with anti-cyclic citrullinated peptide antibody-negative rheumatoid arthritis. Arthritis Rheum 2005;52:3058-62.

22.   van der Helm-van Mil AH, Huizinga TW. Advances in the genetics of rheumatoid arthritis point to subclassification into distinct disease subsets. Arthritis research & therapy 2008;10:205.

23.   van Heemst J, van der Woude D, Huizinga TW, Toes RE. HLA and rheumatoid arthritis: how do they connect? Annals of medicine 2014;46:304-10.

24.   Schellekens GA, de Jong BA, van den Hoogen FH, van de Putte LB, van Venrooij WJ. Citrulline is an essential constituent of antigenic determinants recognized by rheumatoid arthritis-specific autoantibodies. The Journal of clinical investigation 1998;101:273-81.

25.   Vossenaar ER, Zendman AJ, van Venrooij WJ, Pruijn GJ. PAD, a growing family of citrullinating enzymes: genes, features and involvement in disease. BioEssays : news and reviews in molecular, cellular and developmental biology 2003;25:1106-18.

26.   Takizawa Y, Suzuki A, Sawada T, et al. Citrullinated fibrinogen detected as a soluble citrullinated autoantigen in rheumatoid arthritis synovial fluids. Annals of the rheumatic diseases 2006;65:1013-20.

27.   Vossenaar ER, Despres N, Lapointe E, et al. Rheumatoid arthritis specific anti-Sa antibodies target citrullinated vimentin. Arthritis research & therapy 2004;6:R142-50.

28.   Koivula MK, Heliovaara M, Ramberg J, et al. Autoantibodies binding to citrullinated telopeptide of type II collagen and to cyclic citrullinated peptides predict synergistically the development of seropositive rheumatoid arthritis. Annals of the rheumatic diseases 2007;66:1450-5.

29.   Kinloch A, Tatzer V, Wait R, et al. Identification of citrullinated alpha-enolase as a candidate autoantigen in rheumatoid arthritis. Arthritis research & therapy 2005;7:R1421-9.

30.   Ioan-Facsinay A, el-Bannoudi H, Scherer HU, et al. Anti-cyclic citrullinated peptide antibodies are a collection of anti-citrullinated protein antibodies and contain overlapping and non-overlapping reactivities. Annals of the rheumatic diseases 2011;70:188-93.

31.   Rantapaa-Dahlqvist S, de Jong BA, Berglin E, et al. Antibodies against cyclic citrullinated peptide and IgA rheumatoid factor predict the development of rheumatoid arthritis. Arthritis Rheum 2003;48:2741-9.

32.   Nielen MM, van Schaardenburg D, Reesink HW, et al. Specific autoantibodies precede the symptoms of rheumatoid arthritis: a study of serial measurements in blood donors. Arthritis Rheum 2004;50:380-6.

33.   van de Stadt LA, de Koning MH, van de Stadt RJ, et al. Development of the anti-citrullinated protein antibody repertoire prior to the onset of rheumatoid arthritis. Arthritis Rheum 2011;63:3226-33.

34.   van der Woude D, Rantapaa-Dahlqvist S, Ioan-Facsinay A, et al. Epitope spreading of the anti-citrullinated protein antibody response occurs before disease onset and is associated with the disease course of early arthritis. Annals of the rheumatic diseases 2010;69:1554-61.

35.   Kokkonen H, Mullazehi M, Berglin E, et al. Antibodies of IgG, IgA and IgM isotypes against cyclic citrullinated peptide precede the development of rheumatoid arthritis. Arthritis research & therapy 2011;13:R13.

36.   van der Woude D, Syversen SW, van der Voort EI, et al. The ACPA isotype profile reflects long-term radiographic progression in rheumatoid arthritis. Annals of the rheumatic diseases 2010;69:1110-6.

37.   Harre U, Georgess D, Bang H, et al. Induction of osteoclastogenesis and bone loss by human autoantibodies against citrullinated vimentin. The Journal of clinical investigation 2012;122:1791-802.

38. Laurent L, Clavel C, Lemaire O, et al. Fcgamma receptor profile of monocytes and macrophages from rheumatoid arthritis patients and their response to immune complexes formed with autoantibodies to citrullinated proteins. Annals of the rheumatic diseases 2011;70:1052-9.

39. Trouw LA, Haisma EM, Levarht EW, et al. Anti-cyclic citrullinated peptide antibodies from rheumatoid arthritis patients activate complement via both the classical and alternative pathways. Arthritis Rheum 2009;60:1923-31.

40. MacGregor AJ, Snieder H, Rigby AS, et al. Characterizing the quantitative genetic contribution to rheumatoid arthritis using data from twins. Arthritis Rheum 2000;43:30-7.

41. Klareskog L, Catrina AI, Paget S. Rheumatoid arthritis. Lancet (London, England) 2009;373:659-72.

42. Symmons DP, Bankhead CR, Harrison BJ, et al. Blood transfusion, smoking, and obesity as risk factors for the development of rheumatoid arthritis: results from a primary care-based incident case-control study in Norfolk, England. Arthritis Rheum 1997;40:1955-61.

43. Hazes JM, Dijkmans BA, Vandenbroucke JP, de Vries RR, Cats A. Lifestyle and the risk of rheumatoid arthritis: cigarette smoking and alcohol consumption. Annals of the rheumatic diseases 1990;49:980-2.

44. Padyukov L, Silva C, Stolt P, Alfredsson L, Klareskog L. A gene-environment interaction between smoking and shared epitope genes in HLA-DR provides a high risk of seropositive rheumatoid arthritis. Arthritis Rheum 2004;50:3085-92.

45. Klareskog L, Stolt P, Lundberg K, et al. A new model for an etiology of rheumatoid arthritis: smoking may trigger HLA-DR (shared epitope)-restricted immune reactions to autoantigens modified by citrullination. Arthritis Rheum 2006;54:38-46.

46. Stastny P. Mixed lymphocyte cultures in rheumatoid arthritis. The Journal of clinical investigation 1976;57:1148-57.

47. Gregersen PK, Silver J, Winchester RJ. The shared epitope hypothesis. An approach to understanding the molecular genetics of susceptibility to rheumatoid arthritis. Arthritis Rheum 1987;30:1205-13.

48. Huizinga TW, Amos CI, van der Helm-van Mil AH, et al. Refining the complex rheumatoid arthritis phenotype based on specificity of the HLA-DRB1 shared epitope for antibodies to citrullinated proteins. Arthritis Rheum 2005;52:3433-8.

49. Hill JA, Southwood S, Sette A, Jevnikar AM, Bell DA, Cairns E. Cutting edge: the conversion of arginine to citrulline allows for a high-affinity peptide interaction with the rheumatoid arthritis-associated HLA-DRB1*0401 MHC class II molecule. Journal of immunology (Baltimore, Md : 1950) 2003;171:538-41.

50. James EA, Moustakas AK, Bui J, et al. HLA-DR1001 presents "altered-self" peptides derived from joint-associated proteins by accepting citrulline in three of its binding pockets. Arthritis Rheum 2010;62:2909-18.

51. Raychaudhuri S, Sandor C, Stahl EA, et al. Five amino acids in three HLA proteins explain most of the association between MHC and seropositive rheumatoid arthritis. Nature genetics 2012;44:291-6.

52. van der Woude D, Lie BA, Lundstrom E, et al. Protection against anti-citrullinated protein antibody-positive rheumatoid arthritis is predominantly associated with HLA-DRB1*1301: a meta-analysis of HLA-DRB1 associations with anti-citrullinated protein antibody-positive and anti-citrullinated protein antibody-negative rheumatoid arthritis in four European populations. Arthritis Rheum 2010;62:1236-45.

53. Feitsma AL, Worthington J, van der Helm-van Mil AH, et al. Protective effect of noninherited maternal HLA-DR antigens on rheumatoid arthritis development. Proceedings of the National Academy of Sciences of the United States of America 2007;104:19966-70.

54. Begovich AB, Carlton VE, Honigberg LA, et al. A missense single-nucleotide polymorphism in a gene encoding a protein tyrosine phosphatase (PTPN22) is associated with rheumatoid arthritis. American journal of human genetics 2004;75:330-7.

55. Kurreeman FA, Padyukov L, Marques RB, et al. A candidate gene approach identifies the TRAF1/C5 region as a risk factor for rheumatoid arthritis. PLoS medicine 2007;4:e278.

56. Wessels JA, Huizinga TW, Guchelaar HJ. Recent insights in the pharmacological actions of methotrexate in the treatment of rheumatoid arthritis. Rheumatology (Oxford, England) 2008;47:249-55.

57. Montesinos MC, Takedachi M, Thompson LF, Wilder TF, Fernandez P, Cronstein BN. The antiinflammatory mechanism of methotrexate depends on extracellular conversion of adenine nucleotides to adenosine by ecto-5'-nucleotidase: findings in a study of ecto-5'-nucleotidase gene-deficient mice. Arthritis Rheum 2007;56:1440-5.

58. O'Dell JR, Haire CE, Erikson N, et al. Treatment of rheumatoid arthritis with methotrexate alone, sulfasalazine and hydroxychloroquine, or a combination of all three medications. The New England journal of medicine 1996;334:1287-91.

59. Mottonen T, Hannonen P, Leirisalo-Repo M, et al. Comparison of combination therapy with single-drug therapy in early rheumatoid arthritis: a randomised trial. FIN-RACo trial group. Lancet (London, England) 1999;353:1568-73.

60. Elliott MJ, Maini RN, Feldmann M, et al. Randomised double-blind comparison of chimeric monoclonal antibody to tumour necrosis factor alpha (cA2) versus placebo in rheumatoid arthritis. Lancet (London, England) 1994;344:1105-10.

61. Elliott MJ, Maini RN, Feldmann M, et al. Treatment of rheumatoid arthritis with chimeric monoclonal antibodies to tumor necrosis factor alpha. Arthritis Rheum 1993;36:1681-90.

62. Maini RN, Breedveld FC, Kalden JR, et al. Therapeutic efficacy of multiple intravenous infusions of anti-tumor necrosis factor alpha monoclonal antibody combined with low-dose weekly methotrexate in rheumatoid arthritis. Arthritis Rheum 1998;41:1552-63.

63. Klareskog L, van der Heijde D, de Jager JP, et al. Therapeutic effect of the combination of etanercept and methotrexate compared with each treatment alone in patients with rheumatoid arthritis: double-blind randomised controlled trial. Lancet (London, England) 2004;363:675-81.

64. Burger D, Dayer JM, Palmer G, Gabay C. Is IL-1 a good therapeutic target in the treatment of arthritis? Best practice & research Clinical rheumatology 2006;20:879-96.

65. Maini RN, Taylor PC, Szechinski J, et al. Double-blind randomized controlled clinical trial of the interleukin-6 receptor antagonist, tocilizumab, in European patients with rheumatoid arthritis who had an incomplete response to methotrexate. Arthritis Rheum 2006;54:2817-29.

66. Smolen JS, Beaulieu A, Rubbert-Roth A, et al. Effect of interleukin-6 receptor inhibition with tocilizumab in patients with rheumatoid arthritis (OPTION study): a double-blind, placebo-controlled, randomised trial. Lancet (London, England) 2008;371:987-97.

67. Edwards JC, Szczepanski L, Szechinski J, et al. Efficacy of B-cell-targeted therapy with rituximab in patients with rheumatoid arthritis. The New England journal of medicine 2004;350:2572-81.

68. Linsley PS, Nadler SG. The clinical utility of inhibiting CD28-mediated costimulation. Immunological reviews 2009;229:307-21.

69. Genovese MC, Becker JC, Schiff M, et al. Abatacept for rheumatoid arthritis refractory to tumor necrosis factor alpha inhibition. The New England journal of medicine 2005;353:1114-23.

70. Kremer JM, Westhovens R, Leon M, et al. Treatment of rheumatoid arthritis by selective inhibition of T-cell activation with fusion protein

CTLA4Ig. The New England journal of medicine 2003;349:1907-15.

71. Bathon J, Robles M, Ximenes AC, et al. Sustained disease remission and inhibition of radiographic progression in methotrexate-naive patients with rheumatoid arthritis and poor prognostic factors treated with abatacept: 2-year outcomes. Annals of the rheumatic diseases 2011;70:1949-56.

72. Emery P, Durez P, Dougados M, et al. Impact of T-cell costimulation modulation in patients with undifferentiated inflammatory arthritis or very early rheumatoid arthritis: a clinical and imaging study of abatacept (the ADJUST trial). Annals of the rheumatic diseases 2010;69:510-6.

73. Moreland L, Bate G, Kirkpatrick P. Abatacept. Nat Rev Drug Discov 2006;5:185-6.

74. Rudwaleit M, van der Heijde D, Landewe R, et al. The development of Assessment of SpondyloArthritis international Society classification criteria for axial spondyloarthritis (part II): validation and final selection. Annals of the rheumatic diseases 2009;68:777-83.

75. Dougados M, Baeten D. Spondyloarthritis. Lancet (London, England) 2011;377:2127-37.

PART I

A MOLECULAR BASIS FOR THE HLA-RA ASSOCIATION
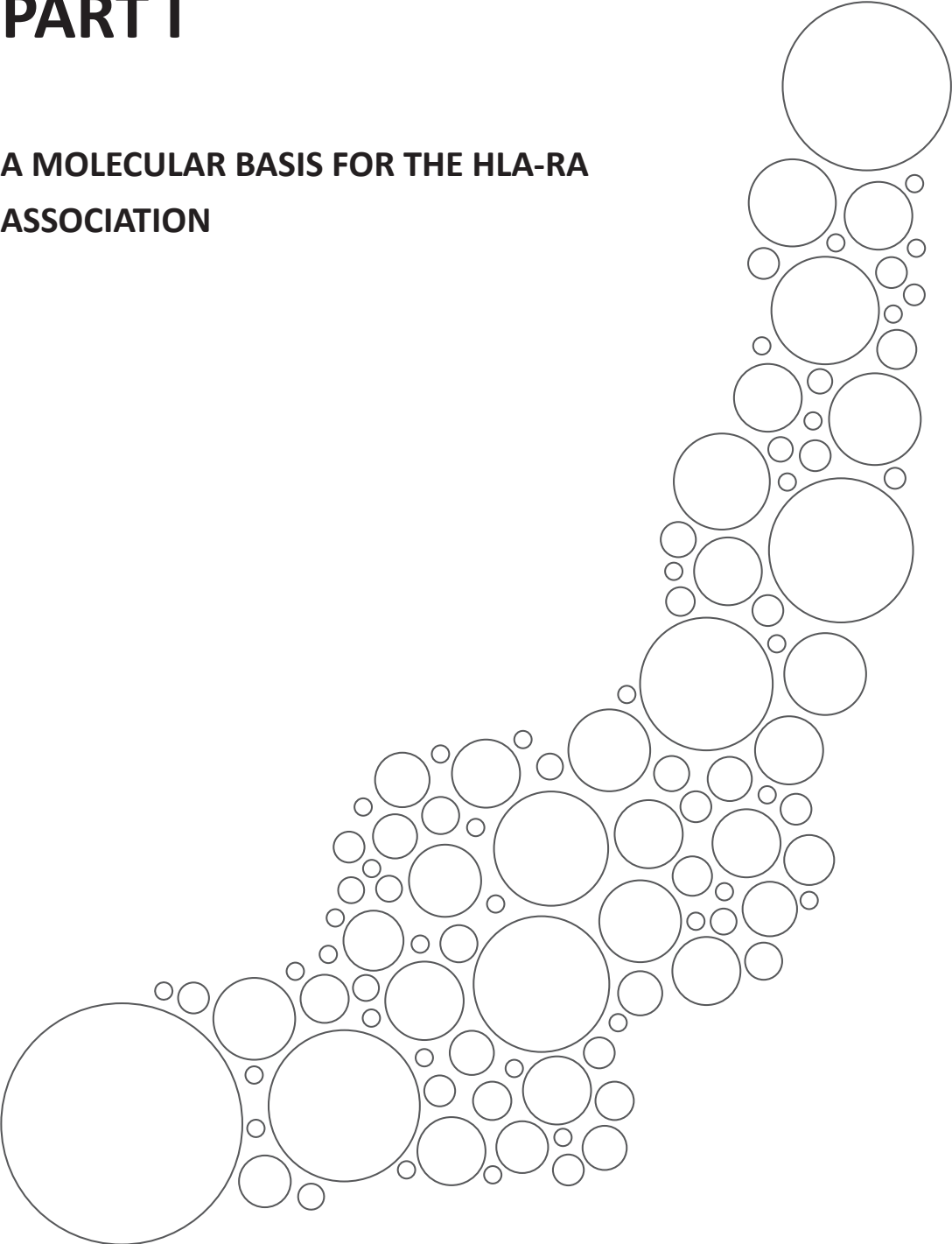
CHAPTER 2

CROSSREACTIVITY TO VINCULIN AND MICROBES PROVIDES A MOLECULAR BASIS FOR HLA-BASED PROTECTION AGAINST RHEUMATOID ARTHRITIS

Diahann T. S. L. Jansen*, Jurgen van Heemst*, Savvas Polydorides, Antonis K. Moustakas, Marieke Bax, Anouk L. Feitsma, Diënne G. Bontrop-Elferink, Martine Baarse, Diane van der Woude, Gert-Jan Wolbink, Theo Rispens, Frits Koning, René R. P. de Vries, George K. Papadopoulos, Georgios Archontis, Tom W.J. Huizinga & René E.M. Toes

* Authors contributed equally
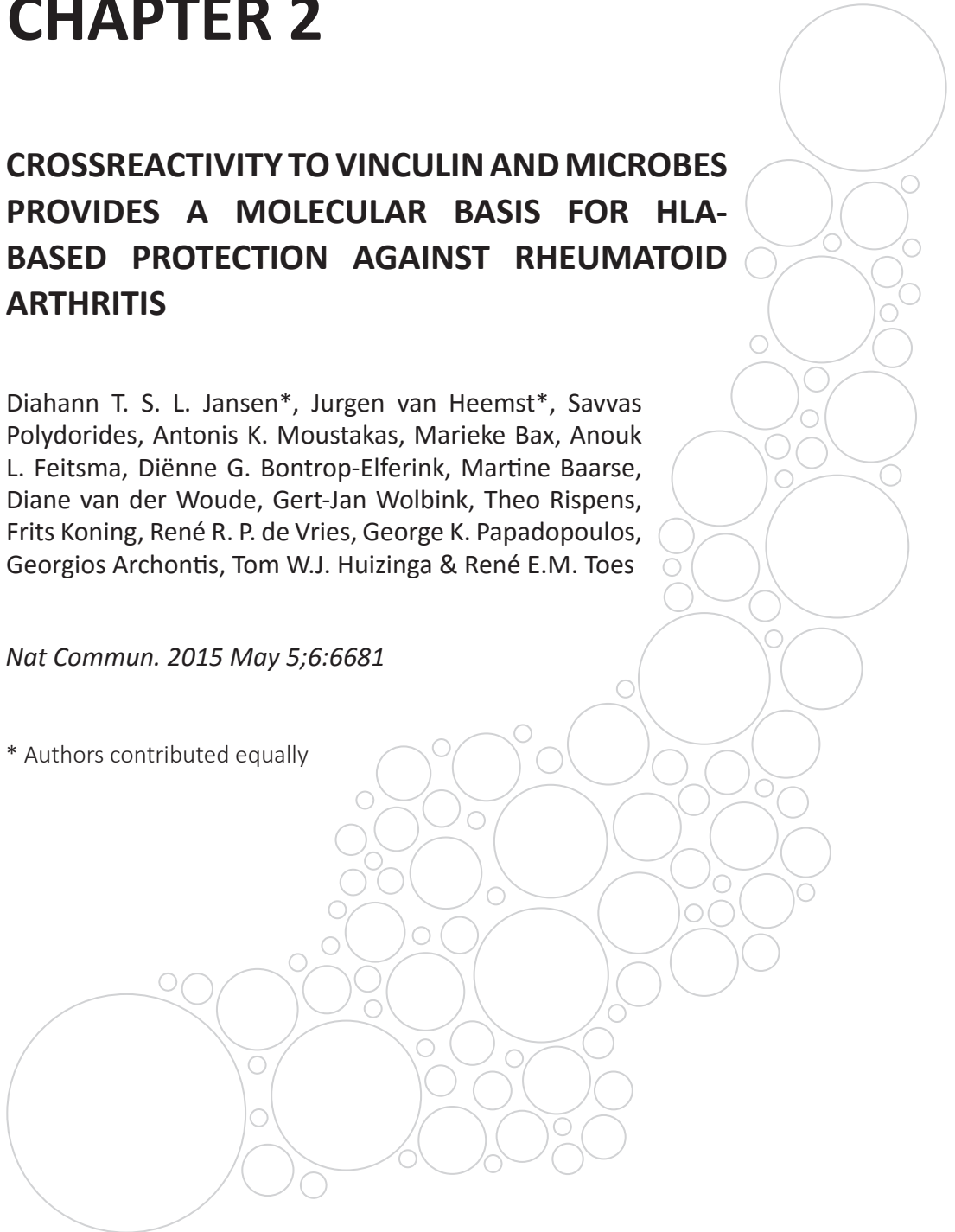
ABSTRACT

The HLA locus is the strongest risk factor for anti-citrullinated protein antibody (ACPA)+ rheumatoid arthritis (RA). Despite considerable efforts in the last 35 years, this association is poorly understood. Here we identify (citrullinated) vinculin, present in the joints of ACPA+ RA patients, as an autoantigen targeted by ACPA and CD4+ T cells. These T cells recognize an epitope with the core sequence DERAA, which is also found in many microbes and in protective HLA-DRB1*13 molecules, presented by predisposing HLA-DQ molecules. Moreover, these T cells crossreact with vinculin-derived and microbial-derived DERAA epitopes. Intriguingly, DERAA-directed T cells are not detected in HLA-DRB1*13+ donors, indicating that the DERAA epitope from HLA-DRB1*13 mediates (thymic) tolerance in these donors and explaining the protective effects associated with HLA-DRB1*13. Together our data indicate the involvement of pathogen-induced DERAA-directed T cells in the HLA-RA association and provide a molecular basis for the contribution of protective/predisposing HLA alleles.

2

INTRODUCTION

Rheumatoid arthritis (RA) is a chronic autoimmune disease affecting synovial joints that can lead to severe disability. Pivotal pathophysiological insight has been obtained by the identification of anti-citrullinated protein antibodies (ACPA)[1,2]. These autoantibodies target proteins that have undergone a post- translational conversion of arginine to citrulline, catalysed by peptidylarginine deiminases (PAD enzymes)[3]. ACPA are highly specific for RA, enriched in the joints of patients and can crossreact between citrullinated antigens that are expressed in the inflamed joints[4-8]. It is clear now that RA represents two main syndromes, ACPA+ and ACPA- disease, each with distinct genetic and environmental risk factors and disease outcome[9-12]. Characteristics of ACPA (for example, isotype usage and epitope spreading) indicate the involvement of CD4+ T cell help in shaping the ACPA response[13].

The most important genetic risk factor for ACPA+ RA is the HLA class II locus and risk is confined to a region with genes encoding for the beta chain of HLA-DR and the alpha and beta chain of HLA-DQ that are in tight linkage disequilibrium (LD) and inherited in haplotypes[14,15]. An understanding of the HLA class II association and the relative contribution of the HLA-DR and HLA-DQ locus has been lacking for the last 35 years.

Next to the association of the predisposing alleles to ACPA+ RA, other HLA molecules are associated with protection. These protective HLA alleles, mainly HLA-DRB1*13, carry the five amino-acid sequence DERAA at positions 70-74 of the beta chain and protect also in the presence of predisposing alleles[16,17]. Intriguingly, protection by these alleles is transferred from mother to child, supporting an active protective role of these alleles, possibly via microchimeric cells influencing thymic selection of CD4+ T cells, and indicating a dominant role of HLA-DRB1*13 in disease protection[18].

HLA-derived peptides are a dominant peptide source presented by HLA class II molecules. We therefore proposed that the protective effect of HLA-DRB1*13 is explained by presentation of an HLA-DRB1*13-derived peptide in the context of other (predisposing) HLA class II molecules[19-21].

It was previously shown that the degradation of HLA-DRB1*13 can result in the presentation of a peptide with the core sequence DERAA by other HLA class II molecules to CD4+ T cells[22]. This could allow for the negative selection of such 'DERAA-directed' CD4+ thymocytes. Interestingly, the DERAA sequence is also found in many microbes and in the self-protein vinculin. Vinculin is expressed in the synovium and was recently shown to be citrullinated in the synovial fluid of an RA patient[4,23]. Likewise, T cells directed to vinculin are found under certain infectious conditions, indicating that T cell tolerance to vinculin is not absolute[24,25]. Molecular mimicry of self-proteins with pathogenic proteins was proposed as an important mechanism to break T cell tolerance[26,27]. Therefore, we postulate that on priming of DERAA-directed T cells by microbes expressing DERAA-containing proteins, T cells crossreactive to vinculin would be able to provide help to B cells reactive to citrullinated vinculin. This would ultimately result in the production of ACPA. In HLA-DRB1*13-positive donors, these T cells

are conceivably deleted, leading to protection against ACPA+ disease.

Here we show that citrullinated vinculin is novel autoantigen for ACPA antibodies. In addition, we demonstrate the presence of a T cell population in HLA-DRB1*13-negative donors that specifically recognize a DERAA-containing vinculin epitope and that crossreact with DERAA sequences derived from pathogens.

METHODS

Cells and sera

HLA-typed buffy coats from healthy volunteers were obtained from the blood bank (Sanquin, The Netherlands). PBMCs and sera from RA patients were derived from patients participating in the Leiden Early Arthritis Clinic cohort[37]. All RA patients fulfilled the American College of Rheumatology (formerly the American Rheumatism Association) 1987 revised criteria for the classification of RA. A total of 178 RA patients were used in the current analyses. Patient samples were compared with 80 control samples from healthy individuals also living in the Leiden area. PBMCs were isolated using a standard Ficoll procedure. The protocols were approved by the Leiden University Medical Center ethics committee and informed consent was obtained.

Peptides

Peptides were synthesized according to standard Fmoc (*N*-(9-fluorenyl)methoxycarbonyl) chemistry using a SyroII peptide synthesizer (Multi- SynTech, Witten, Germany). The integrity of the peptides was checked using reverse-phase high-performance liquid chromatography and mass spectrometry. For vinculin ELISPOT experiments, HLA class II-binding studies and T cell activation studies 15-mer vinculin epitope $VCL_{622-636}$ (VCL-DERAA; REEVFDERAANFENH) was used. To determine the peptide-binding register, the $VCL_{622-636}$ peptide was modified: Truncated on the N- or C terminus or alanine-/arginine-substituted at different positions. For ELISPOT assays against common pathogens, pathogenic peptides were used derived from measles virus (SSRASDERAAHLPTS), influenza A virus (VFEFSDERAANPIVP), human herpesvirus 7 (LAARADERAAFPDVG), *Bordetella pertussis* (SPNLTDER- AAQAGVT), *Staphylococcus aureus* (QDMNDDERAALTMAM), *Haemophilus influenzae* (RFHGDDERAAKVYEN), *Salmonella enteritidis* (PLMMDDERAAKVYEN) and *Propionibacterium acnes* (EEVFTDERAARLSHV). For the generation of T cell lines, these eight pathogenic peptides were pooled.

Cell lines

The following Epstein-Barr virus-transformed lymphoblastoid B cell lines were used: BSM (DRB1*04:01;DQA1*03:01;DQB1*03:02, IHW9032), BOLETH (DRB1*04:01;DQA1*03:01; DQB1*03:02, IHW9031), BM21 (DQA1*05: 01;DQB1*03:01, IHW9043), JSM (DQA1*03:02;DQB1*03:01), APD (DRB1*13:01; DQA1*01:03;DQB1*06:03, IHW9291), BC34 (DRB1*13:02;DQA1*01:02;DQB1 *06:04), WT8 (DQA1*01:02;DQB1*06:02, IHW9017), KAS116 (DRB1*01:01; DQA1*01:02; DQB1*05:01, IHW9003) and 721.82 (DR/DQ-negative)[38].

Cells were maintained in IMDM (Lonza) supplemented with 10% heat-inactivated fetal calf serum. JSM and BC34 cells are derived from healthy HLA-typed donors that were Epstein-Barr virus transformed.

HLA class II competitive peptide-binding assay

Peptide-binding assays were performed, as described previously[39]. In short, cell lysates from HLA class II homozygous B-lymphoblastoid cell lines were incubated on SPVL3- (anti-HLA-DQ) or B8.11.2- (anti-HLA-DR) coated (10 µg/ml3) FluoroNunc 96-well plates at 4 °C overnight. Titration ranges of the tested peptides (0 to 300 µM) were mixed with a fixed concentration (0.6 µM) of biotinylated indicator peptide and added to the wells. Bound indicator peptide was detected using europium-streptavidin (Perkin Elmer, Boston, MA) and measured in a time-resolved fluorometer (PerkinElmer, Wallac Victor2). IC50 values were calculated based on the observed binding of the test peptide against the fixed concentration indicator peptide. The IC50 value depicts the concentration of test peptide required for a loss of 50% of the indicator peptide signal.

Enzyme-linked immunosorbent spot assay

PBMCs were incubated in 96-well Multiscreen HA plates (Millipore) precoated with 5 µg/ml anti-IFNγ capture antibody (clone 1-D1K; Mabtech) at 5×10^5 cells per well and stimulated in X-VIVO medium (LONZA) with 5 µg/ml peptide or with a mix of recall anti- gens consisting of 0.75 Lf/ml tetanus toxoid (Netherlands Vaccine Institute), 5 µg/ml tuberculin purified protein derivative (Netherlands Vaccine Institute) and 0.005% *Candida albicans* (HAL allergy). After 24 h incubation at 37 °C, plates were extensively washed and incubated with 0.3 µg/ml biotin-labelled anti-IFNγ detection antibody (clone 7-B6-1; Mabtech) for 2h at RT, with 1,000 x diluted ExtrAvidin-Alkaline phosphatase (Sigma-Aldrich) for 1h at RT and with 5-Bromo-4-chloro-3-indolyl phosphate/Nitro blue tetrazolium (Sigma-Aldrich). Spots were analysed using the BioSys Bioreader 3000pro. Circular spots with a size of 80-450 µm were included.

Flow cytometry

Polyclonal CD4+ T cell lines were generated by stimulating 3×10^6 PBMCs per well in a 24-well plate with 5 µg/ml peptide for 7 days in IMDM supplemented with 5% human serum (Sanquin). After 7 days, 1.5×10^6 autologous PBMCs per well were plated in 24-well plates for 2h. After 2h, nonadherent cells were removed and adherent cells were pulsed with 5 µg/ml peptide and used as feeders for 10^6 T cells. After 1h, 10 µg/ml brefeldin A was added. Cells were incubated overnight and used for intracellular cytokine staining. The cells were incubated with fluorochrome-conjugated antibodies recognizing CD4, (Clone RPA-T4; BD biosciences), CD14 (Clone 61D3; eBioscience) and CD25 (Clone M-A251; BD biosciences), after which they were permeabilized using CytoFix CytoPerm Kit (BD Biosciences). After washing, cells were incubated with PE-labelled anti-IFNγ or matching isotype control. Cells were taken up in 1% paraformaldehyde until flow cytometric acquisition. Flow cytometry was performed on FACS

Calibur (BD biosciences) or LSR II (BD biosciences). Analysis was performed using FACS Diva (BD biosciences) and FlowJo software.

T cell cloning

JPT57 was generated from an HLA-DRB1*04:05/01:01;DQ8/DQ5 donor. PBMCs were cultured for 7 days in the presence of 10 μg/ml of VCL-DERAA peptide and restimulated with VCL-DERAA-pulsed antigen-presenting cells. After 1 week, cells were restimulated with 150 U/ml rIL-2. After two rounds of restimulation, T cell lines were tested for their specificity. The wells responding to VCL-DERAA peptide were cloned in a limiting dilution of 0.3 cells per well resulting in the isolation of clone JPT57.

T cell clone D2C18 was generated from an HLA-DRB1*04:01;DQ2/DQ8-positive donor. CD4+ T cells and CD14+ monocytes were isolated from PBMCs using antibodies bound to magnetic beads from, respectively, Dynal and Miltenyi. CD4+ T cells were labelled with 1 μM CFSE (Invitrogen) and incubated in a 2:1 ratio with CD14+ monocytes with 30 μg/ml PathMix. After 6 days, $CD3_{pos}CD4_{pos}CD25_{pos}CD14_{neg}$ $DAPI_{neg}CFSE_{low}$ cells were sorted by FACS aria (BD). Isolated CD4+ T cells were rested in medium containing 20 IU/ml rIL-2 (Peprotech). After 3 days, the cells were cloned in a limiting dilution of 0.3 cells per well resulting in the isolation of CD4+ T cell clone D2C18.

T cell activation

To determine IFNγ production by T cell clones in response to peptide stimulation, 50,000 T cells were incubated in a 1:1 ratio with B-LCL lines pulsed with 10 μg/ml of peptide for 3-6h. After 3 days, the supernatant was collected and an IFNγ ELISA (eBioscience) was used to determine the concentration of IFNγ. For measurement of T cell proliferation, 50,000 T cells were incubated in a 1:1 ratio with radiated (3000RAD) autologous PBMCs pulsed with 10 μg/ml of peptide for 3-6h in IMDM supplemented with 5% human serum. After 3 days, cells were cultured for 16-20h with [³H]thymidine (0.5 μCi per well). ³H incorporation was measured by liquid scintillation counting (1450 MicroBeta TriLux; PerkinElmer). Blocking experiments were performed by preincubating antigen-presenting cells for 1h with 20 μg/ml anti-DQ (SPVL3), anti-DR (B8.11.2) and anti-DP (B7.21) blocking antibodies.

Detection of anti-citrullinated vinculin antibodies

Citrullinated vinculin was generated by incubation of 50 μg vinculin protein (Sanbio) in a volume of 200 μl containing 0.1 M Tris-HCl pH 7.6, 0.15 M $CaCl_2$, and 10 U PAD4 (Sigma) for 4h at 37 °C. Unmodified vinculin protein was generated by incubation of vinculin with PAD4 without $CaCl_2$. Citrullinated and unmodified vinculin were loaded onto 10% SDS-polyacrylamide gels and transferred onto blotting membranes. Blots were blocked, washed and incubated in 1:500 diluted serum overnight at 4 °C. The sera were either ACPA+ or ACPA- as determined by ELISA. Blots were incubated with horseradish peroxidase-labelled rabbit anti-human IgG (Dako) and visualized with chemiluminescence (ECL, Amersham). To analyse

reactivity to vinculin by a monoclonal ACPA (anti-cFIB1.1, citrullinated fibrinogen), vinculin- or citrullinated vinculin-coated Nunc plates were incubated with 0.2 µg/ml anti-cFIB1.1 for 2h at room temperature[28]. Bound antibody was detected using horseradish peroxidase-labelled rabbit anti-human IgG (Dako) and visualized with ABTS. Peptide ELISA was performed as described previously using biotinylated peptides coated on streptavidin-precoated plates[40].

B cell activation by JPT57 cells

B cells were isolated from PBMCs of HLA-DQ8-positive healthy donors or ACPA-positive RA patients by magnetic anti-CD19 beads (Invitrogen). B cells were cultured in IMDM supplemented with 10% fetal calf serum, penicillin, streptomycin and glutamax. From healthy subjects, 30,000 B cells were co-cultured with different number of JPT57 cells in the presence of 5 µg/ml anti-IgM (Jackson Immunoresearch Laboratories) and with 10 µg/ml VCL-DERAA or 1 µg/ml PHA in round-bottom 96-well plates. After 7 days, IgG production by B cells was determined using a total IgG ELISA (Bethyl laboratories). From RA patients, 20,000 B cells were pulsed with 10 µg/ml VCL-DERAA peptide and co-cultured with 20,000 JPT57 cells in the presence of 5 µg/ml anti-IgM in round-bottom 96-well plates. After 7 days, ACPA production was determined by ELISA measuring reactivity against the CCP2-peptide in individual wells (EuroDiagnostica).

Energy minimization

Molecular simulations of HLA-DQ8 (A1*0301/B1*302) and HLA-DQ7.3 (A1*0302/B1*0301) complexed with various peptides, experimentally shown to bind to these molecules, were carried out as previously described using the Discover Suite (programmes InsightII and Discover) of Accelrys (San Diego, CA, release of 2005) on a Silicon Graphics Fuel instrument, using a minimization approach previously described[41], that is, 1,000 steps of the steepest gradient method, followed by 1,000 steps of the conjugate gradient method. Records of the energy of every step showed a continuous decrease in energy without any local minima and an energy asymptote for the last 300-400 steps of the conjugate gradient method. The base molecule was the crystal structure of HLA-DQ8 (A1*0301/B1*0302) with bound the insulin B11-23 peptide[42]. The region HLA- DQβ105-112 for which full coordinates were not available in the original data, was constructed by molecular replacement of the respective region from HLA-DR1[43], after superposition of the β-plated sheet regions of the two molecules in the α1β1 domains. The binding registers of the vinculin and the bound microbial peptides were decided from the binding of truncated peptides as well as Arg-substituted peptides in presumed anchor positions; energy minimization of successive registers confirmed the registers predicted from the binding data. The rotamers for the peptide residues were chosen from a library of rotamers provided by the software database, to have no molecular clashes with the residues of HLA-DQ8. Minimizations were carried out either at pH 5.4 (endosomal pH) or 7.4 (extracellular). There are no similarly charged residues (for example, Glu-Glu) with their charged groups so close to each other as to require that one of the residues be

uncharged. Occasionally runs were performed on a Silicon Graphics Octane instrument with previous releases of the same software with very similar results. Figures are drawn using the WebLabViewer v.3.5 and DSViewerPro software of Accelrys, the latter currently freely available on the web. In the figures a side view of the bound peptide with the eye level placed at the level of the peptide backbone and parallel to the HLA-DQ β-sheet floor is visualized with an atomic colour code as in the respective figure legend. In the Supplementary Figures, the α1β1 domains of the modelled HLA-DQ molecules in complex with given bound peptides are depicted in van der Waals surface representation, with colour and depiction conventions identical to those for the other figures. Several visible residues from the HLA-DQ molecule in contact with the antigenic peptide and potential contact with a cognate TCR in canonical orientation are shown in stick form with a transparent surface (atomic colour code: oxygen, red; nitrogen, blue; hydrogen, white; carbon, orange; sulfur, yellow). The antigenic peptide in the groove is shown in space filling form with the same atomic colour code as in Figure 6D-G. Coordinates of all complexes shown in the various figures have been deposited in the Figshare repository under accession codes 1294716.

MD simulations

The simulated system consisted of the entire DQ8 molecule and the 13-residue peptide with the vinculin sequence Glu-Glu-Val-Phe-Asp-Glu-Arg-Ala-Ala-Asn-Phe-Glu-Asn. Titratable residues were assigned their most common ionization state at physiological pH, with the exception of DQ8 residue αGlu31, which was protonated. In the crystallographic structure of the DQ8:insulin complex, residues αGlu31 and βGlu86 are in direct contact[42] and their geometry and interactions with nearby residues and a crystallographic water suggest that at least one of them is protonated. A similar conclusion was reached for a pair of Glu and Asp residues in the pocket P6 of DR and I-E molecules[44]. We used the empirical model Propka[45] and a constant-pH Monte Carlo approach implemented in the program PROTEUS[46] to compute the pK of titratable groups in the crystallographic structure of HLA-DQ8, both in the absence and the presence of the peptides insulin and VCL-DERAA. Both methods agreed that the residues αGlu31 and βGlu86, near pocket P1, are strongly correlated; the predicted pKa values suggested that one of them should be protonated, most probably αGlu31.

The initial coordinates of the protein heavy atoms were taken from the crystallographic structure of the DQ8:insulin complex (PDB accession code 1JK8)[42]. The peptide main chain heavy atoms were placed at the corresponding coordinates of the insulin main chain. Hydrogens were positioned by the HBUILD algorithm of the CHARMM programme[47]. The peptide side chain initial conformations were optimized with the program PROTEUS[45]. An additional control simulation studied the DQ8:insulin complex; for this system, the initial coordinates of the protein and peptide were taken from the corresponding crystallographic structure (PDB accession code 1JK8)[42].

The initial set-up of the simulation system was performed with the CHARMM- GUI interface[48]. A total of 70 crystallographic waters of the DQ8:insulin complex were retained. For the vinculin

complex, crystallographic waters were minimized for 100 steps before the simulation, with the protein and peptide atoms kept fixed. The ligand complexes were immersed in a periodically replicated water box with the shape of a 117-Å truncated octahedron. Overlapping water molecules were omitted and 17 potassium anions were added (14 ions in the insulin complex), to neutralize the total charge. The final complex had 120,324 atoms (6,166 protein- ligand atoms); the insulin complex had 120,504 atoms (6,172 protein-ligand atoms).

The simulations employed the molecular mechanics program CHARMM c37b2 (ref. 47). Protein atomic parameters were taken from the CHARMM36 all-atom force field with a CMAP backbone phi/psi energy correction[49,50]. Water parameters corresponded to the modified TIP3P water model[51,52]. Electrostatic interactions were calculated without truncation by the particle-mesh Ewald method[53], with a parameter $\kappa = 0.34$ for the charge screening, and sixth-order splines for the mesh interpolations. The Lennard-Jones interactions between atom pairs were switched to zero at a cutoff distance of 12Å. The temperature was kept at $T =$ 300 K by a Nose-Hoover thermostat[54] with a mass of 2,000 kcal mol^{-1}ps^{-2} for the thermostat. The pressure was maintained at $P = 1$ atm with a Langevin piston[55,56]. The piston mass was set to 1/20 of the total mass of the system and the collision frequency was set to 20 ps^{-1}. The classical equations of motion were solved by the leap-frog integrator. Bond lengths to hydrogen atoms and the internal water geometry were constrained to standard values via the SHAKE algorithm[57], implemented into CHARMM.

The structure was initially optimized by 100 energy minimization steps with the steepest-descent and adopted-basis Newton-Raphson algorithms. This was followed by an equilibration run, consisting of three 200-ps segments, in which the harmonic force constants were gradually lowered from 10 to 0 kcalmol^{-1}Å^{-2}. The production simulation had a duration of 3 ns (vinculin complex) and 4 ns (vinculin complex with ionized αGlu31 and insulin complex). A total of 300 and 400 snapshots were analysed for the vinculin- and insulin-DQ8 complex, respectively, extracted every 10 ps. All simulations were conducted with version c37b2 of the CHARMM programme[47]. Hydrogen bond occupancies and averaged intermolecular interaction energies were computed by in-house scripts. Molecular visualization was performed using the program VMD[58].

The interaction energies of selected peptide-protein residue pairs were computed by the following equation[59,60].

$$\Delta G_{RR'}^{inte} = \underbrace{\sum_{i\in R}\sum_{j\in R'}\left(E_{ij}^{Coul}+E_{ij}^{GB}\right)}_{\Delta G_{RR'}^{polar}} + \underbrace{\sum_{i\in R}\sum_{j\in R'}E_{ij}^{vW} + \sigma\sum_{i\in R,R'}S_i}_{\Delta D_{RR'}^{nonpolar}}$$

The first and second group of terms on the right-hand side of equation (1) describe, respectively, polar and non-polar interactions between R and R'; 'Coul' denotes Coulombic interaction, 'GB' denotes generalized born interaction, ΔS_i is the change in the solvent accessible surface area of atom on binding and σ is a surface tension coefficient. The residue-

pair interaction energies of equation (1) include solvent-mediated effects via the above GB and surface area terms. In the calculations of Supplementary Figure 15, R and R' are distinct ligand and protein residues.

We employed the GBSW Generalized Born model[61,62], as implemented in the CHARMM programme. The coefficient σ was set to 0.005 kcal mol^{-1}Å^{-2}, for consistency with the GBSW parameterization. To compute the GB contributions, we removed all waters and ions from the simulation system and set the charge to zero for protein and peptide atoms other than those belonging to residues R and R', respectively. The last term contains the difference in solvent accessible surface areas of groups R and R' in the complex and unbound states. Coordinates of all complexes shown in the various figures have been deposited in the Figshare repository under accession code 1294716.

RESULTS

Citrullinated vinculin is a novel target for ACPA

We speculate that the protective effects of HLA-DRB1*13 on the development of ACPA+ RA are related to a T cell response reactive to a sequence that is commonly present in the HLA-DRB1*13 molecule, microorganisms and self-proteins that are targeted by ACPA. Indeed, a 5 amino acid long HLA-DRB1*13-derived sequence (DERAA) is present in many microorganisms and a few self-proteins. Of these self-proteins, the citrullinated protein vinculin attracted our attention. Therefore, we first analysed whether citrullinated vinculin is recognized by ACPA. To this end, we citrullinated vinculin *in vitro* with PAD enzymes and tested both native and citrullinated vinculin for recognition with serum of an ACPA+ RA patient. We observed citrulline-specific recognition of vinculin by serum of an ACPA+ RA patient, but not with an ACPA- patient (Figure 1A). We further confirmed that citrullinated vinculin is a target of ACPA using an ACPA monoclonal antibody (Figure 1B)[28].

Recently, several reports showed the presence of citrullinated vinculin in the synovial fluid of ACPA+ RA patients. In addition, three sites of *in vivo* citrullination on this protein were identified: Arg285, Arg622 and Arg823 [4,23]. When we studied antibody responses to these citrullination sites, we could show recognition by 34% of tested sera from ACPA+ RA patients versus 5% of sera from ACPA- patients (Figure 1C). Sera of ACPA+ RA patients are highly (cross-)reactive towards multiple citrullinated antigens. Indeed, when we quantified responses to citrullinated alpha-enolase, fibrinogen, vimentin and myelin basic protein in patient sera that react to citrullinated vinculin peptides, we could readily demonstrate additional reactivities indicating at ACPA are not exclusively directed against citrullinated vinculin as expected (Figure 1D).

Together these data show that citrullinated vinculin is a self-protein recognized by RA autoantibodies in a citrulline-dependent fashion.
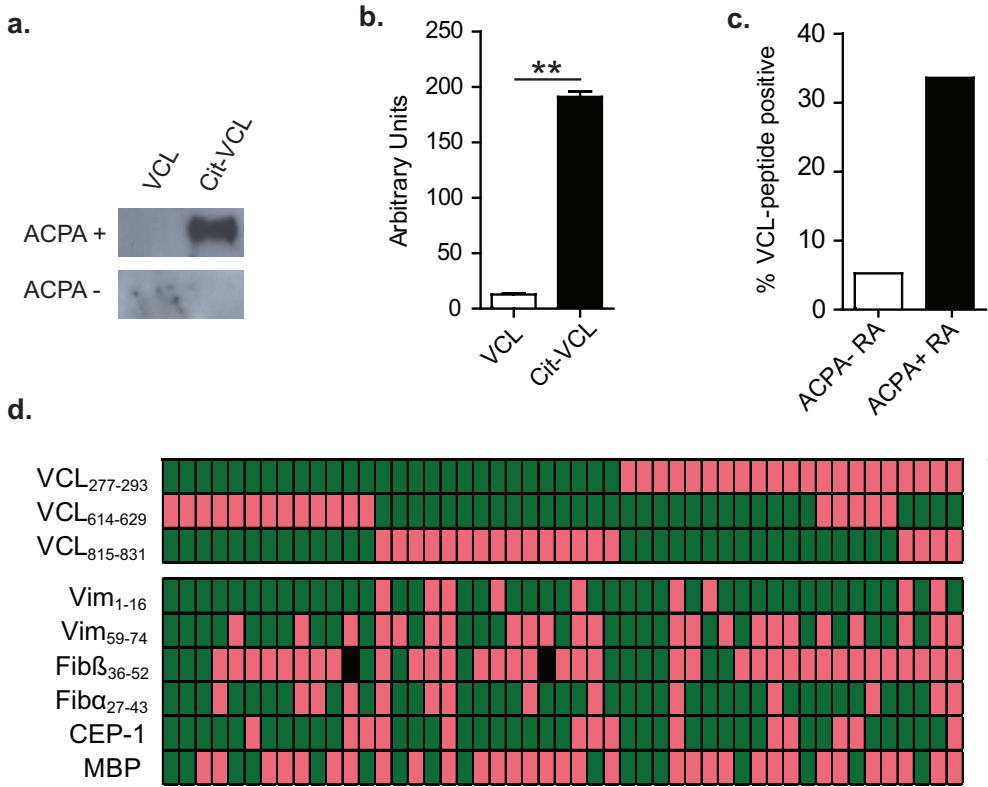
Figure 1. Citrullinated vinculin is a novel autoantigen targeted by ACPA. (A) Western blot (Supplementary Figure 22) of native and citrullinated vinculin protein, stained with the serum of an ACPA+ or an ACPA- RA patient. (B) Enzyme-linked immunosorbent assay (ELISA) of vinculin- or citrullinated vinculin protein-coated plates stained with ACPA monoclonal antibody anti-citFib1.1. Two-sided statistical analysis was performed using a Student's t-test with ** indicating P<0.001. Error bar is S.E.M (C) ELISA of citrullinated vinculin peptides VCL-CIT285$_{277-293}$, VCL-CIT6 22$_{614-651}$, VCL-CIT82 3$_{815-831}$ in serum of anti-CCP2$^+$ (n = 140) versus anti-CCP2$^-$ (n = 38) RA patients. Plot depicts the percentage of patient sera positive for one or more citrullinated vinculin peptides. (D) Heat map depicting all patients positive for one or more citrullinated vinculin epitopes (n = 49) and their serum reactivity towards different citrullinated epitopes derived from vimentin, fibrinogen and alpha-enolase. Red, positive; green, negative; black, undetermined. Error bars are S.E.M.

Vinculin is recognized by T cells from HLA-DRB1*13 negative donors

We next wished to determine whether the DERAA sequence from vinculin is recognized by human CD4+ T cells. To this end, peripheral blood mononuclear cells (PBMCs) were stimulated with a 15-mer vinculin-peptide (VCL$_{622-636}$, REEVFDERAANFENH) (VCL-DERAA) for 24h. We observed a clear reactivity towards this epitope as determined in an interferon-γ (IFNγ)-ELISPOT-assay (Supplementary Figure 1). HLA-DRB1*13, especially HLA-DRB1*13:01, is strongly associated with protection against ACPA+ RA[17]. We hypothesize that HLA-DRB1*13 protects against ACPA+ disease by affecting the generation of DERAA-directed T cells. Therefore, we stratified donors for HLA-DRB1*13:01 status. We observed a striking difference

in IFNγ-producing cells depending on HLA-DRB1*13:01-status. The lack of reactivity in HLA-DRB1*13:01-positive donors was not due to a hampered ability of such donors to respond to T cell antigens as we observed strong response to microbial antigens in both HLA-DRB1*13:01 carriers and non-carriers when stimulated with recall antigens (Figure 2A). We further confirmed this finding in PBMCs stimulated for 4 days (Supplementary Figure 2). The differential ability of HLA-DRB1*13:01-positive donors to respond to VCL-DERAA is most likely not due to a general deficiency to present the VCL-DERAA epitope as these donors were heterozygous and thus expressed other HLA molecules that could potentially present VCL-DERAA. Nonetheless, to further confirm that HLA-DRB1*13:01 affects the ability to generate VCL-DERAA-directed T cell responses, we repeated the experiments in a set-up stratified for HLA using PBMCs from HLA-DRB1*04, HLA-DRB1*13:01 and HLA-DRB1*04/*13:01 heterozygous donors. A significant reduction in IFNγ-producing cells was observed in both HLA-DRB1*13:01 carriers and DRB1*04/*13:01 heterozygous donors as compared with HLA-DRB1*04 carriers. Again, no difference was observed for recall antigens (Figure 2B). These data indicate that the lack of detecting VCL-DERAA-directed T cells is not explained by the inability of HLA-DRB1*13 molecules to present VCL-DERAA, but rather the result of a dominant effect associated with the presence of HLA-DRB1*13.

Thus, vinculin is an autoantigen recognized by circulating VCL-DERAA-directed CD4+ T cells. In HLA-DRB1*13:01 carriers these T cells are absent. This effect, like the protective effects of HLA-DRB1*13:01 on the development of ACPA+ RA, was present in a dominant fashion, consistent with the notion that HLA-DRB1*13 affects the generation of DERAA-directed T cells, possibly during thymic selection.
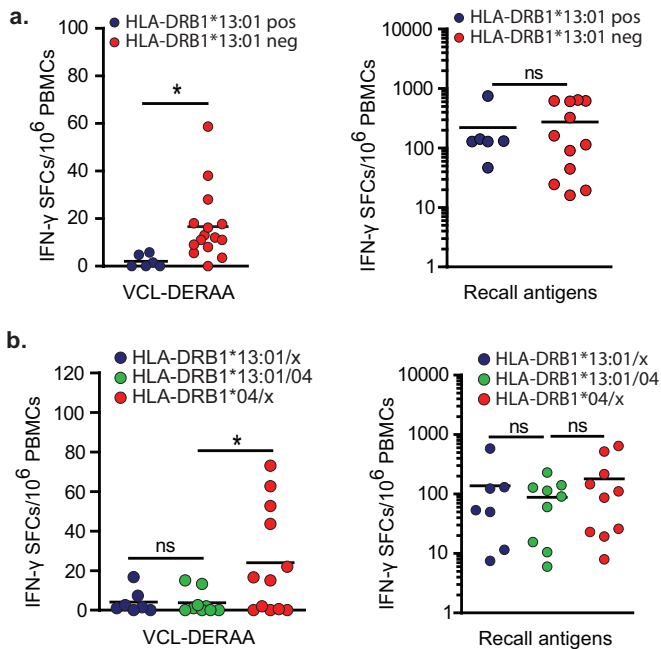

Figure 2. Citrullinated vinculin is a novel autoantigen targeted by CD4+ T cells in HLA-DRB1*13-negative donors. (**A**) IFNγ ELISPOT of PBMCs from healthy individuals stimulated for 24h with VCL-DERAA peptide REEVFDERAANFENH (*n* = 21) or with a mix of recall antigens (tetanus, tuberculin, candida, *n* = 18). Donors were stratified based on HLA-DRB1*13:01 status. (**B**) IFNγ ELISPOT of PBMCs of HLA-DRB1*13:01 carriers (*n* = 7), HLA-DRB1*04 carriers (*n* = 12) and HLA-DRB1*13:01/DRB1*04 donors (*n* = 9), stimulated for 24 h with VCL-DERAA peptide or with a mix of recall antigens. Each dot represents a unique donor. Two-sided statistical analyses of ELISPOT data were performed using a Mann-Whitney U-test with * indicating *p*<0.05. Neg, negative; NS, not significant; Pos, positive

2

Presentation of Vinculin-DERAA by RA-predisposing HLA-DQ molecules

HLA-DRB1 alleles predisposing to ACPA+ RA in the Caucasian population are collectively called HLA shared epitope (SE) alleles[14,15,29]. The most common HLA-SE alleles are HLA-DRB1*04:01 and HLA-DRB1*01:01. Using HLA-DR-binding assays, we examined the ability of VCL-DERAA to bind to these HLA molecules, but we could not detect any binding of VCL-DERAA to these alleles (Table 1, Supplementary Figure 3A, 3B). The HLA class II region is known for its strong LD. Genes that encode for the HLA-DR-beta chains are inherited in haplotypes with genes that encode for the alpha and beta chain of HLA-DQ. The predisposing HLA-SE alleles are in tight LD with HLA-DQ5 (DQA1*01;DQB1*05:01), HLA-DQ7.3 (DQA1*03:02;DQB1*03:01) and HLA-DQ8 (DQA1*03:01;DQB1*03:02) (Figure 3A, 3B). In Figure 3B, the distribution of HLA-DQ molecules in SE+ healthy donors is depicted, showing that these donors are HLA-DQ5-, HLA-DQ7.3- or HLA-DQ8-positive. We therefore next studied the binding of VCL-DERAA to these HLA-DQ alleles and observed binding of the VCL-DERAA peptide to HLA-DQ5, DQ7.3 and DQ8 (Table 1, Supplementary Figure 3C-E). These data indicate that VCL-DERAA can be presented by HLA-DQ molecules in LD with predisposing HLA-SE alleles.

To obtain an indication whether the VCL-DERAA can be presented by more HLA molecules, we also studied the ability of additional HLA-DR and HLA-DQ molecules encoded by HLA haplotypes that protect or have no influence on the development of ACPA+ RA. We could not detect binding of VCL-DERAA to these HLA class II alleles (Table 1, Supplementary Figure 3F-K). Likewise, using an IFNγ ELISPOT, VCL-DERAA-directed T cells were absent in donors negative for predisposing HLA-DQ molecules (Supplementary Figure 4).

These data indicate that HLA-DQ molecules that predispose to ACPA+ disease present the VCL-DERAA peptide, whereas the analysed HLA-DQ and HLA-DR molecules not associated with disease do not present VCL-DERAA.
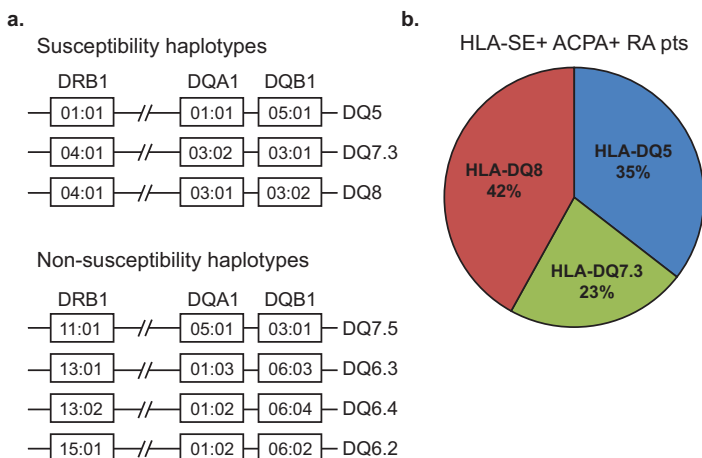

Figure 3. Presentation to vinculin-DERAA-directed T cells is restricted to RA-predisposing HLA-DQ molecules. (A) Schematic representation of the LD between the HLA-DRB1, HLA-DQA1 and HLA-DQB1 gene in studied haplotypes associated or not associated with susceptibility to ACPA+ RA. (B) Distribution of HLA-DQ molecules in ACPA+ RA patients positive for HLA-DR SE alleles (*n* = 31).

Table 1 | Presentation to vinculin-DERAA-directed T cells is restricted to RA-predisposing HLA-DQ molecules.

Assocation	Subtype	HLA allele	IC50 (μM)
Susceptibility haplotypes	HLA-DR	DRB1*01:01	>300
		DRB1*04:01	>300
	HLA-DQ	DQ5	39
		DQ7.3	11
		DQ8	14
Non-susceptibility haplotypes	HLA-DR	DRB1*13:01	>300
		DRB1*13:02	>300
	HLA-DQ	DQ6.2	>300
		DQ6.3	>300
		DQ6.4	>300
		DQ7.5	>300

Affinity of VCL-DERAA for associated HLA class II molecules. Affinity was determined by a competitive binding assay using high-affinity biotinylated peptides. Results are depicted as IC50 value, the concentration of test peptide (μM) where 50% of biotinylated peptide is bound. Experiments were performed at least three times and the average IC50 value between the different experiments is shown.

Table 1. Presentation of vinculin-DERAA-directed T cells is restricted to RA-predisposing HLA-DQ molecules. Affinity of VCL-DERAA for associated HLA class II molecules. Affinity was determined by a competitive binding assay using high-affinity biotinylated peptides. Results are depicted as IC50 value, the concentration of test peptide (μM) where 50% of biotinylated peptide is bound. Experiments were performed at least three times and the average IC50 value between the different experiments is shown.

HLA-DQ-restricted recognition of VCL-DERAA by T cells

To further confirm the presence of VCL-DERAA-directed T cells and their HLA-restriction, we isolated CD4+ T cell clone JPT57, which was specific for VCL-DERAA. As shown in Supplementary Figure 5, this clone proliferated readily and produced large amounts of IFNγ when stimulated with the VCL-DERAA peptide.

When cultured with B cells from ACPA+ RA patients pulsed with the VCL-DERAA epitope, the clone not only upregulated CD40L, but also enhanced the production of ACPA in culture, indicating that such T cells have a phenotype compatible with the ability to provide 'help' to ACPA-producing B cells (Supplementary Figure 6).

To further confirm that HLA-DQ molecules present the VCL-DERAA peptide, we stimulated the clone with VCL-DERAA-pulsed HLA-typed antigen-presenting cells preincubated with HLA class II blocking antibodies (Supplementary Figure 7). In concordance with the binding studies, anti-HLA-DQ antibodies abrogated T cell recognition. Interestingly, we observed that JPT57 can recognize VCL-DERAA, presented by both HLA-DQ7.3 and HLA-DQ8 suggesting that this epitope is presented in a similar binding register by these HLA molecules (Supplementary Figure 8).

Together HLA class II presentation and T cell recognition of VCL-DERAA was restricted to HLA-DQ molecules that are associated with RA susceptibility.

Identification of microbe-specific T cells targeting DERAA epitopes

We next investigated the presence of the DERAA sequence in microorganisms. A Blast search showed that DERAA is found in 66% of bacteria and 4% of viruses (Figure 4A). This large number represents a major challenge to identify potential 'crossreactive microorganisms'. To select for relevant microorganisms, we restricted the search to those microorganisms that can cause disease or symptoms in humans and are present in the western world. This approach
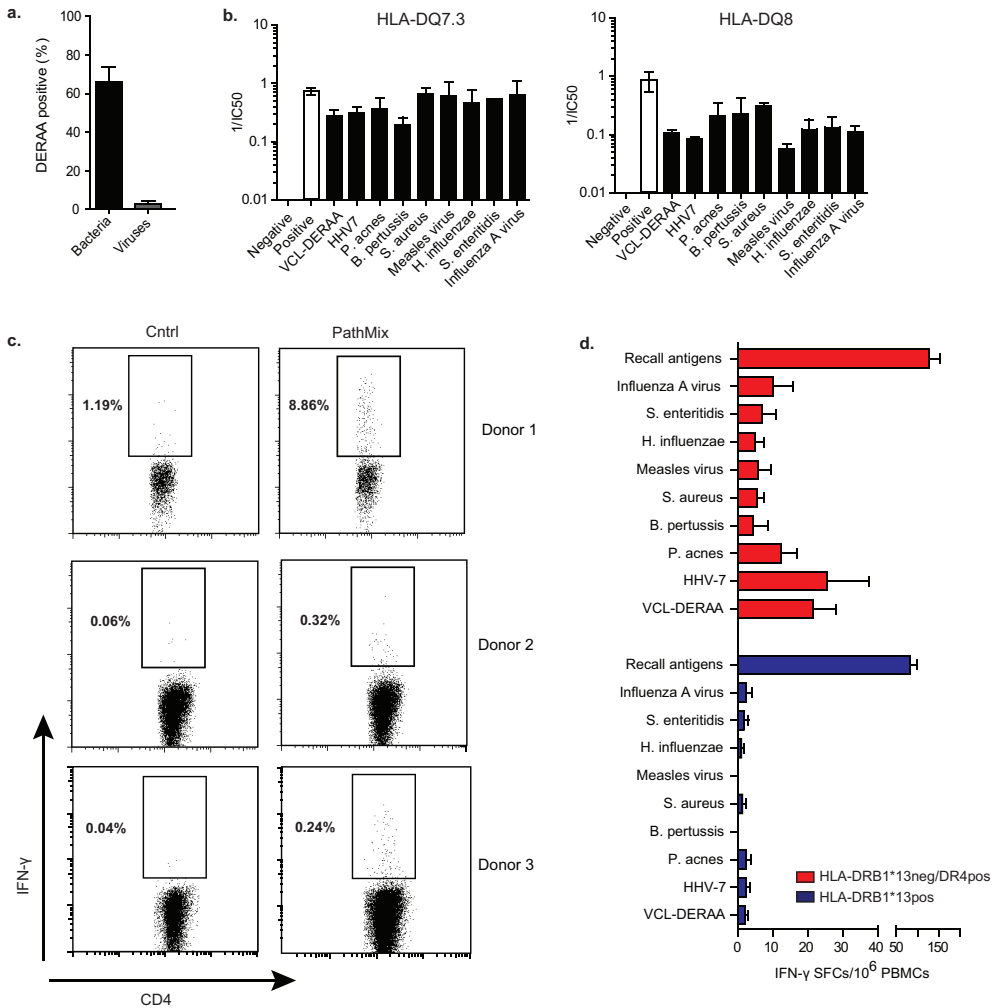
Figure 4. Identification of pathogen-specific T cells targeting DERAA epitopes in HLA-DRB1*13 negative donors.
(A) Frequency of bacteria or viruses positive for a DERAA-containing protein as identified using the NCBI BLAST. List of all bacteria or viruses in blast database was generated and for three random sets of 50 bacteria/viruses a blast search for DERAA was performed. Error bars indicate the S.D. between the three analysed sets. (B) Competitive binding of pathogen-derived DERAA epitopes to HLA-DQ7.3 or HLA-DQ8. Binding experiments were performed at least three times and plots show pooled experiments, the error bars show the variation between the different experiments. (C) Flow cytometry staining of PathMix-directed T cell lines restimulated with PathMix pulsed or unpulsed antigen-presenting cells. Plots are gated on CD14neg/CD4pos/CD25pos T cells. (D) ELISPOT of PBMCs of healthy individuals of HLA-DRB1*13:01 donors (*n* = 5) and HLA-DQ7.3/DQ8 donors (*n* = 8) stimulated for 24h with DERAA-containing peptides and recall antigens. Error bars indicate the variation between different donors. Error bars are S.E.M.

left us with 219 candidate sequences. We then synthesized eight DERAA-containing peptides from common recall microbes including several bacteria (*P. acnes, S enteritidis, B. pertussis, S. aureus*) and viruses (measles virus, influenza A and human herpesvirus 7). Interestingly, all of these peptides were presented by HLA-DQ7.3 and DQ8 molecules showing that these
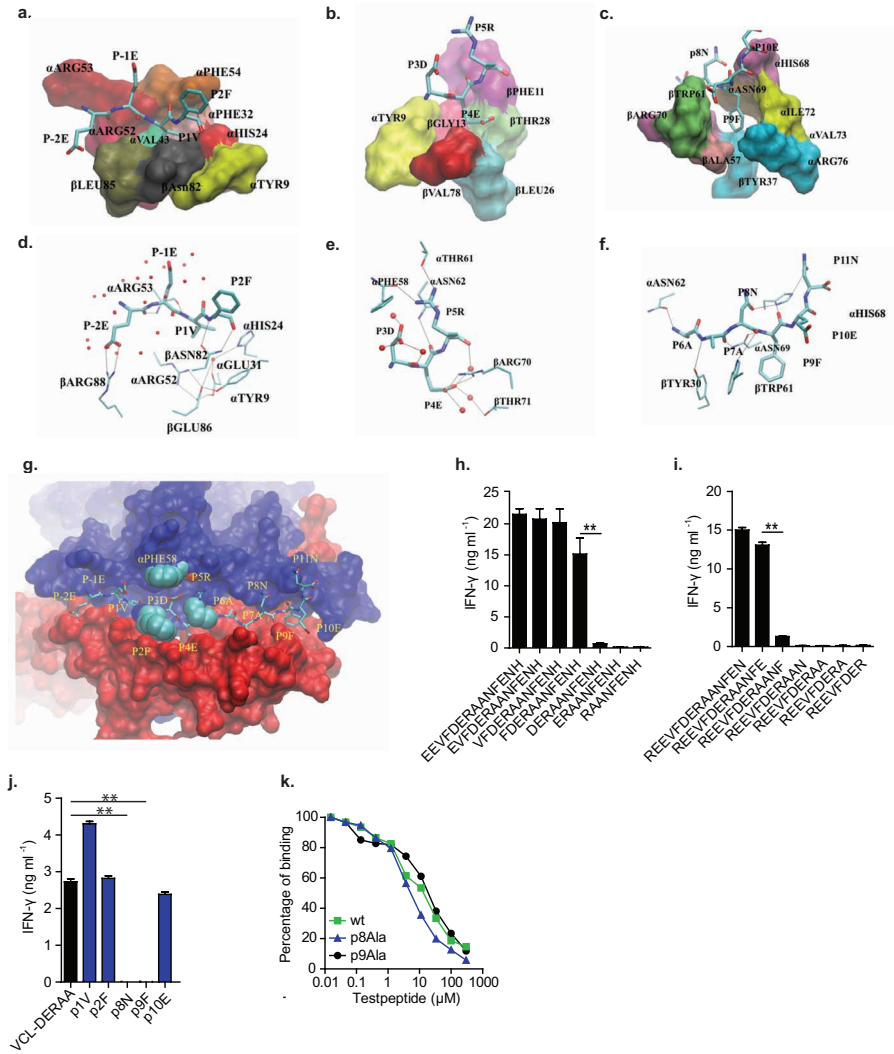
HLA molecules can efficiently accommodate both the VCL-DERAA epitope as well as microbe-derived DERAA epitopes (Figure 4B).

To determine whether these microbial-derived epitopes are recognized by human T cells, we generated T cell lines by stimulating PBMCs from three healthy HLA-DQ8-positive donors for 7 days with a pool of the eight pathogen-derived peptides (PathMix). Next we determined the presence of PathMix-specific CD4+ IFNγ-producing T cells. As shown in Figure 4C, such T cells were readily detectable. Using limiting dilutions, we isolated T cell clone D2C18, further confirming the presence of 'microbial-DERAA-directed' T cells (Supplementary Figure 9). Next we also analysed the presence of 'microbial-DERAA- directed' T cells by ELISPOT directly *ex vivo,* allowing the analyses of more donors at higher throughput. Interestingly, PBMCs from HLA-DRB1*13:01 carriers displayed a significantly reduced reaction against these peptides, indicating that the presence of HLA-DRB1*13 also affects the formation of T cell responses against DERAA epitopes from microbes (Figure 4D).

Together these data indicate that HLA-DQ alleles associated with ACPA+ RA efficiently present both VCL-DERAA and microbe-derived DERAA epitopes and that microbe-specific T cells directed to DERAA epitopes are readily detected. The presence of HLA-DRB1*13:01 affects the formation of these T cell responses.

Predicting crossreactive microbes by modelling vinculin-DERAA presentation

The data presented above demonstrate the presence of microbial- and VCL-DERAA-directed T cells, but do not show if a single T cell receptor (TCR) can react with both epitopes. To facilitate the search for possible 'crossreactive' DERAA epitopes out of all microbe-derived DERAA sequences, we first determined the binding register of VCL-DERAA using HLA class II-binding assays with amino (N)- and carboxyl (C)- terminally truncated and amino-acid-substituted VCL-DERAA peptides as detailed in the Supplementary Note and in Supplementary Figures 10-14. Together these experiments support **V**FD**E**R**AA**N**F** (anchors in bold) as the core binding register for both HLA-DQ7.3 and HLA-DQ8. All-atom molecular dynamics (MD) simulations showed that residues Val625 (P1), Glu628 (P4) and Phe633 (P9) make numerous intermolecular polar and non-polar interactions in the respective pockets. In Figure 5A-F, we highlight key intermolecular interactions between the VCL-DERAA epitope and the HLA-DQ8 molecule. A detailed discussion of the MD results and a quantitative assessment of the intermolecular interactions can be found in the supplementary data (Supplementary Figures 15 and 16, Supplementary Table 1 and Supplementary Note). The MD simulations also indicated that the long protruding side chains of Glu623 (P-2) Glu624 (P-1), Phe626 (P2), Asp627 (P3), Arg629 (P5), Asn632 (P8), Glu634 (P10) and Asn635 (P11) are exposed and could potentially interact with crossreactive TCRs (Figure 5G). Subsequently, we also further confirmed the obtained model using a second type of molecular modelling: energy minimization, which further confirmed possible TCR-contact residues (Supplementary Figures 17 and 18).

Figure 5. Molecular modelling of HLA:VCL-DERAA complexes identifies critical TCR-contact residues. (A-C) Non-polar contacts between the VCL-DERAA peptide and HLA-DQ8 in pockets P1 (A), P4 (B) and P9 (C). Protein residues are depicted in a surface representation, in distinct colours. (D-F) Hydrogen bonds between the VCL-DERAA peptide and HLA-DQ8 in pockets P1 (D), P4 (E) and P9 (F). Peptide and protein groups are shown, respectively, in thick and thin licorice representation and water molecules as small spheres. Hydrogens are omitted, with the exception of the extra hydrogen in protonated aGlu31. (G) TCR view of the DQ8:VCL-DERAA complex. The peptide main chain is shown in licorice; domains α and β are shown in a surface representation, coloured, respectively, in blue and red. Side chains P-2E, P-1E, P2F, P3D, P5R, P8N, P10E and P11N are facing towards the TCR-binding site. The P2F and αPhe58 side chains and the non-polar moiety of P5R form a non-polar cluster, which faces towards the TCR-binding site; the average P2F ring-αPhe58 ring distance is ~8Å. (H-J) IFNγ ELISA on supernatant of T cell clone JPT57 stimulated with unpulsed HLA-DQ8-positive antigen-presenting cells and N-truncated (H), C-truncated (I) or alanine-substituted (J) VCL-DERAA peptides. (K) Competitive binding of the VCL-DERAA peptide, and alanine-substituted VCL-DERAA peptides to HLA-DQ8. Binding experiments were performed at least three times and plots show pooled experiments, the error bars show the variation between the different experiments. Experiments involving JPT57 were performed three times and show a representative experiment. Two-sided statistical analysis was performed using a Student's t-test with ** indicating $p<0.001$. Error bars are S.E.M.

To functionally confirm whether a TCR would indeed interact with (some of the) potential TCR-contact residues within the VCL-DERAA peptide, we next determined how the epitope is recognized by the VCL-DERAA-directed T cell clone JPT57. Phe626 (P2) interacts with the JPT57-TCR as its removal results in a large decrease in recognition without affecting HLA-DQ8 binding. (Figure 5H, Supplementary Figure 12). C-terminal truncations resulted in a large decrease in T cell recognition after the removal of Glu634 (P10), showing that this residue is also important for JPT57-TCR interaction (Figure 5I). Thus, the data obtained using the VCL-DERAA-directed T cell clone as a functional read-out, are in line with the HLA-binding and molecular modelling studies indicating the sequence **V**FD**E**R**AA**N**F**E (anchors in bold) as the minimal epitope required for activation of JPT57. Next we performed alanine substitutions within the minimal epitope to remove critical TCR-interacting residues. Substituting Asn632 (P8) and Phe633 (P9) dramatically impacted T cell recognition, without affecting the binding affinity of VCL-DERAA (Figure 5J, 5K).

Together these data indicate **V**FD**E**R**AA**N**F** (anchors in bold) as the most likely core binding register for HLA-DQ7.3 and HLA-DQ8 and Asn632 and Phe633 as important residues for JPT57-TCR recognition.

TCR crossreactivity between vinculin and bacterial antigens

Identifying microbes that crossreact with vinculin was challenging due to the large number of potential candidates. Therefore, we used the data presented above to determine if a single TCR can crossreact both to DERAA sequences from microbes and the self-protein vinculin.

As we identified the Asn632 and Phe633 at P8 and P9, respectively, as important for JPT57-TCR interactions, we use the molecular modelling to predict which viral and bacterial epitopes are likely to bind to HLA-DQ8 and harbor P8Asn or P9Phe and are thus likely to crossreact with JPT57. From the 15 peptides identified (Supplementary Table 2), three were able to activate JPT57 in a T cell stimulation assay at concentrations similar to those used for the vinculin peptide. These epitopes were derived from *Campylobacter coli, Lactobacillus curvatus* and *Lactobacillus sakei* and crossreacted with JPT57 in an HLA-DQ-dependent manner (Figure 6A). Peptide-binding studies revealed that these three peptides bind with an intermediate binding affinity to HLA-DQ7 and HLA-DQ8 (Figure 6B-6C). Molecular models of these bacterial peptides in HLA-DQ8 illustrate the similarities with VCL-DERAA (Figure 6D-G, Supplementary Figures 19-21).

Thus, these data show that the RA-susceptibility alleles HLA-DQ7 and HLA-DQ8 can present both VCL-DERAA and related microbe-derived epitopes to T cells and that such T cells can be crossreactive to vinculin and bacterial epitopes, thereby providing an explanation for the presence of activated self-reactive CD4+ T cells directed to vinculin in peripheral blood.
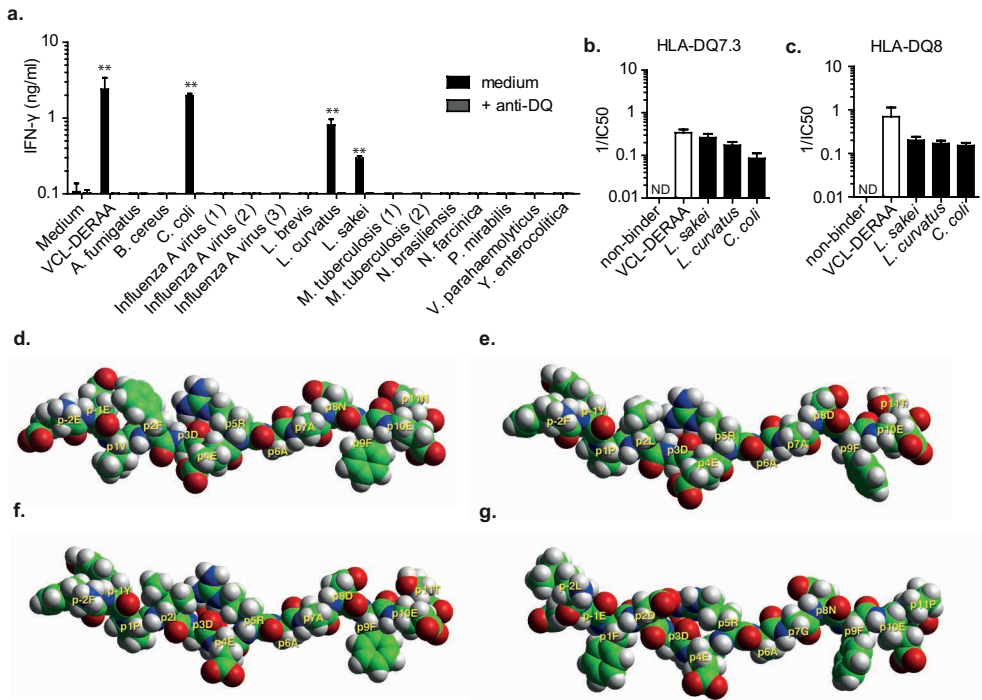
Figure 6. TCR crossreactivity of vinculin and bacterial DERAA epitopes. (A) IFNγ ELISA on supernatant of T cell clone JPT57 stimulated with HLA-DQ8-positive B-LCLs and alanine-substituted VCL-DERAA peptides. This experiment was performed three times, the plot shows a representative experiment. Two-sided statistical analysis was performed using a Student's t-test with * indicating *p*<0.05 and ** indicating *p*<0.001. (B-C) Competitive binding of HLA-DQ7.3 (B) and HLA-DQ8 (C) to a non-binding negative control peptide, an unbiotinylated positive control peptide and epitopes from *Lactobacillus curvatus*, *Lactobacillus sakei* and *Campylobacter coli*. Binding experiments were performed three times. The error bars show the variation between the different experiments. (D-G) Side views of HLA-DQ8 complexed with the vinculin-DERAA peptide (D) and peptides derived from *Lactobacillus curvatus* (E), *Lactobacillus sakei* (F) and *Campylobacter coli* (G) in space-filling mode at pH 7.4 (extracellular), obtained by energy minimization as described in the methods section. Each peptide is shown in atomic colour code: oxygen, red; nitrogen, blue; hydrogen, white; carbon, green; sulfur, yellow. Error bars are S.E.M.

DISCUSSION

The strong connection between the HLA locus and RA has been known for more than 35 years. The complex HLA class II associations and the diverse ACPA responses in RA patients suggest the presence of multiple aetiological pathways. To unravel these pathways, identifying the relevant autoantigens is crucial. We here present evidence favouring the involvement of vinculin in the emergence of ACPA+ disease. This cytoskeletal protein was recently found to be citrullinated *in vivo* in the synovial fluid. We now show that it is recognized by ACPA as well, thereby adding it to a still selective list of targets. Moreover, we identified an epitope from vinculin recognized by CD4+ T cells restricted to HLA-DQ molecules predisposing to ACPA+ RA. The core amino-acid sequence (DERAA) is also present in many pathogens and in HLA-DRB1*13, a molecule encoded by an HLA locus associated with protection against ACPA+ RA.

We have also shown that a single TCR can recognize both a vinculin-DERAA epitope as well as DERAA epitopes from microbes, indicating the crossreactive nature of 'DERAA'-directed T cell responses. More importantly, such T cell responses appear absent from donors carrying HLA-DRB1*13 as DERAA-directed T cell responses to either pathogen- or vinculin-derived DERAA epitopes were lacking in these subjects. Even donors that harboured HLA-DRB1*13 next to predisposing HLA alleles were unable to respond to vinculin-DERAA.

Together these data indicate a novel pathway that explains several of the protective and predisposing HLA-effects associated with ACPA+ RA (Figure 7). In short, recognition of citrullinated vinculin by B cells will lead to the presentation of the 'VCL-DERAA' epitope in the context of HLA class II molecules. The HLA-DQ molecules genetically linked to the predisposing HLA-SE-molecules are particularly good in presenting DERAA-containing peptides. The DERAA-directed T cells primed against various pathogens harbouring DERAA-containing proteins cross-react with the VCL-DERAA peptide and provide help to the B cells, ultimately leading to a strong ACPA response. Subjects born with HLA-DRB1*13, will present the HLA-DRB1*13-derived DERAA-peptide in the thymus, leading to tolerization of the DERAA-directed T cell response and hence the inability to provide help to ACPA-producing B cells via this pathway and thereby the emergence of ACPA+ RA (Figure 7).

The variation of HLA-DR and HLA-DQ molecules in the human population is enormous. We have shown that predisposing HLA-DQ molecules are particularly good at presenting the VCL-DERAA epitope. Interestingly, the absence of VCL-DERAA affinity for a wide variety of other tested HLA-DR or HLA-DQ molecules could indicate a selective presentation by these HLA risk molecules. Next to a role of predisposing haplotypes, we also focussed on the protective effect of HLA-DRB1*13 alleles. However, the DERAA sequence can also be found in other HLA-DRB1 alleles (*04:02, *11:02, *11:03), which are rare in Caucasian populations. These alleles have previously been implicated in protection from ACPA+ RA, but their allele frequency hampers functional studies[30-32]. Interestingly, it has been previously reported that the processing of these alleles results in the generation of a similar HLA-DERAA epitope suggesting that these alleles could all protect via the pathway that we have described[22].

The place in time at which HLA-DR13 mediates protection from the development of ACPA and/or ACPA+ disease, or its relation to epitope spreading of the ACPA response is currently not known and would be relevant to determine in future studies. Recent evidence showed that the ACPA response matures before disease onset and that the HLA system could be involved in this[13,33]. It is intriguing to speculate that infections such as by DERAA-containing microbes are involved in this expansion. Molecular mimicry of self-proteins with pathogenic proteins was proposed as a mechanism to break T cell tolerance, allowing the development of autoimmune disease[26,27]. Interestingly, the DERAA sequence is also present in proteins from many (common) microbes allowing priming of DERAA-directed T cells. In mouse models, it was shown that low-avidity T cells to tissue-restricted antigens can persist without signs of anergy and unresponsiveness. Infection lowers the threshold for T cell activation

resulting in the induction of autoimmunity and memory formation[34]. Infection could also induce autoimmunity via molecular mimicry of microbial proteins with self-proteins. We now identified crossreactive epitopes from the gut-residing bacteria *L. sakei, L. curvatus* and *C. coli.* It was shown that acute gastrointestinal infections can induce loss of T cell tolerance to (commensal) gut microbes, resulting in the activation of microbiota-specific T cells, their differentiation to inflammatory effector cells and formation of memory T cells[35]. A recent study on the fecal microbiota of RA patients compared with controls demonstrated a significant increase in *Lactobacillus* species, together providing a rationale for a role of such bacterial species in the formation of DERAA-directed T cell responses[36].

Together our study provides a mechanistic clue on the HLA-RA connection, including both predisposing and protective HLA effect, and warrants further studies addressing the possibility to target DERAA-directed T cells in the prevention of ACPA+ RA.
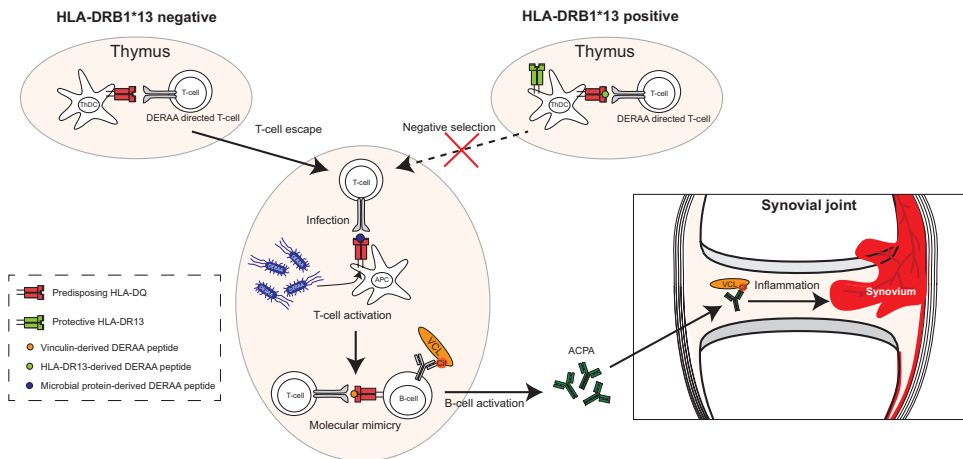

Figure 7. Schematic representation of the proposed role of DERAA-directed CD4+ T cells in ACPA+ RA. DERAA-directed T cells are restricted to RA-predisposing HLA-DQ5, -DQ7.3 and -DQ8 molecules. In carriers of these HLA-DQ molecules, DERAA-directed T cells can become activated on contact with microbes. These activated T cells can subsequently crossreact with a DERAA epitope derived from vinculin resulting in the activation of citrulline-directed B cells and the production of ACPA directed to citrullinated vinculin or vinculin-linked proteins. Citrullinated vinculin is present in the synovial compartment and is a target of ACPA. Binding of ACPA to its target can induce antibody-mediated effector mechanisms thereby contributing to synovial inflammation. In HLA-DRB1*13-positive individuals, a HLA-DRB1*13-derived DERAA epitope is presented by predisposing HLA-DQ molecules to CD4+ T cells resulting in their negative selection, thereby protecting against the development of ACPA+ RA.

REFERENCES

1. Schellekens, G. A., de Jong, B. A., van den Hoogen, F. H., van de Putte, L. B. & van Venrooij, W. J. Citrulline is an essential constituent of antigenic determinants recognized by rheumatoid arthritis-specific autoantibodies. J. Clin. Invest. 101, 273-281 (1998).

2. Girbal-Neuhauser, E. et al. The epitopes targeted by the rheumatoid arthritis-associated antifilaggrin autoantibodies are posttranslationally generated on various sites of (pro)filaggrin by deimination of arginine residues. J. Immunol. 162, 585-594 (1999).

3. Anzilotti, C., Pratesi, F., Tommasi, C. & Migliorini, P. Peptidylarginine deiminase 4 and citrullination in health and disease. Autoimmun. Rev. 9, 158-160 (2010).

4. van Beers, J. J. et al. The rheumatoid arthritis synovial fluid citrullinome reveals novel citrullinated epitopes in apolipoprotein E, myeloid nuclear differentiation antigen, and beta-actin. Arthritis Rheum. 65, 69-80 (2013).

5. Vossenaar, E. R. et al. The presence of citrullinated proteins is not specific for rheumatoid synovial tissue. Arthritis Rheum. 50, 3485-3494 (2004).

6. Ioan-Facsinay, A. et al. Anti-cyclic citrullinated peptide antibodies are a collection of anti-citrullinated protein antibodies and contain overlapping and non-overlapping reactivities. Ann. Rheum. Dis. 70, 188-193 (2011).

7. Amara, K. et al. Monoclonal IgG antibodies generated from joint-derived B cells of RA patients have a strong bias toward citrullinated autoantigen recognition. J. Exp. Med. 210, 445-455 (2013).

8. Snir, O. et al. Antibodies to several citrullinated antigens are enriched in the joints of rheumatoid arthritis patients. Arthritis Rheum. 62, 44-52 (2010).

9. van Gaalen, F. A. et al. Autoantibodies to cyclic citrullinated peptides predict progression to rheumatoid arthritis in patients with undifferentiated arthritis: a prospective cohort study. Arthritis Rheum. 50, 709-715 (2004).

10. Rantapaa-Dahlqvist, S. et al. Antibodies against cyclic citrullinated peptide and IgA rheumatoid factor predict the development of rheumatoid arthritis. Arthritis Rheum. 48, 2741-2749 (2003).

11. Huizinga, T. W. et al. Refining the complex rheumatoid arthritis phenotype based on specificity of the HLA-DRB1 shared epitope for antibodies to citrullinated proteins. Arthritis Rheum. 52, 3433-3438 (2005).

12. Verpoort, K. N. et al. Association of HLA-DR3 with anti-cyclic citrullinated peptide antibody-negative rheumatoid arthritis. Arthritis Rheum. 52, 3058-3062 (2005).

13. Willemze, A., Trouw, L. A., Toes, R. E. & Huizinga, T. W. The influence of ACPA status and characteristics on the course of RA. Nat. Rev. Rheumatol. 8, 144-152 (2012).

14. Stastny, P. Mixed lymphocyte cultures in rheumatoid arthritis. J. Clin. Invest. 57, 1148-1157 (1976).

15. Raychaudhuri, S. et al. Five amino acids in three HLA proteins explain most of the association between MHC and seropositive rheumatoid arthritis. Nat. Genet. 44, 291-296 (2012).

16. Shadick, N. A. et al. Opposing effects of the D70 mutation and the shared epitope in HLA-DR4 on disease activity and certain disease phenotypes in rheumatoid arthritis. Ann. Rheum. Dis. 66, 1497-1502 (2007).

17. van der Woude, D. et al. Protection against anti-citrullinated protein antibody-positive rheumatoid arthritis is predominantly associated with HLA- DRB1*1301: a meta-analysis of HLA-DRB1 associations with anti-citrullinated protein antibody-positive and anti-citrullinated protein antibody-negative rheumatoid arthritis in four European populations. Arthritis Rheum. 62, 1236-1245 (2010).

18. Feitsma, A. L. et al. Protective effect of noninherited maternal HLA-DR antigens on

2

rheumatoid arthritis development. Proc. Natl Acad. Sci. USA 104, 19966-19970 (2007).

19.   Chicz, R. M. et al. Predominant naturally processed peptides bound to HLA- DR1 are derived from MHC-related molecules and are heterogeneous in size. Nature 358, 764-768 (1992).

20.   Collado, J. A. et al. Composition of the HLA-DR-associated human thymus peptidome. Eur. J. Immunol. 43, 2273-2282 (2013).

21.   Adamopoulou, E. et al. Exploring the MHC-peptide matrix of central tolerance in the human thymus. Nat. Commun. 4, 2039 (2013).

22.   Snijders, A. et al. An HLA-DRBl-derived peptide associated with protection against rheumatoid arthritis is naturally processed by human APCs. J. Immunol. 166, 4987-4993 (2001).

23.   Romero, V. et al. Immune-mediated pore-forming pathways induce cellular hypercitrullination and generate citrullinated autoantigens in rheumatoid arthritis. Sci. Transl. Med. 5, 209ra150 (2013).

24.   di Marzo Veronese, F. et al. Autoreactive cytotoxic T lymphocytes in human immunodeficiency virus type 1-infected subjects. J. Exp. Med. 183, 2509-2516 (1996).

25.   Propato, A. et al. Apoptotic cells overexpress vinculin and induce vinculin- specific cytotoxic T cell cross-priming. Nat. Med. 7, 807-813 (2001).

26.   Oldstone, M. B., Nerenberg, M., Southern, P., Price, J. & Lewicki, H. Virus infection triggers insulin-dependent diabetes mellitus in a transgenic model: role of anti-self (virus) immune response. Cell 65, 319-331 (1991).

27.   Wucherpfennig, K. W. & Strominger, J. L. Molecular mimicry in T cell- mediated autoimmunity: viral peptides activate human T cell clones specific for myelin basic protein. Cell 80, 695-705 (1995).

28.   van de Stadt, L. A. et al. Monoclonal anti-citrullinated protein antibodies selected on citrullinated fibrinogen have distinct targets with different cross- reactivity patterns. Rheumatology

52, 631-635 (2013).

29.   Gregersen, P. K., Silver, J. & Winchester, R. J. The shared epitope hypothesis. An approach to understanding the molecular genetics of susceptibility to rheumatoid arthritis. Arthritis Rheum. 30, 1205-1213 (1987).

30.   de Vries, N., Tijssen, H., van Riel, P. L. & van de Putte, L. B. Reshaping the shared epitope hypothesis: HLA-associated risk for rheumatoid arthritis is encoded by amino acid substitutions at positions 67-74 of the HLA-DRB1 molecule. Arthritis Rheum. 46, 921-928 (2002).

31.   van der Helm-van Mil, A. H. et al. An independent role of protective HLA class II alleles in rheumatoid arthritis severity and susceptibility. Arthritis Rheum. 52, 2637-2644 (2005).

32.   Shadick, N. A. et al. Opposing effects of the D70 mutation and the shared epitope in HLA-DR4 on disease activity and certain disease phenotypes in rheumatoid arthritis. Ann. Rheum. Dis. 66, 1497-1502 (2007).

33.   Hensvold, H. A. et al. Environmental and genetic factors in the development of anticitrullinated protein antibodies (ACPAs) and ACPA-positive rheumatoid arthritis: an epidemiological investigation in twins. Ann. Rheum. Dis. 74, 375-380 (2013).

34.   Enouz, S., Carrie, L., Merkler, D., Bevan, M. J. & Zehn, D. Autoreactive T cells bypass negative selection and respond to self-antigen stimulation during infection. J. Exp. Med. 209, 1769-1779 (2012).

35.   Hand, T. W. et al. Acute gastrointestinal infection induces long-lived microbiota-specific T cell responses. Science 337, 1553-1556 (2012).

36.   Liu, X., Zou, Q., Zeng, B., Fang, Y. & Wei, H. Analysis of fecal lactobacillus community structure in patients with early rheumatoid arthritis. Curr. Microbiol. 67, 170-176 (2013).

37.   de Rooy, D. P., van der Linden, M. P., Knevel, R., Huizinga, T. W. & van der Helm-van Mil, A. H. Predicting arthritis outcomes—what can be learned from the Leiden Early Arthritis Clinic? Rheumatology 50, 93-100 (2011).

38.   Erlich, H., Lee, J. S., Petersen, J. W., Bugawan, T. & DeMars, R. Molecular analysis of HLA class I and class II antigen loss mutants reveals a homozygous deleteion of the DR, DR, and part of the DP region: implications for class II gene order. Hum. Immunol. 16, 205-219 (1986).

39.   Stepniak, D. et al. Large-scale characterization of natural ligands explains the unique gluten-binding properties of HLA-DQ2. J. Immunol. 180, 3268-3278 (2008).

40.   Shi, J. et al. Autoantibodies recognizing carbamylated proteins are present in sera of patients with rheumatoid arthritis and predict joint damage. Proc. Natl Acad. Sci. USA 108, 17372-17377 (2011).

41.   Moustakas, A. K. et al. Structure of celiac disease-associated HLA-DQ8 and non-associated HLA-DQ9 alleles in complex with two disease-specific epitopes. Int. Immunol. 12, 1157-1166 (2000).

42.   Lee, K. H., Wucherpfennig, K. W. & Wiley, D. C. Structure of a human insulin peptide-HLA-DQ8 complex and susceptibility to type 1 diabetes. Nat. Immunol. 2, 501-507 (2001).

43.   Murthy, V. L. & Stern, L. J. The class II MHC protein HLA-DR1 in complex with an endogenous peptide: implications for the structural basis of the specificity of peptide binding. Structure 5, 1385-1396 (1997).

44.   Fremont, D. H., Hendrickson, W. A., Marrack, P. & Kappler, J. Structures of an MHC class II molecule with covalently bound single peptides. Science 272, 1001-1004 (1996).

45.   Rostkowski, M., Olsson, M. H., Sondergaard, C. R. & Jensen, J. H. Graphical analysis of pH-dependent properties of proteins predicted using PROPKA. BMC Struct. Biol. 11, 6 (2011).

46.   Simonson, T. et al. Computational protein design: the Proteus software and selected applications. J. Comput. Chem. 34, 2472-2484 (2013).

47.   Brooks, B. R. et al. CHARMM: the biomolecular simulation program. J. Comput. Chem. 30, 1545-1614 (2009).

48.   Jo, S., Kim, T., Iyer, V. G. & Im, W. CHARMM-GUI: a web-based graphical user interface for CHARMM. J. Comput. Chem. 29, 1859-1865 (2008).

49.   MacKerell, A. D. et al. All-atom empirical potential for molecular modeling and dynamics studies of proteins. J. Phys. Chem. B 102, 3586-3616 (1998).

50.   Mackerell, Jr. A. D., Feig, M. & Brooks, III C. L. Extending the treatment of backbone energetics in protein force fields: limitations of gas-phase quantum mechanics in reproducing protein conformational distributions in molecular dynamics simulations. J. Comput. Chem. 25, 1400-1415 (2004).

51.   Jorgensen, W. L., Chandrasekhar, J., Madura, J. D., Impey, R. W. & Klein, M. L. Comparison of simple potential functions for simulating liquid water. J. Chem. Phys. 79, 926-935 (1983).

52.   Neria, E., Fischer, S. & Karplus, M. Simulation of activation free energies in molecular systems. J. Chem. Phys. 105, 1902-1921 (1996).

53.   Darden, T., York, D. & Pedersen, L. Particle Mesh Ewald: an N.Log(N) method for Ewald sums in large systems. J. Chem. Phys. 98, 10089-10092 (1993).

54.   Nose, S. A. Unified formulation of the constant temperature molecular- dynamics methods. J. Chem. Phys. 81, 511-519 (1984).

55.   Hoover, W. G. Canonical dynamics - equilibrium phase-space distributions. Phys. Rev. A 31, 1695-1697 (1985).

56.   Feller, S. E., Zhang, Y. H., Pastor, R. W. & Brooks, B. R. Constant-pressure molecular-dynamics simulation - the Langevin Piston method. J. Chem. Phys. 103, 4613-4621 (1995).

57.   Ryckaert, J. P., Ciccotti, G. & Berendsen, H. J. C. Numerical-integration of cartesian equations of motion of a system with constraints - molecular- dynamics of N-alkanes. J. Comput. Phys. 23, 327-341 (1977).

2

58.   Humphrey, W., Dalke, A. & Schulten, K. VMD: visual molecular dynamics. J. Mol. Graph. 14, 33-38 (1996).

59.   Tamamis, P., Morikis, D., Floudas, C. A. & Archontis, G. Species specificity of the complement inhibitor compstatin investigated by all-atom molecular dynamics simulations. Proteins 78, 2655-2667 (2010).

60.   Tamamis, P. et al. Insights into the mechanism of C5aR inhibition by PMX53 via implicit solvent molecular dynamics simulations and docking. BMC Biophys. 7, 5 (2014).

61.   Im, W., Lee, M. S. & Brooks, III C. L. Generalized born model with a simple smoothing function. J. Comput. Chem. 24, 1691-1702 (2003).

62.   Chen, J., Im, W. & Brooks, III C. L. Balancing solvation and intramolecular interactions: toward a consistent generalized Born force field. J. Am. Chem. Soc. 128, 3728-3736 (2006).
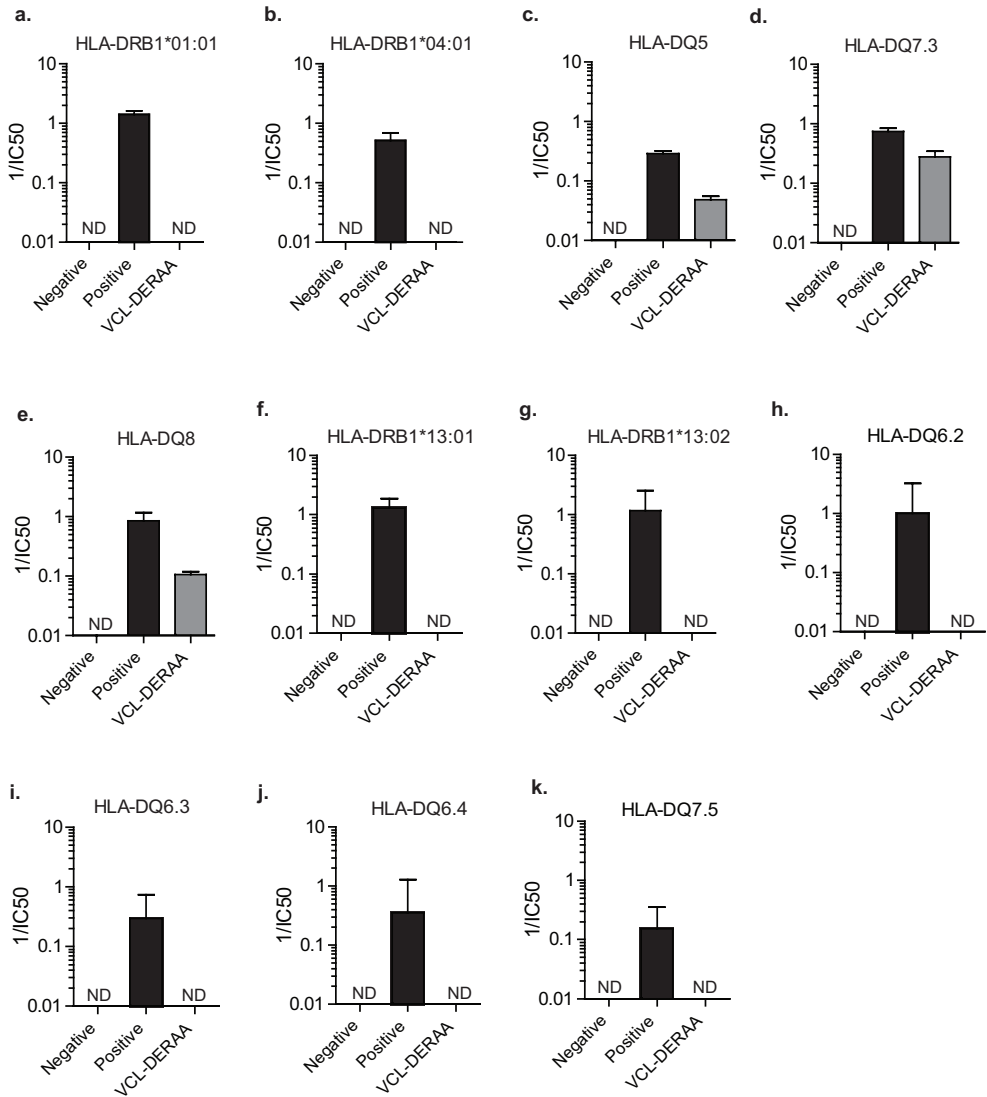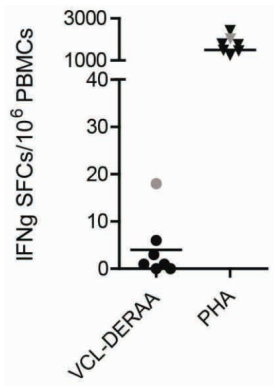
SUPPLEMENTARY FIGURES
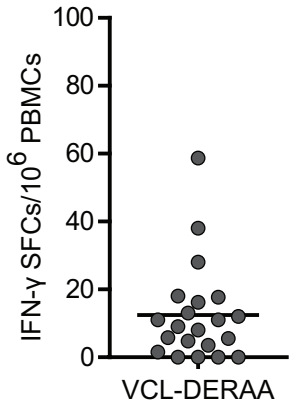
Supplementary Figure 1. Vinculin is an autoantigen recognized by circulating CD4+ T cells. IFNγ ELISPOT of PBMC from healthy individuals (*n*=21) stimulated for 24h with VCL-DERAA peptide REEVFDERAANFENH. Each dot represents a unique donor.
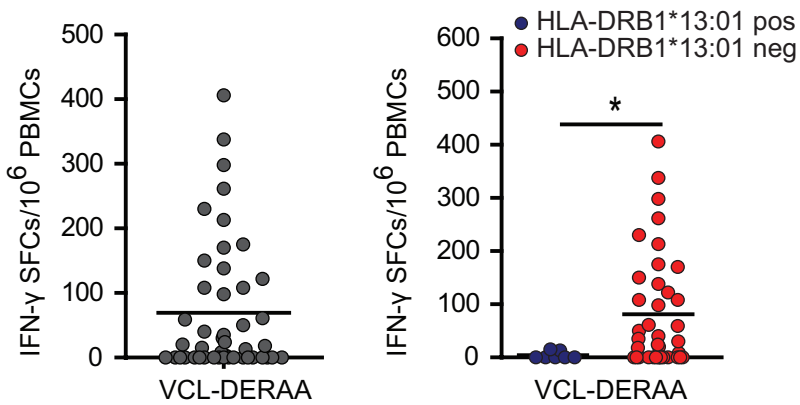

Supplementary Figure 2. Vinculin is an autoantigen recognized by circulating CD4+ T cells of HLA-DRB1*13-negative donors. IFNγ ELISPOT of PBMC from healthy individuals stimulated for 4d with VCL-DERAA peptide REEVFDERAANFENH (Left panel). Stratification of donors in two distinct groups based on the presence or absence of HLA-DRB1*13:01 (Right panel). Each dot represents a unique donor (*n*=46). Two-sided statistical analyses of ELISPOT data were performed using a Mann-Whitney U test with * indicating *p* > 0.05.

Supplementary Figure 3. Presentation to vinculin-DERAA-directed T cells is restricted to RA-predisposing HLA-DQ molecules. Competitive binding of a non-binding negative control peptide, an unbiotinylated positive control peptide and the VCL-DERAA peptide to HLA-DRB1*01:01 (A), HLA-DRB1*04:01 (B), HLA-DQ5 (C), HLA-DQ7.3 (D), HLA-DQ8 (E), HLA-DRB1*13:01 (F), HLA-DRB1*13:02 (G), HLA-DQ6.2 (H), HLA-DQ6.3 (I), HLA-DQ6.4 (J) or HLA-DQ7.5 (K). IC50 is the concentration of test-peptide (pM) where 50% of biotinylated peptide is bound, ND = non-detectable (IC50 > 300 pM). All experiments were performed at least three times and bars show pooled experiments, the error bars show the variation between the different experiments in S.E.M.

Supplementary Figure 4. Vinculin is not recognized by circulating CD4+ T cells of donors negative for predisposing HLA-DQ molecules. IFNγ ELISPOT of PBMC from healthy individuals negative for HLA-DQ5, HLA-DQ7.3 or HLA-DQ8 (*n*=6) stimulated for 24h with VCL-DERAA peptide REEVFDERAANFENH or PHA. PBMC from an HLA-DQ8+ individual was used as a positive control (Gray dot).
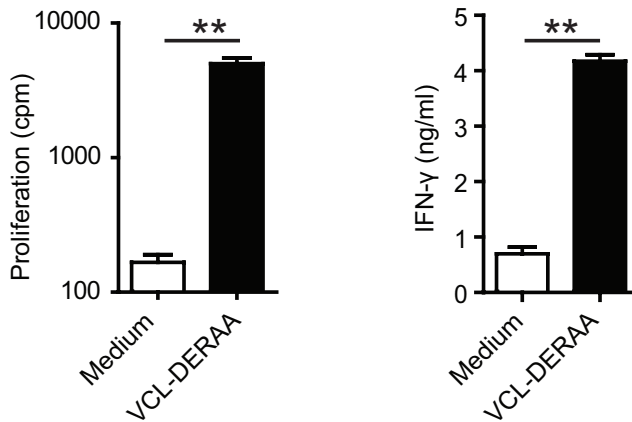
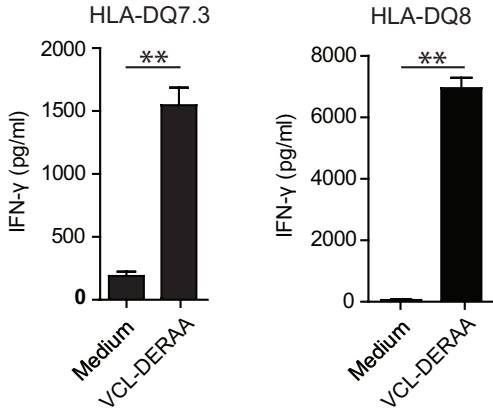**Supplementary Figure 5. T cell clone JPT57 specifically recognized the VCL-DERAA epitope.** ^{3}H-thymidine incorporation and IFNγ production upon stimulation of T cell clone JPT57 with unpulsed and VCL-DERAA pulsed autologous APCs. Data are representative of at least three independent experiments. Two-sided statistical analysis was performed using a student's t-test with ** indicating $p < 0.001$. Error bar is S.E.M.
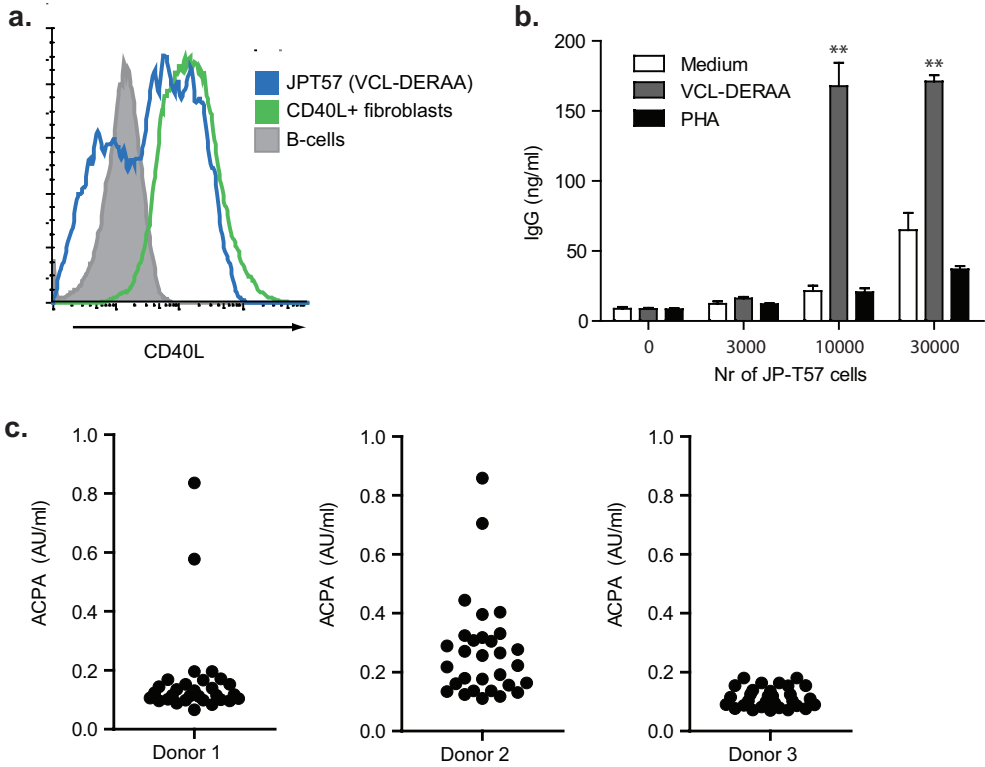
Supplementary Figure 6. Activated JPT57 cells can activate ACPA-producing B cells. (A) Flow cytometry analysis of CD40L expression on JPT57 cells stimulated with VCL-DERAA-pulsed APCs, CD40L-transfected fibroblasts and EBV-transformed B cells. (B) Co-culture of VCL-DERAA-pulsed HLA-DQ8-positive B cells from healthy subjects with increasing numbers of JPT57 cells in the presence of anti-IgM. The experiment was repeated three times and the plot shows a representative experiment. (C) Co-culture of VCL-DERAA-pulsed HLA-DQ8-positive B cells from three ACPA-positive RA patients with JPT57 (1:1) in the presence of anti-IgM. Activation of ACPA-producing B cells was determined by CCP2 ELISA. Each dot represents a different well. Statistical analysis was performed using a student's t-test with ** indicating $p > 0.001$. Error bars are S.E.M.
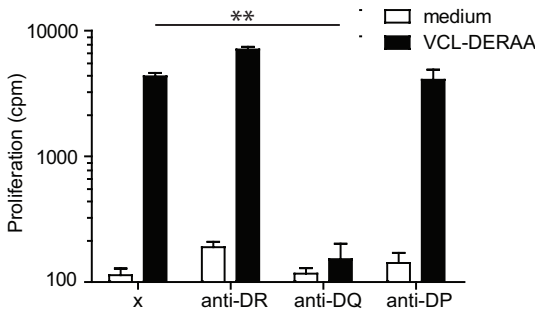
Supplementary Figure 7. Vinculin-DERAA-directed T cell clone JPT57 is HLA-DQ-restricted. ^{3}H-thymidine incorporation of JPT57 stimulated with feeders, pulsed or unpulsed with VCL-DERAA in the presence of HLA class II blocking antibodies. Data are representative of at least three independent experiments. Two-sided statistical analysis was performed using a student's t-test with ** indicating $p < 0.001$. Error bars are S.E.M.

Supplementary Figure 8. Vinculin-DERAA-directed T cell clone JPT57 is restricted to HLA-DQ7.3 and HLA-DQ8. IFNγ production by JPT57 cells stimulated with HLA-DQ7.3 or HLA-DQ8 homozygous EBV-transformed B cells. Data are representative of at least three independent experiments. Two-sided statistical analysis was performed using a student's t-test with ** indicating $p < 0.001$. Error bars are S.E.M.
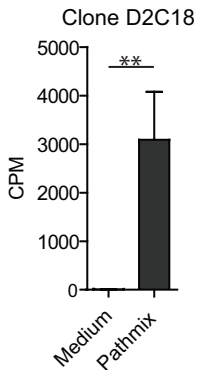

Supplementary Figure 9. Identification of a Pathmix directed T cell clone in an HLA-DRB1*13 negative donor. ^{3}H-thymidine incorporation upon stimulation of T cell clone D2C18 with unpulsed and salmonella-DERAA-pulsed autologous monocytes. The experiment was repeated two times and the plot shows a representative experiment. Two-sided statistical analysis was performed using a student's t-test with ** indicating $p > 0.001$. Error bar is S.E.M.
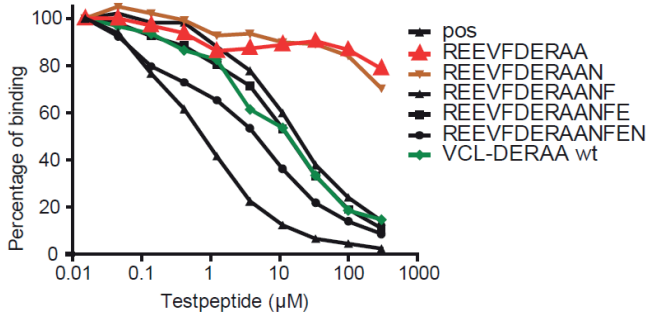
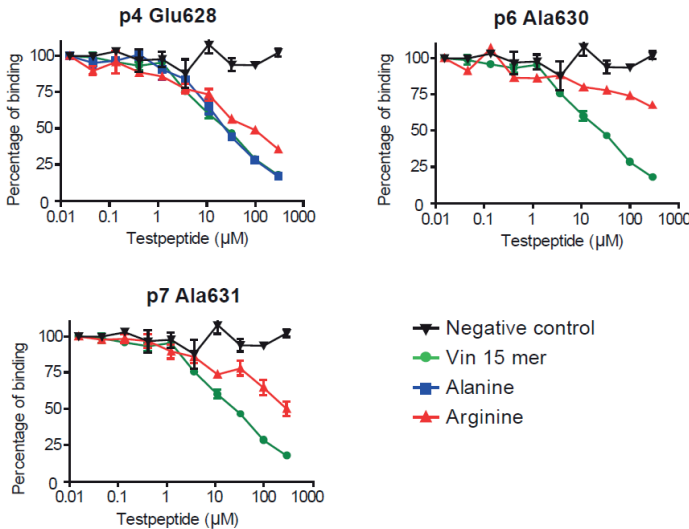**Supplementary Figure 10. Truncation of Phe633 results in loss of binding to HLA-DQ8.** Competitive binding of HLA-DQ8 to an unbiotinylated positive control peptide and C-truncated VCL-DERAA peptides. The experiment was repeated three times and plots show a representative experiment.
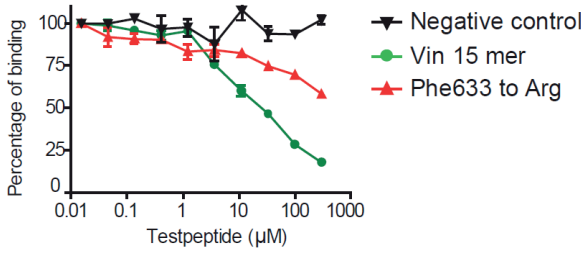
Supplementary Figure 11. Arginine substituting Phe633 negatively impacts binding affinity to HLA-DQ8. Competitive binding of a negative control peptide, the native VCL-DERAA peptide and the VCL-DERAA peptide with Phe633 substituted to arginine. Experiments were performed three times and plots show a representative experiment.
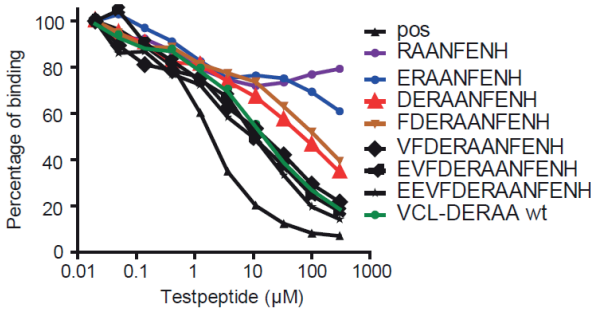
Supplementary Figure 12. N-terminal truncation of Val625 lowers the binding affinity to HLA-DQ8. Competitive binding of HLA-DQ8 to an unbiotinylated positive control peptide and N-truncated VCL-DERAA peptides. The experiment was repeated three times and plots show a representative experiment.

Supplementary Figure 13. Arginine-substitutions of residues implicated to interact with binding pockets negatively impacts binding to HLA-DQ8. Competitive binding of a negative control peptide, the native VCL-DERAA peptide and the VCL-DERAA peptide with Glu628, Ala630 and Ala631 substituted to alanine or arginine. Experiments were performed three times and plots show a representative experiment.

Supplementary Figure 14. HLA-DQ7.3 presents VCL-DERAA in a similar binding register as HLA-DQ8. Competitive binding of HLA-DQ7.3 to an unbiotinylated positive control peptide and C-truncated and N-truncated VCL-DERAA peptides. The experiment was repeated three times and plots show a representative experiment.
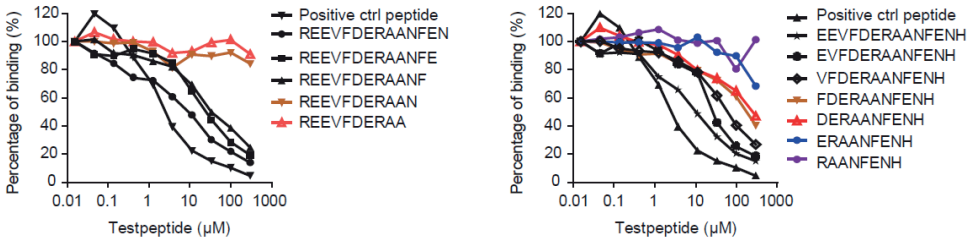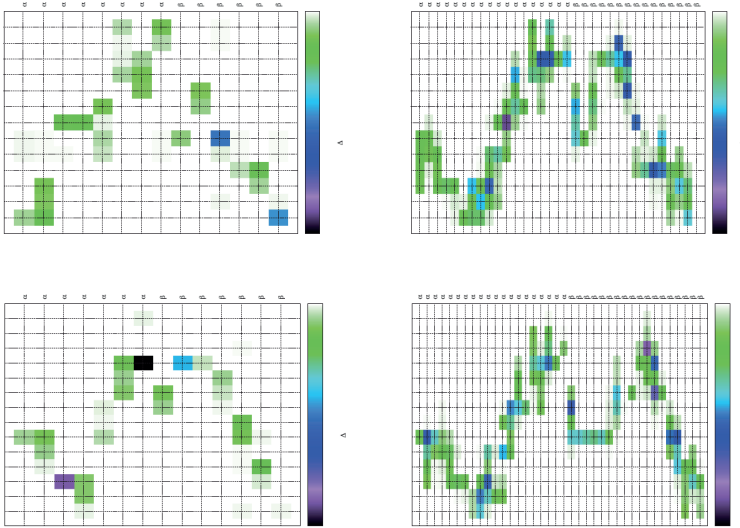

Supplementary Figure 15. Interaction free-energies (in kcal/mol) for selected peptide-ligand residue pairs, averaged over the MD trajectories. The left and right panels correspond, respectively, to polar (GB+Coulomb) and non-polar (vW + SA) interactions, computed with Eq. (1) of the methods. Rows from top to bottom correspond, respectively, to the DQ8:VCL-DERAA and DQ8:insulin complexes.
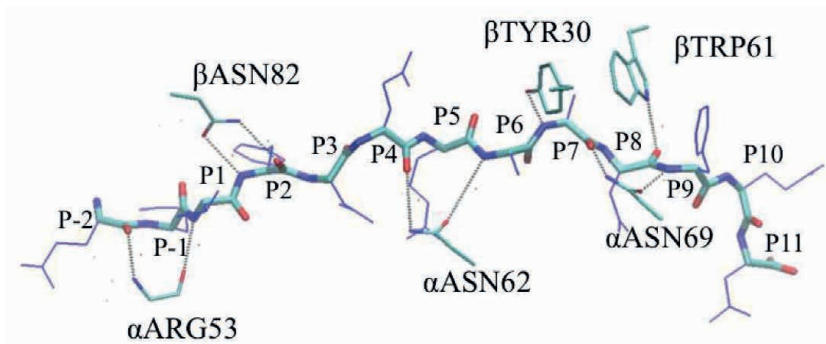
Supplementary Figure 16. Hydrogen bonds between the VCL-DERAA peptide mainchain and DQ8. The peptide mainchain is shown in thick licorice and its sidechains are displayed in blue lines. DQ8 groups are shown in thin licorice. Hydrogen bonds with occupancy smaller than 20% are omitted. A comprehensive list of all hydrogen bonds is included in Supplementary Table 1.
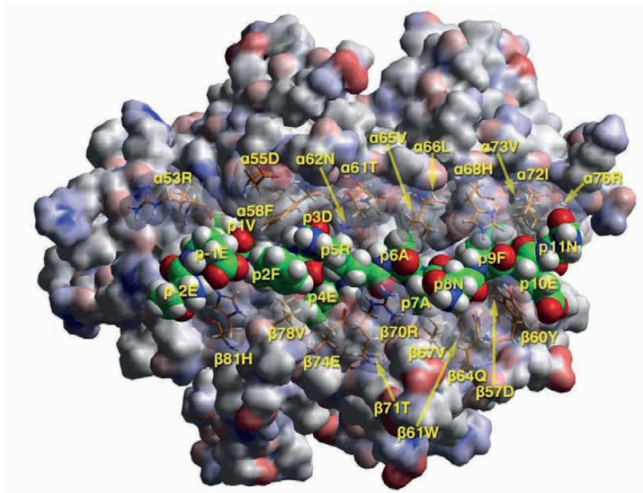
Supplementary Figure 17. TCR view of the complex of HLA-DQ7.3 with the VCL-DERAA epitope in the groove at pH 7.4 (extracellular). The α1β1 domain of the modelled HLA-DQ molecule is in van der Waals surface representation, colored according to atomic charges (negative = red, positive = blue, neutral = gray, partial charges shades in-between). Several visible residues from the HLA-DQ molecule in contact with the antigenic peptide and potential contact with a cognate TCR in canonical orientation are shown in stick form with a transparent surface (atomic color code: oxygen, red; nitrogen, blue; hydrogen, white; carbon, green; sulfur, yellow). The antigenic peptide in the groove is shown in space-filling form, with identical colour conventions as in Figure 6D-G. Anchors p1V and p9F point into the plane of the paper (screen) and are only partly seen. In vivo, p5R may not interact with p2F (cation-π interaction) because the former might more favorably interact with water molecules from the solvent. In this allele p4E makes an even weaker anchor than in DQ8, because of β13Gly-->Ala and β26Leu-->Tyr substitutions (DQ8 -->DQ7) that leaves less space available at the base of pocket 4.
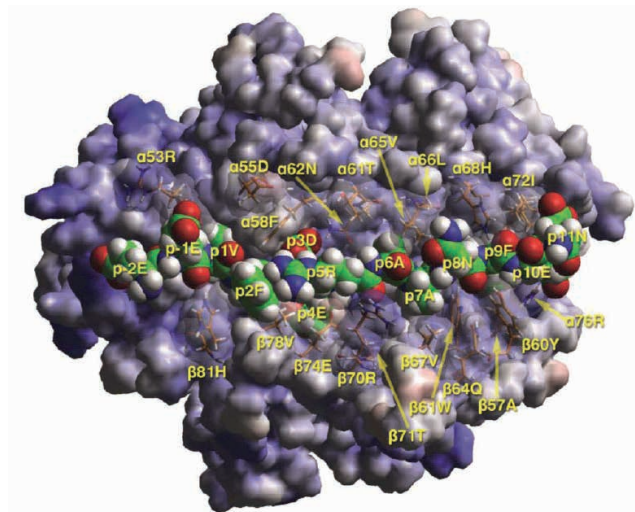
Supplementary Figure 18. TCR view of the complex of HLA-DQ8 with the VCL-DERAA epitope in the groove at pH 7.4 (extracellular). Depiction and colour conventions as in Suppl. Figure 16. Anchors P1V and P9F point into the plane of the paper (screen) and are only partially seen. In vivo, P5R may not interact with P2F (cation-π interaction) because the former might more favorably interact with water molecules from the solvent.
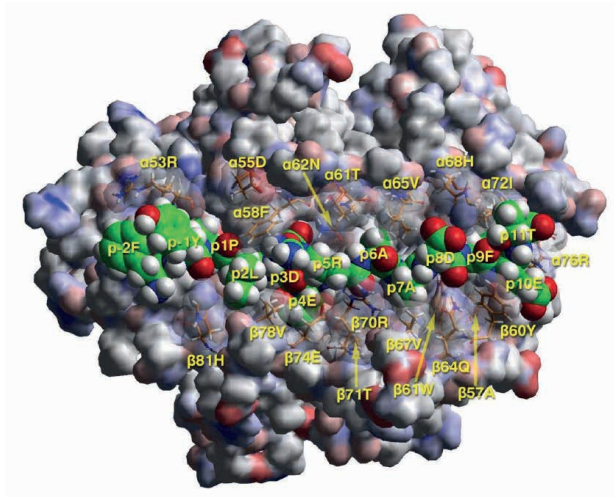
Supplementary Figure 19. TCR view of the complex of HLA-DQ8 with the *L. curvatus* epitope in the groove at pH 7.4 (extracellular). Depiction and colour conventions as in Suppl. Figure 16. Anchors P1P and P9F point into the plane of the paper (screen) and are only partially seen.

Supplementary Figure 20. TCR view of the complex of HLA-DQ8 with the *L. Sakei* epitope in the groove at pH 7.4 (extracellular). Depiction and colour conventions as in Suppl. Figure 16. Anchors P1P and P9F point into the plane of the paper (screen) and are only partially seen.
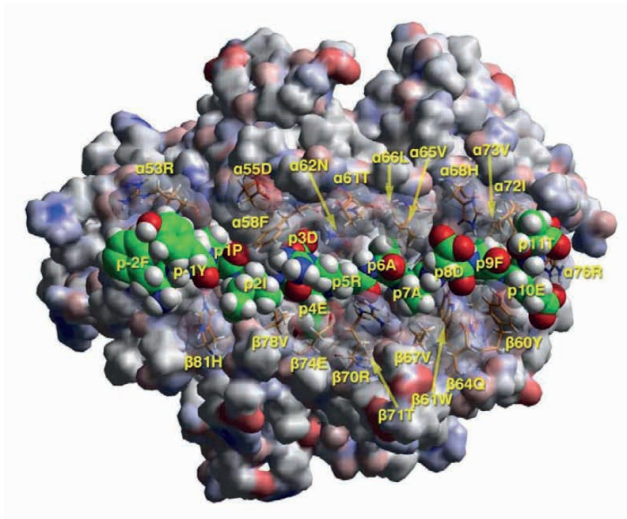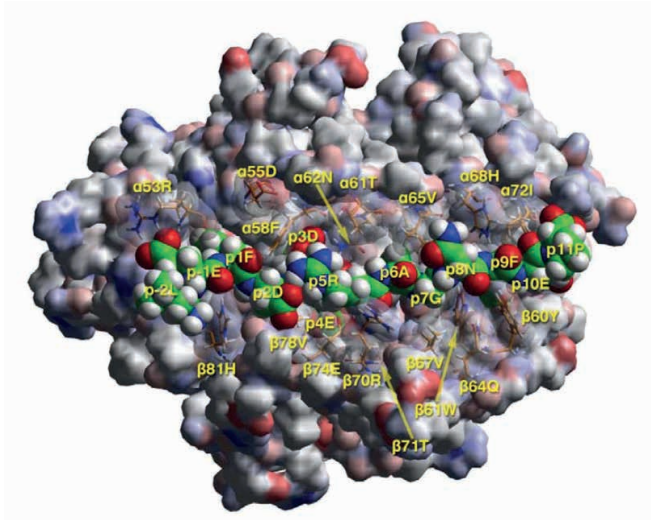
Supplementary Figure 21. TCR view of the complex of HLA-DQ8 with the *C. coli* epitope in the groove at pH 7.4 (extracellular). Depiction and colour conventions as in Suppl. Figure 16. Anchors P1P and P9F point into the plane of the paper (screen) and are only partially seen.
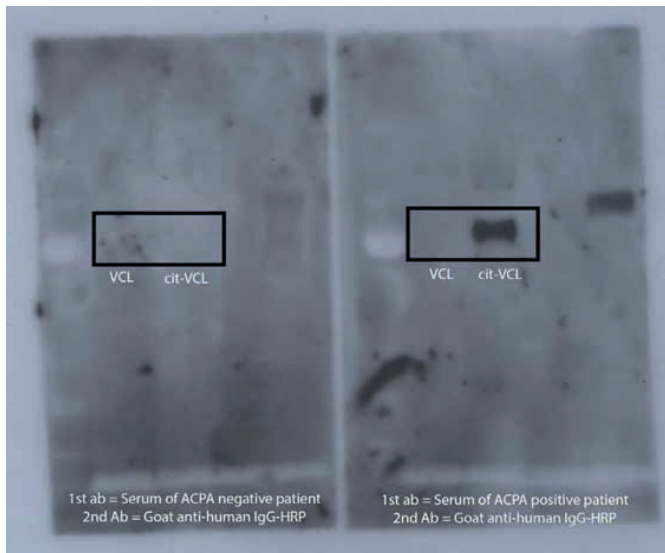
Supplementary Figure 22. Unedited blot of Figure 1A.

Donor	Acceptor	Occupancy (%)
Water	**P-2E** (sc)	381
P-2E (Nter)	Water	188
βArg88 (sc)	P-2E(sc)	165
αArg53 (mc)	P-2E (mc)	42.7
αArg53 (sc)	P-2E (sc)	41.3
aPhe51 (mc)	P-2E (sc)	29.8*
αPhe51 (mc)	P-2E (Nter)	18.1*
Water	**P-1E**(sc)	535
Water	P-1E (mc)	62.9
P-1E (mc)	Water	56.7
βAsn82 (sc)	P-1E(mc)	20.5*
βHis81-Side	P-1E(mc)	16.6*
Water	**P1V** (mc)	79.3
P1V(mc)	αArg53 (mc)	76.9
P2F(mc)	βAsn82 (sc)	85.6
βAsn82 (sc)	P2F (mc)	68.5
Water	**P3D**(sc)	301
Water	P3D (mc)	64.2
αAsnN62 (sc)	P3D (sc)	46.9*
αTyr22 (sc)	P3D (sc)	36.6*
Water	**P4E**(sc)	269
βArg70 (sc)	P4E (sc)	160.4
βThr71 (sc)	E6 (sc)	64.7*
βThr28 (sc)	E6 (sc)	38.5*
αAsn62 (sc)	P4E(mc)	36
	(Continued)	

2

(Continued)		
Donor	**Acceptor**	**Occupancy (%)**
P5R (sc)	Water	118
Water	P5R (mc)	98.3
P5R(sc)	αThr61 (sc)	76.9
P5R (sc)	αPhe58 (mc)	74.1
Water	**P6A**(mc)	118
P6A(mc)	αAsn62 (sc)	88.5
P7A(mc)	βTyr30 (sc)	65.4
P8N (mc)	Water	70.4
Water	P8N (sc)	70.4
Water	P8N (mc)	47.5
βTrp61 (sc)	P8N(mc)	41.9
P8N (sc)	Water	38.7
P8N (sc)	αAsn69 (sc)	35.0
αHis68 (sc)	P8N (sc)	19.2
Water	**P9F** (mc)	65.6
P9F(mc)	αAsn69 (sc)	38.8
Water	**P10E** (sc)	555
Water	P10E (mc)	62.8
P10E (mc)	Water	48.6
Water	**P11N** (Cter)	461
Water	P11N (sc)	117.5
P11N (mc)	Water	54.7
P11N (sc)	Water	44.0
P11N(sc)	αHis68 (sc)	21.3
αArg76 (sc)	P11N(sc)	33.2

Supplementary Table 1. Statistics of intermolecular hydrogen bonds in the DQ8:VCL-DERAA complex. Hydrogen bonds were considered present if the D-A distance I_{DA} was smaller than 3.5 Å, and the angle $\theta_{D-H...A}$ was larger than 150°. The (*) denotes water-mediated interactions; "sc" and "mc" denote side-chain and main-chain groups.

	p-2	p-1	p1	p2	p3	p4	p5	p6	p7	p8	p9	p10	p11
VCL-DERAA	E	E	V	F	D	E	R	A	A	N	F	E	N
Aspergillus fumigatus	V	T	A	E	D	E	R	A	A	M	F	F	R
Bacillus cereus	V	A	V	P	D	E	R	A	A	N	A	I	A
Campylobacter coli	L	E	F	D	D	E	R	A	G	N	F	E	P
Influenza A virus	F	E	F	S	D	E	R	A	A	N	P	I	V
Influenza A virus	F	E	L	S	D	E	R	A	A	N	P	I	V
Influenza A virus	F	E	L	S	D	E	R	A	A	N	P	V	V
Lactobacillus brevis	L	V	T	D	D	E	R	A	A	I	F	K	A
Lactobacillus curvatus	F	Y	P	L	D	E	R	A	A	D	F	E	T
Lactobacillus sakei	F	Y	P	I	D	E	R	A	A	D	F	E	T
Mycobacterium tuberculosis	A	L	P	F	D	E	R	A	A	V	F	L	R
Mycobacterium tuberculosis	A	M	P	F	D	E	R	A	A	V	F	L	R
Nocardia brasiliensis	A	L	P	F	D	E	R	A	A	I	F	L	R
Nocardia farcinica	A	L	L	A	D	E	R	A	A	L	F	A	R
Proteus mirabilis	V	I	T	D	D	E	R	A	A	V	F	Y	G
Proteus penneri													
Proteus stuartii													
Vibrio parahaemolyticus	Y	D	E	L	D	E	R	A	A	W	F	Y	E
Yersinia enterocolitica	L	E	D	Y	D	E	R	A	A	N	G	Y	D

Supplementary Table 2. Microbe derived epitopes with molecular mimicry to vinculin-DERAA.

2

SUPPLEMENTARY NOTE 1

Functional Identification of the primary binding register of VCL-DERAA in HLA-DQ7.3 and DQ8.

To establish the primary binding register of VCL-DERAA in HLA-DQ8, we performed HLA class II binding assay with N- and C-terminal truncated VCL-DERAA peptides. Upon C-terminal truncations, we observed a dramatic drop in binding affinity upon removal of Phe633 (Supplementary Figure 9). This observation made us speculate that this residue is interacting with the p9 pocket of HLA-DQ8. The p9 pocket of HLA-DQ8 is shaped by several different amino acids including α68His and α76Arg. Due to the presence of these positively charged amino acids, the pocket has a preference for negatively charged amino acids. Therefore, we substituted Phe633 for an arginine and observed a drop in binding capacity (Supplementary Figure 10).

Next, we performed N-terminal truncations. We performed a slight drop in binding affinity upon removal of Val625. The removal of Phe626 had no further effect, but removal of Asp627 resulted in a complete loss of binding affinity (Supplementary Figure 11). The N-terminal truncation of Val625 does not result in a complete loss of binding affinity. This is in agreement with previous data on binding of truncated peptides to HLA-DQ molecules and their mouse homologues H2-A, where p1 and p2 positions may be empty, provided the C-terminus of the peptide extends to p11 or beyond[1, 2]. Indeed, upon truncation of Asp627, the residue proposed to interact with p3, we did observe a complete loss of binding affinity.

Finally, we performed alanine and arginine substitutions of Glu628, Ala630 and Ala631 that are proposed to interact with respectively the p4, p6 and p7 pocket further confirmed the proposed core register (Supplementary Figure 12).

Together this data supports **V**FD**E**RAAN**F** (anchors in bold) as the primary binding register of the VCL-DERAA epitope in HLA-DQ8. Next, we also examined the binding register of this epitope in HLA-DQ7.3 using N- and C-terminal truncated VCL-DERAA epitopes. We observed striking similarities with the previously performed binding assays to HLA-DQ8 (Supplementary Figure 13).

Together these data indicate that VCL-DERAA binds in a similar binding register to both HLA-DQ7.3 and HLA-DQ8.

Molecular Dynamics simulations of HLA-DQ:VCL-DERAA complexes

We studied the structure and interactions of the HLA-DQ8:VCL-DERAA complex in the binding register determined above via atomic-detail MD simulations. Figure 5 shows important hydrogen-bonding patterns and intermolecular nonpolar contacts in pockets P1, P4 and P9. Supplementary Figure 14 displays interaction free energies of selected protein-peptide residue pairs. These values are averaged over the MD trajectories and include solvent effects (see Methods).

The peptide P1V side chain forms nonpolar contacts with several surrounding residues (αTyr9, αHis24, αPhe32, αVal43, αArg52, αArg53, αPhe54, βVal78, βHis81, βAsn82, βLeu85)

at the P1 pocket (Figure 5 and Supplementary Figure 14). Residues αArg52, βGlu86, αGlu31, αTyr9 and αHis24 form the same dense network of interactions, as in the crystallographic DQ8:insulin complex[3] and additional MD simulations of the DQ8:insulin complex; αHis24 replaces a water-mediated interaction with the insulin P1E side chain by a water-mediated interaction with the βGlu86 side chain. In the second anchor pocket, the P4E side chain is surrounded by a large number of water molecules (on average, 6 waters are positioned with their oxygen atom within 4 Å of the side chain), and makes a strong interaction with αArg70. Pocket P9 has a preference for negatively charged residues, which can form a salt bridge with αArg76 [3-5]. In the VCL-DERAA complex this pocket accepts a Phe residue. The P9F side chain is placed between βTrp61 and αIle72, and makes several additional nonpolar contacts with residues αHis68, αAsn69, αVal73, αArg76, βTyr37, βAla57, and βTyr60. The αArg76 side chain interacts with the C-terminal residue P11Asn (Supplementary Figure 14 and Supplementary Table 1).

The protein interactions with VCL-DERAA anchor residues P1V, P9F are weaker than the interactions with insulin residues P1E and P9E, in the DQ8:insulin complex (Supplementary Figure 14). In the latter, residues P1E and P9E form salt bridges with αHis24 and βArg76, respectively; similarly, insulin residue P4Y forms stronger nonpolar contacts with the protein, relative to VCL-DERAA residue P4E (Supplementary Figure 14)[3]. These differences are in line with the weaker, relative to insulin, VCL-DERAA affinity for DQ8.

The interactions described so far involve the side chains of anchor residues. The peptide backbone makes several additional intermolecular hydrogen bonds (Supplementary Table 1 and Supplementary Figure 15) which are consistent with the conserved peptide-protein interactions of the MHCII binding motif[6-8]. Furthermore, the N- and C-terminal residues form salt bridges with the protein (P-2E- βArg88, P-2E- βArg53, P11N- αArg76).

As discussed above, our IFN-γ ELISA measurements suggest that residues P2F, P8N, P9F and P10E are important TCR contacts, as they affect T cell recognition. The P2F side chain packs against the α-helix of the β1 domain of HLA-DQ8 and makes direct contacts with several of its residues (Figure 5G and Supplementary Figure 14). Its opposite side is exposed to solvent, and is positioned near the side chain ring of αPhe58. During the simulation, the two rings remain approximately parallel to each other, at an average mutual distance of ~ 8 Å. The P2F and αPhe58 rings and the nonpolar moiety of P5R form a hydrophobic cluster (Figure 5G), which could play a role in TCR recognition. The side chains of the important TCR contact residues P8N and P10E side chains are also solvent-exposed and make few interactions with the protein. Among the other residues of the DERAA sequence, the P3D and P5R side chains face also toward the TCR binding region and form a stable salt-bridge interaction.

SUPPLEMENTARY REFERENCES

1.   Scott, C.A., Peterson, P.A., Teyton, L., & Wilson, I.A. Crystal structures of two I-Ad-peptide complexes reveal that high affinity can be achieved without large anchor residues. Immunity. 8, 319-329 (1998).

2.   He, X.L. et al. Structural snapshot of aberrant antigen presentation linked to autoimmunity: the immunodominant epitope of MBP complexed with I-Au. Immunity. 17, 83-94 (2002).

3.   Lee, K.H., Wucherpfennig, K.W., & Wiley, D.C. Structure of a human insulin peptide-HLA-DQ8 complex and susceptibility to type 1 diabetes. Nat. Immunol. 2, 501-507 (2001).

4.   Kwok, W.W., Domeier, M.L., Raymond, F.C., Byers, P., & Nepom, G.T. Allele-specific motifs characterize HLA-DQ interactions with a diabetes-associated peptide derived from glutamic acid decarboxylase. J. Immunol. 156, 2171-2177 (1996).

5.   Godkin, A. et al. Use of eluted peptide sequence data to identify the binding characteristics of peptides to the insulin-dependent diabetes susceptibility allele HLA-DQ8 (DQ 3.2). Int. Immunol. 9, 905-911 (1997).

6.   Stern, L.J. et al. Crystal structure of the human class II MHC protein HLA-DR1 complexed with an influenza virus peptide. Nature 368, 215-221 (1994).

7.   Jardetzky, T.S. et al. Crystallographic analysis of endogenous peptides associated with HLA-DR1 suggests a common, polyproline II-like conformation for bound peptides. Proc. Natl. Acad. Sci. U. S. A 93, 734-738 (1996).

8.   Painter, C.A. & Stern, L.J. Conformational variation in structures of classical and non- classical MHCII proteins and functional implications. Immunol. Rev. 250, 144-157 (2012).

2

PART II

THE WORKING MECHANISM OF THE
BIOLOGICAL ABATACEPT
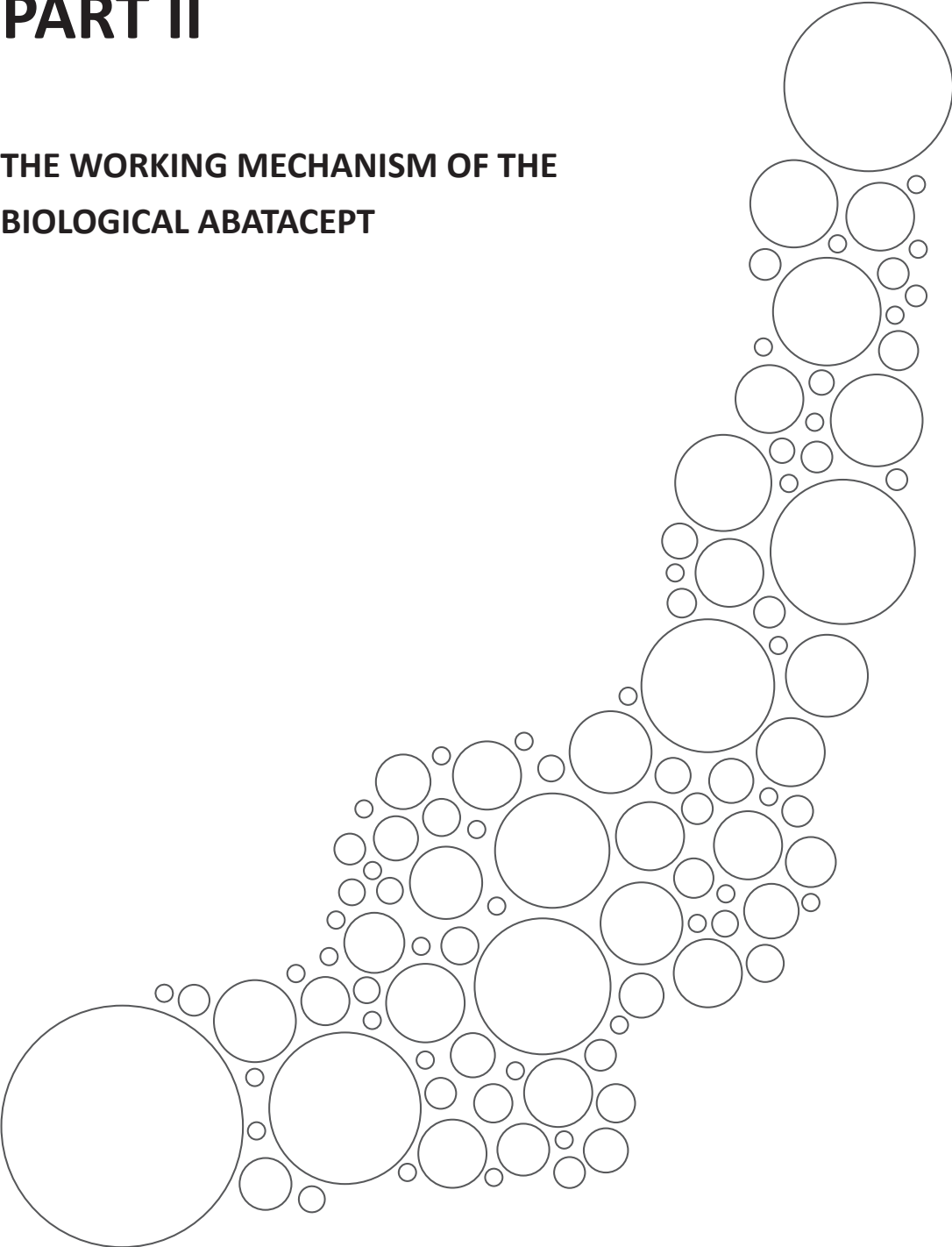
CHAPTER 3

ABATACEPT DECREASES DISEASE ACTIVITY IN THE ABSENCE OF CD4+ T CELLS IN THE COLLAGEN INDUCED ARTHRITIS MODEL

Diahann T.S.L. Jansen*, Hanane el Bannoudi*, Ramon Arens, Kim L.L. Habets, Marjolijn Hameetman. Tom W.J. Huizinga, Jeroen N. Stoop & René E.M. Toes

* Authors contributed equally

ABSTRACT

Introduction Abatacept is a fusion protein of human CTLA-4 and the Fc portion of human IgG1. It is believed to be effective in the treatment of rheumatoid arthritis by inhibiting co-stimulation of T cells via blocking CD28-B7 interactions as CTLA-4 binds to both B7.1 (CD80) and B7.2 (CD86). However, the interaction of CD28 with B7 molecules is crucial for activation of naive cells, whereas it is unclear whether the action of already activated CD4+ T cells, which are readily present in established disease, also depends on this interaction.

The aim of this study was to determine whether the mode of action of Abatacept depends solely on its ability to halt T cell activation in established disease.

Methods Arthritis was induced in thymectomized male DBA/1 mice by immunisation with bovine collagen type II. The mice were subsequently depleted for CD4+ T cells. Abatacept or control treatment was started when 80% of the mice showed signs of arthritis. Arthritis severity was monitored by clinical scoring of the paws and anti-collagen antibody levels over time were determined by ELISA.

Results Treatment with Abatacept in the absence of CD4+ T cells resulted in lower disease activity. This was associated with decreasing levels of collagen specific IgG1 and IgG2a antibodies while the antibody levels in control or CD4+ T cell-depleted mice increased over time.

Conclusion These results show that Abatacept decreased disease activity in the absence of CD4+ T cells indicating that the mode of action of Abatacept in established arthritis does not entirely depend on its effects on CD4+ T cell activation.

INTRODUCTION

Rheumatoid arthritis (RA) is a chronic inflammatory autoimmune disease affecting the joints in approximately 1% of the world population[1,2]. Patients with RA can be treated with non-steroidal anti-inflammatory drugs (NSAIDs) or with disease-modifying anti-rheumatic drugs (DMARDs). NSAIDs can alleviate disease symptoms, but do not impede the underlying inflammatory events or inhibit joint destruction, however, DMARDs do affect the disease process in all these respects[3]. Abatacept, a fusion protein of human CTLA-4 and the Fc portion of human IgG1, is a (biological) DMARD and is an effective therapy for established RA[4,5]. It is believed to be effective by blocking the co-stimulation of T cells through disruption of CD28-B7 interactions as CTLA-4 binds to B7.1 (CD80) and B7.2 (CD86) on antigen presenting cells (APC)[6].

CTLA-4-Ig has been tested in the collagen induced arthritis (CIA) model in mice and rats as a preventative treatment and on the first day of clinical onset resulting in lower clinical scores and reduced joint damage[7-9]. However, Abatacept is used to treat RA patients that failed anti-TNF treatment. It is likely that, in this phase of disease, the underlying autoimmune response is fully matured. Likewise, it is conceivable that the action of Abatacept does not fully depend on its ability to inhibit T cell responses as fully developed T cell responses are less dependent on CD28 co-stimulation. Indeed, CD28-B7 interactions are important for the activation of naive T cells, but this is less well-established for the activation of memory CD4+ T cells[10]. CD28-B7 costimulation of memory CD4+ T cells has been described to disturb IL-2 production and proliferation, however, production of other cytokines and expression of activation markers CD25 and CD69 are not affected indicating an incomplete dependence on this pathway[11]. Therefore, it is of interest to study the effect of Abatacept in the established phase of arthritis models as it is more alike the human situation with respect to the developmental phase of the underlying auto-immune response. In addition, much can be learned about the pathogenesis of human disease by understanding the mode of action of therapeutic interventions. The latter is exemplified through the use of e.g. anti-TNF or IL-6R blocking agents showing the pivotal role of these cytokines in inflammation. Nonetheless, the exact mode of action of several DMARDs used in RA treatment is still largely unclear, such as methotrexate or sulfasalazine.

A recent study described the comparison of anti-TNF treatment (Adalimumab) and Abatacept in a head-to-head study revealing similar efficacy in time based on clinical, functional and radiographic outcomes[12]. Intriguingly, anti-TNF therapy is thought to have a quick mode of action as it directly inhibits inflammation by blocking TNF, while Abatacept is thought to be effective after a longer time period as the effect of costimulation blockade will not become apparent directly. Consequently, similar efficacy of Adalimumab and Abatacept indicates a different mode of action of Abatacept in addition to costimulation blockade. Therefore, we now investigated whether the mode of action of Abatacept solely depends on its ability to halt T cell activation. We report a decrease in disease progression and activity after Abatacept

3

treatment in the absence of CD4+ T cells indicating that the mode of action of Abatacept in established arthritis does not entirely depend on its effects on CD4+ T cell activation.

METHODS

Mice

Male DBA/1 mice were obtained from our own breeding colony (originally obtained from Charles River). Thymectomized DBA/1 mice were purchased from Harlan. All mice were housed under specific pathogen-free conditions in individually ventilated cages at the animal facility of LUMC. All experiments were performed in accordance with national legislation and approved by the Ethical Committee for Animal Experimentation of Leiden University (approval number 11085 and 12217).

Induction of CIA and evaluation of arthritis

CIA was induced in 8-10 week old male DBA/1 mice as described before[13]. A clinical score was assigned based on a scoring protocol were each swollen or red phalanx was given 0.5 point and 1 point per toe. A red or swollen knuckle was given 1 point as well as a red or swollen footpad and a swollen ankle/wrist was given 5 points. The maximum score for each paw is 15 points resulting in a maximum score of 60 points per mouse. Disease progression was monitored till a maximum of 90 days after induction of CIA. Change in clinical score was calculated by subtracting the clinical score at start of treatment for every scoring time point after start of treatment till the end of follow up to correct for the difference in clinical score at start of treatment as the mice did not develop arthritis at the same time.

Treatment

Treatment was started when 80% of the mice showed signs of arthritis. The mice were randomized over the different treatment groups according to their score to assure that the mean clinical score of all groups was comparable at start of treatment. On day 0 of treatment, 100 µg GK1.5 (rat anti-mouse CD4 mAb), was administered intraperitoneally to the mice that received CD4+ T cell depletion to acquire CD4 depletion at start of treatment. This was weekly continued till the end of the experiment. For the different treatment regimens, mice were injected intraperitoneally with 500 µl PBS, 100 µg GK1.5, 1 mg Abatacept (Bristol-Myers Squibb), 100 µg GK1.5 in combination with 1 mg Abatacept, 1 mg isotype for Abatacept (Roche) or 1 mg isotype in combination with 100 µg GK1.5 on day 1, 3, 5, 8, 12 and 19.

Evaluation of CD4+ T cell counts

To confirm that CD4+ T cell depletion after GK1.5 treatment was complete, blood was collected on day 0, 12, 22, 35 and at the end of the experiment. The blood was lysed and subsequently stained with CD3 PerCP Cy5.5 (145-2C11), CD4 FITC (RM4-4), CD8 APC (Ly 2 53-6.7) from BD Pharmingen and CD45 efluor 450 (30-F11) from eBioscience. All samples were evaluated by a BD LSRFortessa cell analyser (BD Biosciences) and analysed using BD FACSDIVA

software (BD Biosciences) and FlowJo version 7.6.5 (Tree Star Inc).

Measurement of serum antibodies by ELISA

Anti-collagen type II and total IgG antibody levels were determined as described before[14]. In short, Nunc Maxisorp plates (Thermo Scientific) were coated with 2 µg/ml bovine type II collagen (Chondrex) or 3 µg/ml murine type II collagen (Chondrex) for antigen specific antibodies or with 0.5 µg/ml goat anti-mouse IgG (Southern Biotechnology) for total antibodies. IgG, IgG1 and IgG2a were detected using goat anti-mouse IgG HRP, goat anti-mouse IgG1 HRP and goat anti-mouse IgG2a HRP respectively (all Southern Biotech). Enzyme activity was visualized using ABTS. Serial dilutions from pooled sera of arthritic mice were used as standard to calculate arbitrary units (AU).

Measurement of supernatant antibody titers

At sacrifice bone marrow and spleen cells were isolated and 200.000 cells per well were cultured in IMDM (Lonza) containing 10% fetal calf serum (Gibco), glutamax, penicillin, streptomycin (Invitrogen) and 2-mercaptoethanol. After 7 or 14 days of culture supernatant was harvested and total IgG levels were determined by ELISA.

Statistical analysis

Statistical analysis was performed using GraphPad Prism version 5 (GraphPad Software Inc.). The Abatacept and CD4 depletion combination treated group and control treated group were compared using the Student's T-test or the Mann-Whitney U test as appropriate according to data distribution. p-values <0.05 were considered to be significant.

RESULTS

Abatacept decreased disease activity in mice depleted of CD4+ T cells by GK1.5

CTLA-4-Ig treatment has been used in the CIA model as a preventative intervention[7-9]. However, CTLA-4-Ig has not been tested in established disease where most of the disease-associated T cells are thought to be already activated or to have differentiated into memory T cells. Hence, it is not known whether its mode of action is also mediated through T cell inhibition in this disease phase. To investigate this, CIA was induced and treatment was started when 80% of the mice showed signs of arthritis. One day before start of treatment, CD4+ T cells were depleted by intraperitoneal administration of the CD4+ T cell depleting mAb GK1.5 and GK1.5 treatment was continued weekly until the end of follow up. Intriguingly, mice treated with the combination of CD4 depletion and Abatacept showed a significant decrease in disease activity compared to the mice treated with GK1.5 only or PBS control (Figure 1B and 1C). In contrast, CD4 depletion only did not significantly alter arthritis development compared to the control group (Figure 1B and 1C). Abatacept treatment in combination with CD4 depletion did not result in a lower number of affected paws, however, combination treatment did reduce the number of severely affected paws (clinical score >=5) (Figure 1D and 1E). In addition, novel paws that developed inflammation after start of therapy, displayed a lower disease score.
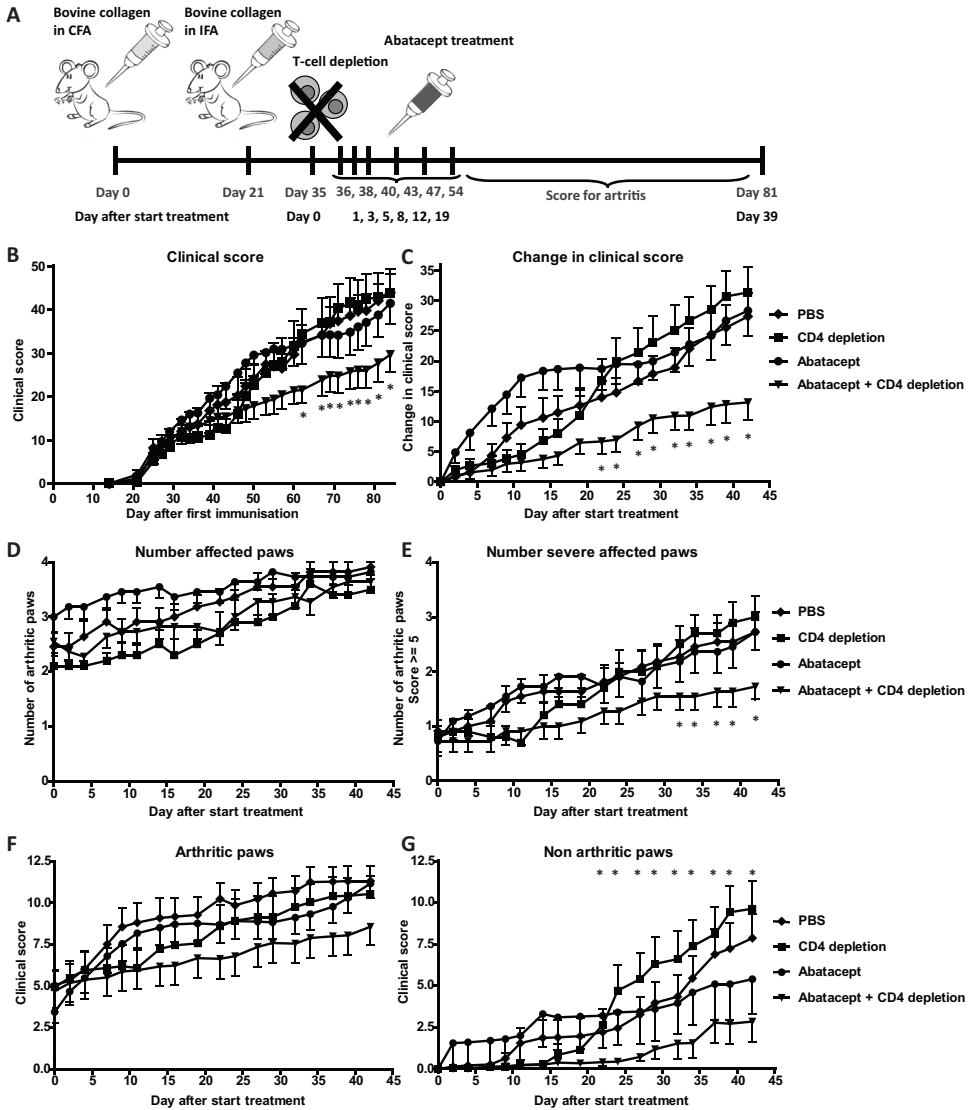
Figure 1. Abatacept decreased disease activity in mice depleted of CD4+ T cells by GK1.5. (A) Collagen induced arthritis was induced in male DBA/1 mice and when 80% of the mice showed signs of arthritis, treatment was started. One day before start of treatment CD4+ T cells were depleted by intraperitoneal administration of GK1.5 and the depletion was continued until the end of follow up. Treatment was administered by intraperitoneal injection of either PBS (diamonds), GK1.5 (CD4 depletion) (squares), Abatacept (circles) or the combination of GK1.5 and Abatacept (triangle). The mice were scored 3 times per week for inflammation in the paws to monitor disease progression. (B) Clinical score over time of the different treatment groups. (C) Change in clinical score from day of start of treatment over time of the different treatment groups. (D) Number of affected paws per treatment from the day of start of treatment over time. (E) Number of affected paws with a clinical score of 5 or higher (considered as severe affected paws) per treatment from the day of start of treatment. (F) Clinical score of paws that showed signs of arthritis at start of treatment over time per treatment. (G) Clinical score of paws that did not show signs of arthritis at start of treatment per treatment over time. Values are mean ± SEM, n=11 per treatment group. Statistical analysis was performed using the Student's T-test. * p<0.05 Abatacept + CD4 depletion vs CD4 depletion

Thus Abatacept treatment did not prevent arthritis development in non-affected joints, but it did reduce clinical score of affected joints (Figure 1F and 1G). Similar results were also obtained in an independent replication experiment (data not shown).
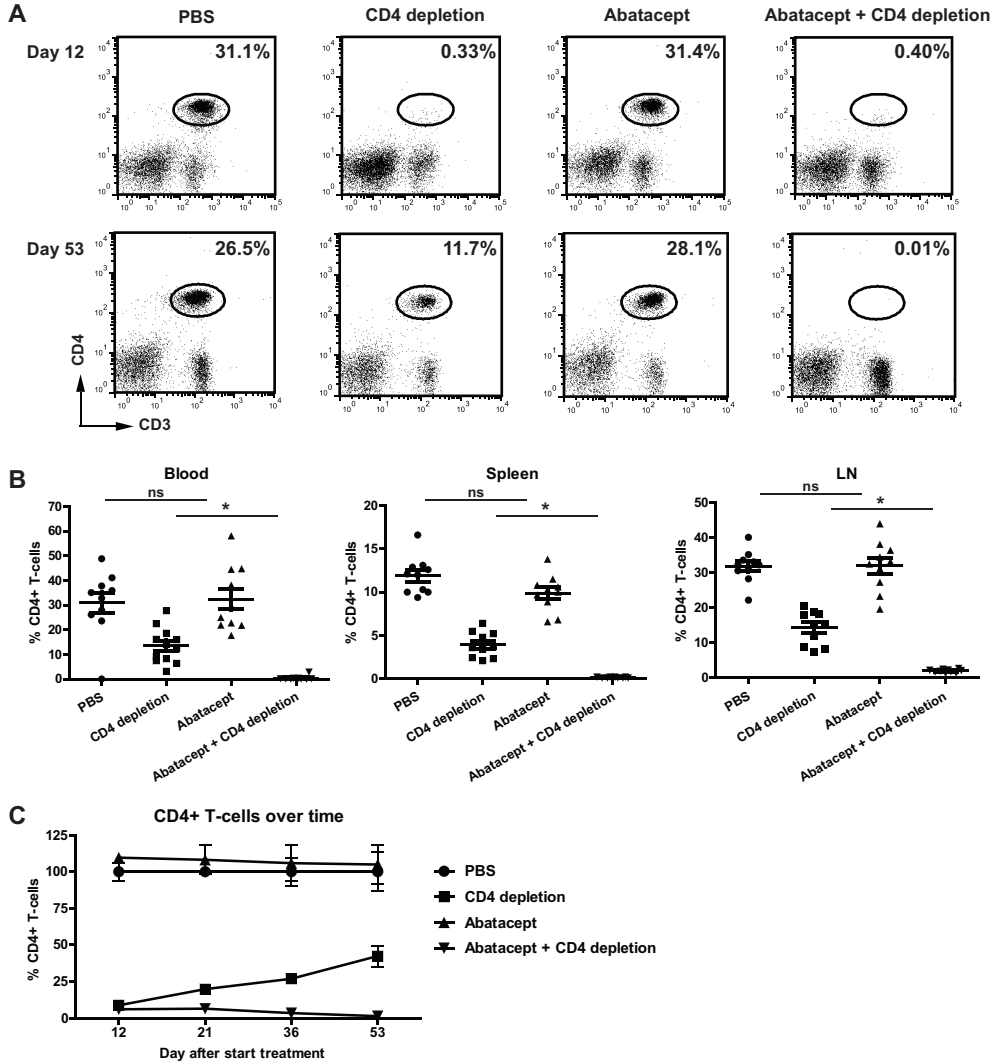
Figure 2. Incomplete CD4+ T cell depletion by GK1.5 over time. The presence of CD4+ T cells in the blood was monitored over time using flow cytometry. Blood was collected by tail incision during the experiment or cardiac puncture at sacrifice. After red blood cell lysis, blood mononuclear cells were cell-surface stained for CD45, CD3, CD4 and CD8. Cells were gated on CD45 and subsequently on CD3 and CD4. (A) Dotplots of representative mice of each treatment group on day 12 and day 53 after start of treatment (end of experiment). (B) Summary of the percentage of CD4+ T cells per treatment at the end of follow up is depicted for the blood, spleen and inguinal lymph node (LN). Each symbol represents 1 mouse. (C) Summary of CD4+ T cells in the blood over time as a percentage of the PBS treated group. Values are mean ± SEM, *n*=11 per treatment group. Statistical analysis was performed using the Student's T-test. * *p*<0.05 Abatacept + CD4 depletion vs CD4 depletion, ns=not significant

To confirm complete CD4+ T cell depletion CD4+ T cell frequencies were evaluated in blood of GK1.5-treated mice. On day 12 after start of treatment CD4+ T cells were correctly depleted as expected. However, on day 53 CD4+ T cell depletion was not complete anymore. In contrast, mice receiving the combination of Abatacept and CD4 depletion were still depleted of CD4+ T cells (Figure 2A). This was also the case in the spleen and inguinal lymph node (Figure 2B). Examining the frequency of CD4+ T cells over time indicated that from day 12 onwards the CD4+ T cell frequencies gradually increased until the end of the experiment. Nonetheless, at this time point CD4+ T cell frequencies were still significantly lower compared to the groups that did not receive GK1.5 (Figure 2C). In contrast, CD4+ T cells in the mice receiving the combination of GK1.5 and Abatacept treatment remained depleted (Figure 2C), conceivably as a result from the prevention of the development of an anti-rat antibody response against GK1.5 by Abatacept. Together, these results show that Abatacept is also effective in a situation where CD4+ T cell number is greatly reduced, suggesting a T cell-independent effect of Abatacept that inhibits the progression of arthritis.

Abatacept decreased disease activity in thymectomized mice depleted of CD4+ T cells

Although the data presented above point to a CD4+ T cell independent effect of Abatacept in the treatment of arthritis, they do not show such effects in a conclusive manner as CD4+ T cells returned after initial depletion. To ascertain that the CD4+ T cells were completely depleted during the treatment, a more stringent method of CD4+ T cell depletion was implemented. CIA was induced in mice that were thymectomized at 6 weeks after birth. After immunisation with collagen type II and arthritis development, CD4+ T cell depletion was performed using GK1.5. Because the mice were thymectomized, no new T cells could reappear in CD4+ T cell-depleted mice. Again, we observed that treatment with Abatacept resulted in reduced disease activity in CD4+ T cell-depleted mice (Figure 3B). Likewise, a reduced clinical score of paws that were not arthritic at the start of treatment was observed (Figure 3C) as well as a reduced number of severely affected paws, but Abatacept treatment did not prevent arthritis development in joints not affected at start of therapy (data not shown). Abatacept only treatment did not modulate the clinical score compared to PBS treatment (data not shown). To confirm that CD4+ T cells were completely depleted, CD4+ T cell frequencies were monitored over time by flow cytometry. Contrary to treatment with GK1.5 only (Figure 2), thymectomy in combination with GK1.5 treatment resulted in complete depletion of CD4+ T cells in mice receiving CD4 depletion (alone or in combination with Abatacept) (Figure 3D). These results indicate that Abatacept treatment results in decreased disease activity in the absence of CD4+ T cells.

Reduced antibody levels after treatment with Abatacept in the absence of CD4+ T cells

Collagen type II specific antibodies play a crucial role in the development of CIA[15]. Therefore, collagen type II specific and total IgG levels were determined over time in serum of the thymectomized mice by ELISA. Treatment with Abatacept in the absence of CD4+ T cells
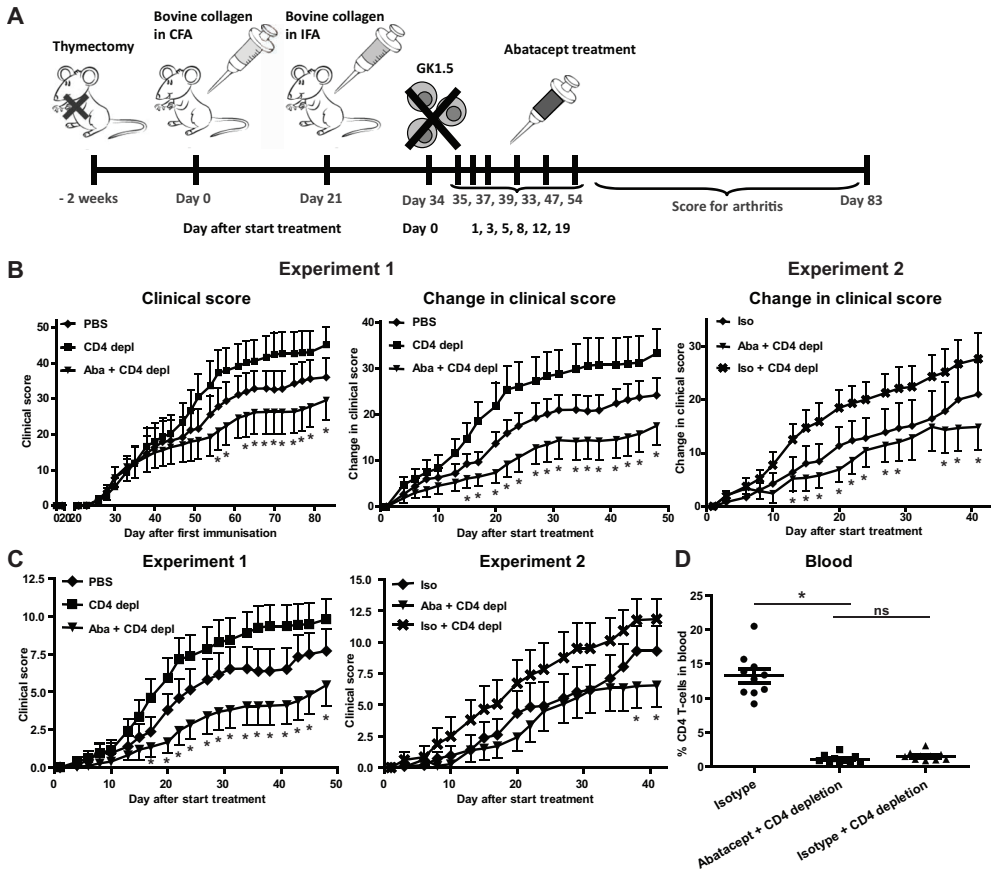
Figure 3. Abatacept decreased disease activity in thymectomized mice depleted of CD4+ T cells. (A) Collagen induced arthritis was induced in male DBA/1 mice 2 weeks after they were thymectomized. When 80% of the mice showed signs of arthritis, treatment was started. One day before start of treatment CD4+ T cells were depleted by intraperitoneal administration of GK1.5 and the depletion was continued till the end of follow up. Treatment was administered by intraperitoneal injection of PBS (diamonds), GK1.5 (squares; CD4 depl) or the combination of GK1.5 and Abatacept (triangle; Aba + CD4 depl). The mice were scored 3 times per week for inflammation in the paws to monitor disease progression. (B) Clinical score and change in clinical score from day of start of treatment over time of the different treatment groups (Experiment 1). n=10 per treatment group. The same experiment was independently repeated in another 10 mice per treatment group and an isotype for Abatacept was used as control treatment (diamond; iso) and in combination with CD4 depletion (cross; iso + CD4 depl) (Experiment 2). Change in clinical score from day of start of treatment is depicted. In C the clinical score of the paws that did not show signs of arthritis at the start of treatment is depicted for Experiment 1 and 2. The frequency of CD4+ T cells in blood at the end of follow up was determined by flow cytometry depicted in D. Abatacept only treatment is not depicted for readability of the graphs. Values are mean ± SEM. Statistical analysis was performed using the Student's T-test. * p<0.05 Abatacept + CD4 depletion vs control group, ns=not significant

resulted in decreased total IgG2a levels over time compared to control (Figure 4). More importantly, also a decrease in bovine collagen type II (immunisation antigen) and murine collagen type II (autoantigen) levels was detected after treatment with Abatacept and GK1.5 (Figure 4). This result was not specific for the IgG2a isotype as decreased IgG1 levels were

observed as well (Figure 4). Together, these results indicate that Abatacept treatment leads to a reduction in disease activity as well as collagen specific antibody levels in the absence of CD4+ T cells.
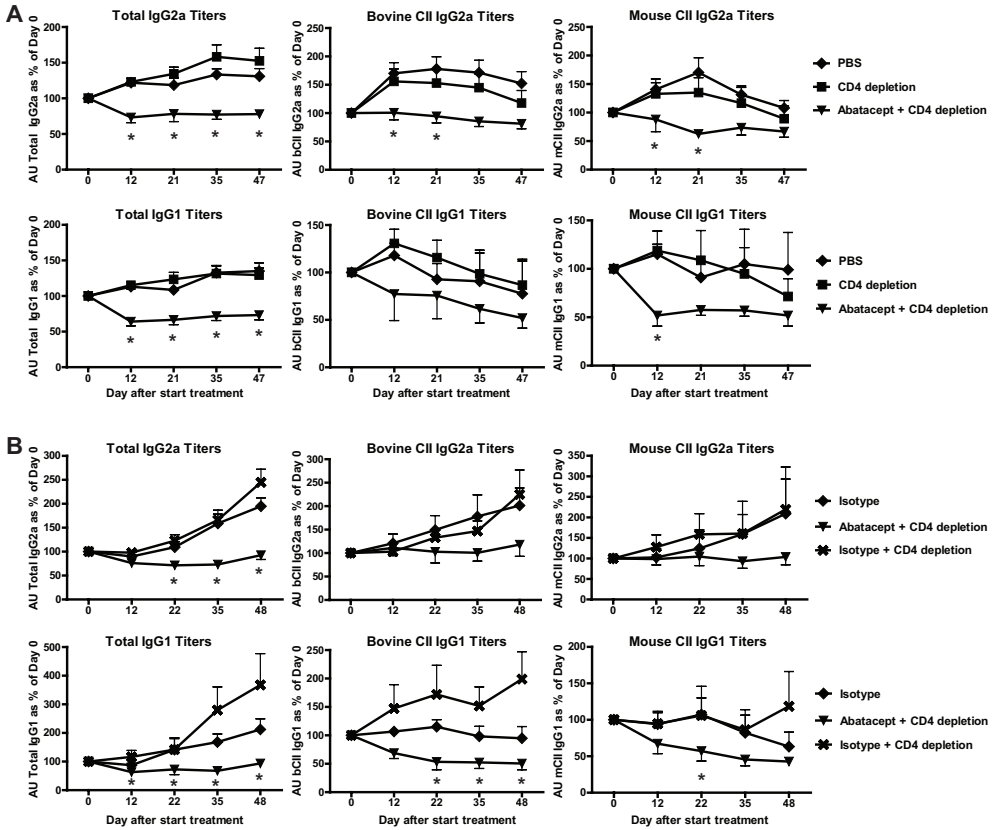
Figure 4. Reduced antibody levels after treatment with Abatacept in the absence of CD4+ T cells. Antibody levels were determined by ELISA over time. Serum samples were collected on day 0, 12, 21-22, 35 and 47-48 after start of treatment and total IgG2a and IgG1 levels were determined in the thymectomized mice. In addition, bovine and mouse collagen type II specific IgG2a and IgG1 levels were determined. Levels are depicted as percentage of day 0 in A. Figure B depicts an independent experiment including the isotype for Abatacept. Abatacept only treatment is not depicted for readability of the graphs, but showed comparable results to Abatacept + CD4 depletion. Levels are depicted as percentage of day 0. Values are mean ± SEM, *n*=10 per treatment group. Statistical analysis was performed using the Mann-Whitney U test. * *p*<0.05 Abatacept + CD4 depletion vs control group

Reduced antibody levels in supernatant of *ex vivo* cultured spleen and bone marrow cells after treatment with Abatacept in the absence of CD4+ T cells

The data presented above suggests that Abatacept treatment could directly affect the number and/or activity of antibody-secreting B cells. To study whether Abatacept in addition to the inhibition of costimulation of T cells also affected the antibody producing capacity of spleen and bone marrow derived B cells, we next isolated spleen- and bone marrow cells from

treated animals. Total IgG levels in the supernatant of *ex vivo* cultured, but not stimulated, spleen and bone marrow cells were subsequently analysed by ELISA (Figure 5). Spleen cells of mice treated with Abatacept and CD4 depletion produced lower IgG levels after 7 and 14 days of culture compared to spleen cells of mice receiving only CD4 depletion, although the percentage of B cells and plasma cells, as analysed by flow cytometry, was comparable between the different treatment groups (data not shown). This reduction in IgG production was also observed in the supernatant of cultured bone marrow cells indicating a loss of antibody producing capacity after Abatacept treatment in the absence of CD4+ T cells.
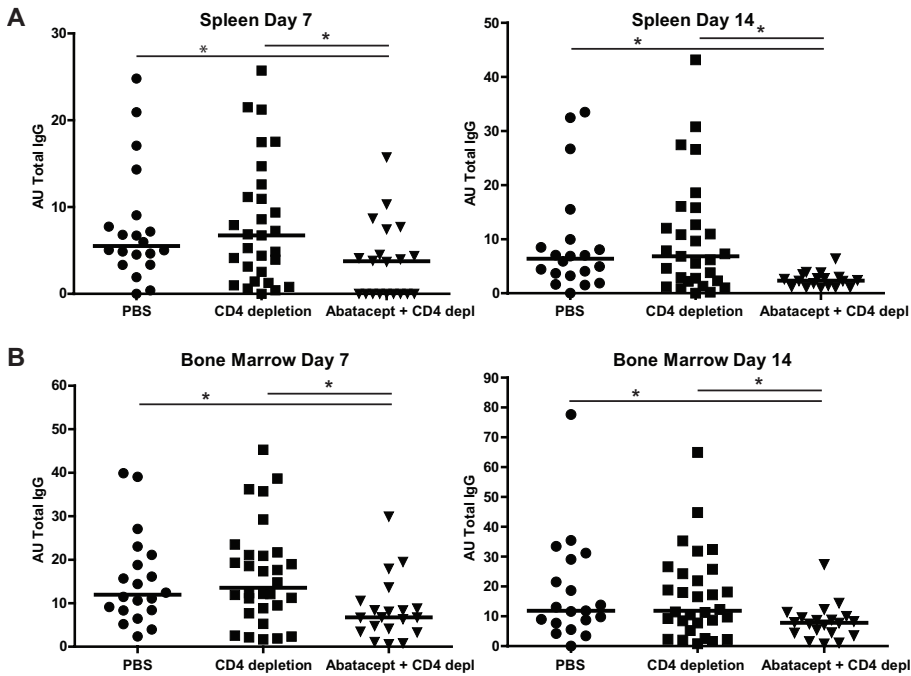
Figure 5. Abatacept decreased antibody levels detected in supernatant of *ex vivo* spleen and bone marrow cells in the absence of CD4+ T cells. At sacrifice spleen and bone marrow cells were collected and cultured without stimulation for 7 or 14 days and IgG production was measured in the supernatant by ELISA. (A) Summary of the IgG levels detected in supernatant of spleen cells of Experiment 1 and 2. The IgG levels of the PBS and isotype treated mice are combined and depicted as 'PBS' and the CD4 depletion and combination of isotype and CD4 depletion treated groups are combined and depicted as 'CD4 depletion'. (B) Summary of the IgG levels detected in supernatant of bone marrow cells cultured for 7 or 14 days of Experiment 1 and 2. Statistical analysis was performed using the Mann-Whitney U test. * *p*<0.05 Abatacept + CD4 depletion vs control group

DISCUSSION

Abatacept is an effective treatment in RA and is thought to block costimulation of T cells by inhibiting CD28-B7 interactions as Abatacept binds to both B7.1 and B7.2[6]. The interaction of CD28 with both B7 molecules is crucially important for the activation of naive T cells whereas its role in the activation of already activated/memory CD4+ T cells is less clear. As such CD4+ T cells are readily present in established disease, we investigated whether Abatacept is still

effective in the absence of CD4+ T cells in the established disease phase of the CIA model. Our study revealed that Abatacept treatment is able to decrease disease activity in the absence of CD4+ T cells, indicating that the mode of action mediated by Abatacept in CIA does not solely depend on its ability to block costimulation of T cells. In addition, Abatacept treatment is also capable of reducing collagen-specific and total antibody levels in a T cell independent setting. To evaluate the mode of action of Abatacept in established disease, CD4+ T cells were depleted using the rat anti-mouse CD4 antibody, GK1.5. Remarkably, after 12 days of depletion the CD4+ T cells gradually reappeared in mice treated with GK1.5 only. Interestingly, the CD4+ T cells remained properly depleted in mice treated with the combination of Abatacept and GK1.5. This observation is most likely explained by the notion that mice treated with GK1.5 develop an anti-rat antibody response ultimately neutralizing the CD4 depleting antibodies. This illustrates that Abatacept is also capable of blocking costimulation and thereby the activation of naive T cells, preventing the development of the anti-rat response. Therefore, the depletion of CD4+ T cells by GK1.5 in mice treated with Abatacept resulting in the complete and sustained depletion of CD4+ T cells until the end of follow up. For this reason, we also depleted CD4+ T cells in thymectomized mice to prevent the reappearance of new T cells when the GK1.5 treatment became less effective and we obtained similar results.

Our results indicate that CD4+ T cells are not required for disease progression once arthritis is established, since the mice treated with GK1.5 only showed comparable or a trend towards more severe disease progression as compared to the control groups. These observations are in line with the observation by Morgan *et al.* describing that lethal irradiation of mice with CIA, followed by syngeneic bone marrow transplantation, results in continuation of the disease even though the T cells were depleted[16]. Thus, CD4+ T cells are not required for arthritis progression once the disease has become clinically manifest in the CIA model. The presented results are obtained in a mouse model, however, it is not known whether Abatacept has a direct effect on other cell types in addition to T cells in the human situation. Nonetheless, a recent study in RA, comparing head-to-head anti-TNF and Abatacept treatment reported comparable efficacy based on clinical, functional and radiographic outcomes[12]. Intriguingly, no difference in the rate of response was noted as similar improvements were observed over time. As one could speculate that a T cell targeting drug would require more time to mediate its beneficial effects compared to a TNF inhibitor, this observation could be compatible with the notion that Abatacept has a different mode of action in addition to the blocking effect on T cell costimulation in humans as well.

The observation that Abatacept is capable of decreasing disease activity in the absence of CD4+ T cells does not contradict with the 'dogma' that the mode of action of Abatacept is mediated through blockade of costimulation and thereby activation of (naive) CD4+ T cells. However, our results do indicate that Abatacept also has another mode of action in addition to its effects on costimulation. A limitation of our study is that we did not elucidate the mechanism responsible for the inhibitory effect of Abatacept on arthritis. In this respect

Abatacept is no different from other DMARDs as methotrexate for which the exact mode of action is also not elucidated. Nonetheless, it would be interesting to delineate these additional modes of action[17] as it could allow for a more refined targeted therapy and additional insights into the etiological pathways of disease.

Recently, Rozanski *et al.* have described that CD28 serves as a survival factor for long lived plasma cells. Loss of CD28 or B7.1 (CD80) and B7.2 (CD86) caused significant loss of long lived plasma cells resulting in decreased antibody titers[18]. As Abatacept prevents the binding of CD28 to CD80/86, this survival signal could be abrogated leading to loss of plasma cells and consequently a decrease in antibody titers. Indeed, this would be in line with our observation of decreased antibody levels after Abatacept treatment, reduction of clinical scores as well as our observation of decreased antibody production by cultured spleen and bone marrow cells from CD4+ T cell depleted mice treated with Abatacept. Likewise, in the BXD2 mouse model of autoimmune disease it has been reported that elevated expression of activation induced cytidine deaminase (AID) in recirculating follicular CD86+ B cells and increased germinal centre activity are associated with the production of autoantibodies[19]. Treatment with CTLA-4-Ig resulted in normalization of AID expression in the B cells and suppression of IgG autoantibodies, which could explain the decrease in IgG titers we observed after Abatacept treatment in the absence of CD4+ T cells.

The CD4+ T cell independent effect of Abatacept could also be explained by the induction of nitric oxide synthase (NOS) or indoleamine 2,3-dioxygenase (IDO) by antigen presenting cells[20-22]. IDO is an enzyme that degrades the essential amino acid tryptophan resulting in local depletion of tryptophan[23], which leads to cell cycle arrest[24,25] and thereby inhibition of T cell proliferation and expansion of the immune response[26-28]. IDO has been implicated in disease aetiology as, for example, it has been reported that CTLA-4 on regulatory T cells can induce IDO in APCs[29], but that regulatory T cells from RA patients fail to induce such expression due to low CTLA-4 expression[30]. In addition to the suppressing effect of IDO on proliferating effector T cells, IDO expressing dendritic cells are able to promote the activation of regulatory T cells[31] and the differentiation of naïve T cells to regulatory T cells[23,32] which could explain the inflammation suppressing effects of Abatacept. However, Davis *et al.*[33] reported inhibition of naïve and memory T cell proliferation and effector function in the absence of IDO induction, indicating that Abatacept could also have other mechanisms of action.

Abatacept could also have an effect on osteoclast precursors explaining the anti-erosive effects of Abatacept[34,35] or on monocytes by modulating their migratory capacity)[36]. Direct effects on macrophages have also been described resulting in decreased cytokine production and reduction of the inflammatory reaction[37-40] which could account for the beneficial effects in the treatment of RA.

In conclusion, Abatacept is thought to block costimulation of T cells by blocking the interaction between CD28 and B7 resulting in inhibition of T cell activation. However, Abatacept reduced disease progression and activity in the absence of CD4+ T cells in the CIA mouse model

indicating that Abatacept can exert its action in established arthritis independent from its effects on CD4+ T cell activation. Since a head-to-head comparison of anti-TNF and Abatacept treatment resulted in comparable efficacy with a similar time course, it is tempting to speculate that Abatacept could have an effect on other cell types in addition to T cells in human RA as well.

REFERENCES

1.   Silman AJ, Pearson JE. Epidemiology and genetics of rheumatoid arthritis. Arthritis Res 2002;4 Suppl 3:S265-S72.

2.   Gabriel SE. The epidemiology of rheumatoid arthritis. Rheum Dis Clin North Am 2001;27:269-81.

3.   Smolen JS, Steiner G. Therapeutic strategies for rheumatoid arthritis. Nat Rev Drug Discov 2003;2:473-88.

4.   Kremer JM, Westhovens R, Leon M, et al. Treatment of rheumatoid arthritis by selective inhibition of T-cell activation with fusion protein CTLA4Ig. N Engl J Med 2003;349:1907-15.

5.   Genovese MC, Becker JC, Schiff M, et al. Abatacept for rheumatoid arthritis refractory to tumor necrosis factor alpha inhibition. N Engl J Med 2005;353:1114-23.

6.   Emery P. The therapeutic potential of costimulatory blockade with CTLA4Ig in rheumatoid arthritis. Expert Opin Investig Drugs 2003;12:673-81.

7.   Webb LM, Walmsley MJ, Feldmann M. Prevention and amelioration of collagen-induced arthritis by blockade of the CD28 co-stimulatory pathway: requirement for both B7-1 and B7-2. Eur J Immunol 1996;26:2320-8.

8.   Knoerzer DB, Karr RW, Schwartz BD, Mengle-Gaw LJ. Collagen-induced arthritis in the BB rat. Prevention of disease by treatment with CTLA-4-Ig. J Clin Invest 1995;96:987-93.

9.   Kliwinski C, Kukral D, Postelnek J, et al. Prophylactic administration of abatacept prevents disease and bone destruction in a rat model of collagen-induced arthritis. J Autoimmun 2005;25:165-71.

10.   Boesteanu AC, Katsikis PD. Memory T cells need CD28 costimulation to remember. Semin Immunol 2009;21:69-77.

11.   Ndejembi MP, Teijaro JR, Patke DS, et al. Control of memory CD4 T cell recall by the CD28/B7 costimulatory pathway. J Immunol 2006;177:7698-706.

12.   Schiff M, Weinblatt ME, Valente R, et al. Head-to-head comparison of subcutaneous abatacept versus adalimumab for rheumatoid arthritis: two-year efficacy and safety findings from AMPLE trial. Ann Rheum Dis 2014;73:86-94.

13.   Stoop JN, Liu BS, Shi J, et al. Antibodies specific for carbamylated proteins precede the onset of clinical symptoms in mice with collagen induced arthritis. PLoS One 2014;9:e102163.

14.   van Duivenvoorde LM, Han WG, Bakker AM, et al. Immunomodulatory dendritic cells inhibit Th1 responses and arthritis via different mechanisms. J Immunol 2007;179:1506-15.

15.   Luross JA, Williams NA. The genetic and immunopathological processes underlying collagen-induced arthritis. Immunology 2001;103:407-16.

16.   Morgan ME, Flierman R, van Duivenvoorde LM, et al. Effective treatment of collagen-induced arthritis by adoptive transfer of CD25+ regulatory T cells. Arthritis Rheum 2005;52:2212-21.

17.   Cutolo M, Nadler SG. Advances in CTLA-4-Ig-mediated modulation of inflammatory cell and immune response activation in rheumatoid arthritis. Autoimmun Rev 2013;12:758-67.

18.   Rozanski CH, Arens R, Carlson LM, et al. Sustained antibody responses depend on CD28 function in bone marrow-resident plasma cells. J Exp Med 2011;208:1435-46.

19.   Hsu HC, Wu Y, Yang P, et al. Overexpression of activation-induced cytidine deaminase in B cells is associated with production of highly pathogenic autoantibodies. J Immunol 2007;178:5357-65.

20.   Deppong CM, Parulekar A, Boomer JS, Bricker TL, Green JM. CTLA4-Ig inhibits allergic airway inflammation by a novel CD28-independent, nitric oxide synthase-dependent mechanism. Eur J Immunol 2010.

21.   Grohmann U, Orabona C, Fallarino F, et al. CTLA-4-Ig regulates tryptophan catabolism in vivo. Nat Immunol 2002;3:1097-101.

3

22.   Munn DH, Sharma MD, Mellor AL. Ligation of B7-1/B7-2 by human CD4+ T cells triggers indoleamine 2,3-dioxygenase activity in dendritic cells. J Immunol 2004;172:4100-10.

23.   Mellor AL, Munn DH. IDO expression by dendritic cells: tolerance and tryptophan catabolism. Nat Rev Immunol 2004;4:762-74.

24.   Munn DH, Sharma MD, Baban B, et al. GCN2 kinase in T cells mediates proliferative arrest and anergy induction in response to indoleamine 2,3-dioxygenase. Immunity 2005;22:633-42.

25.   Lee GK, Park HJ, Macleod M, Chandler P, Munn DH, Mellor AL. Tryptophan deprivation sensitizes activated T cells to apoptosis prior to cell division. Immunology 2002;107:452-60.

26.   Mellor AL, Keskin DB, Johnson T, Chandler P, Munn DH. Cells expressing indoleamine 2,3-dioxygenase inhibit T cell responses. J Immunol 2002;168:3771-6.

27.   Mellor AL, Baban B, Chandler P, et al. Cutting edge: induced indoleamine 2,3 dioxygenase expression in dendritic cell subsets suppresses T cell clonal expansion. J Immunol 2003;171:1652-5.

28.   Terness P, Bauer TM, Rose L, et al. Inhibition of allogeneic T cell proliferation by indoleamine 2,3-dioxygenase-expressing dendritic cells: mediation of suppression by tryptophan metabolites. J Exp Med 2002;196:447-57.

29.   Fallarino F, Grohmann U, Hwang KW, et al. Modulation of tryptophan catabolism by regulatory T cells. Nat Immunol 2003;4:1206-12.

30.   Cribbs AP, Kennedy A, Penn H, et al. Treg cell function in rheumatoid arthritis is compromised by ctla-4 promoter methylation resulting in a failure to activate the indoleamine 2,3-dioxygenase pathway. Arthritis Rheumatol 2014;66:2344-54.

31.   Sharma MD, Baban B, Chandler P, et al. Plasmacytoid dendritic cells from mouse tumor-draining lymph nodes directly activate mature Tregs via indoleamine 2,3-dioxygenase. J Clin Invest 2007;117:2570-82.

32.   Chen W, Liang X, Peterson AJ, Munn DH, Blazar BR. The indoleamine 2,3-dioxygenase pathway is essential for human plasmacytoid dendritic cell-induced adaptive T regulatory cell generation. J Immunol 2008;181:5396-404.

33.   Davis PM, Nadler SG, Stetsko DK, Suchard SJ. Abatacept modulates human dendritic cell-stimulated T-cell proliferation and effector function independent of IDO induction. Clin Immunol 2008;126:38-47.

34.   Bozec A, Zaiss MM, Kagwiria R, et al. T cell costimulation molecules CD80/86 inhibit osteoclast differentiation by inducing the IDO/tryptophan pathway. Sci Transl Med 2014;6:235ra60.

35.   Axmann R, Herman S, Zaiss M, et al. CTLA-4 directly inhibits osteoclast formation. Ann Rheum Dis 2008;67:1603-9.

36.   Bonelli M, Ferner E, Goschl L, et al. Abatacept (CTLA-4IG) treatment reduces the migratory capacity of monocytes in patients with rheumatoid arthritis. Arthritis Rheum 2013;65:599-607.

37.   Cutolo M, Soldano S, Montagna P, et al. CTLA4-Ig interacts with cultured synovial macrophages from rheumatoid arthritis patients and downregulates cytokine production. Arthritis Res Ther 2009;11:R176.

38.   Cutolo M, Soldano S, Contini P, et al. Intracellular NF-kB-decrease and IKBalpha increase in human macrophages following CTLA4-Ig treatment. Clin Exp Rheumatol 2013;31:943-6.

39.   Wenink MH, Santegoets KC, Platt AM, et al. Abatacept modulates proinflammatory macrophage responses upon cytokine-activated T cell and Toll-like receptor ligand stimulation. Ann Rheum Dis 2012;71:80-3.

40.   Brizzolara R, Soldano S, Montagna P, et al. [CTLA4-Ig interferes and downregulates the proinflammatory activities of rheumatoid synovial macrophages in monoculture]. Reumatismo 2011;63:80-5.

3

CHAPTER 4

CONVERSION TO SERONEGATIVE STATUS AFTER ABATACEPT TREATMENT IN PATIENTS WITH EARLY AND POOR PROGNOSTIC RHEUMATOID ARTHRITIS IS ASSOCIATED WITH BETTER RADIOGRAPHIC OUTCOMES AND SUSTAINED REMISSION

Diahann T. S. L. Jansen, Paul Emery, Josef S. Smolen, Rene Westhovens, Manuela Le Bars, Sean E. Connolly, June Ye, Rene E. M. Toes & Tom W. J. Huizinga
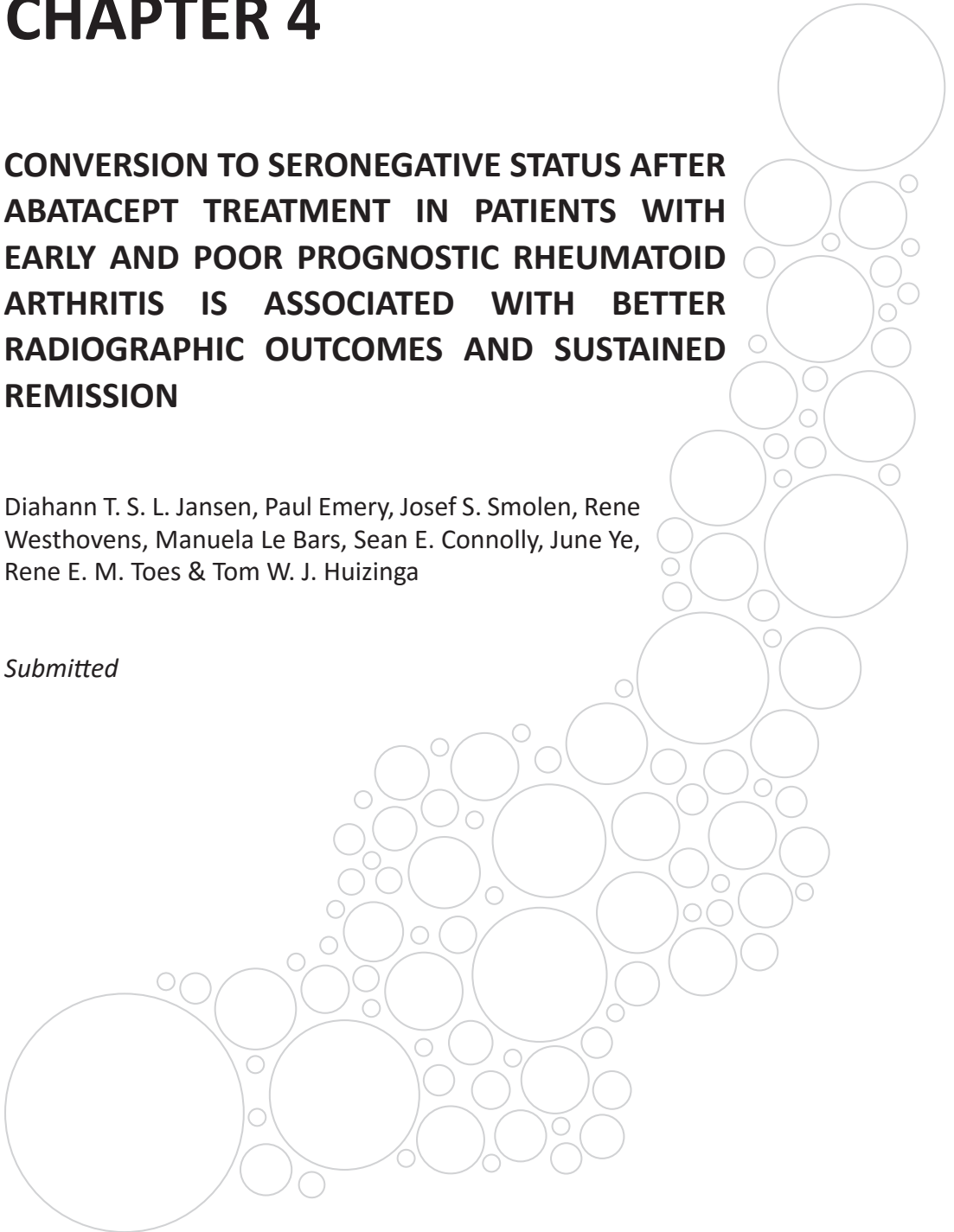
ABSTRACT

Introduction This post hoc analysis evaluated the effects of the T cell co-stimulation blocker abatacept on anti-citrullinated protein antibodies (ACPA) and rheumatoid factor (RF) in early rheumatoid arthritis (RA), and the association between changes in serological status and clinical response.

Methods Data from a double-blind, randomised and controlled phase III study (AGREE) in methotrexate (MTX)-naive patients with early RA with poor prognostic factors were used in this analysis. Patients were randomised to abatacept (~10 mg/kg intravenously according to weight range) or placebo, plus MTX over 12 months followed by open-label abatacept plus MTX for a further 12 months. Autoantibody titres were determined by enzyme-linked immunosorbent assay at baseline and 6 and 12 months of the double-blind phase. Conversion to seronegative status was evaluated and its association with clinical response was assessed at months 6 and 12.

Results Patients receiving abatacept plus MTX showed a greater decrease in ACPA (but not RF) titres and higher rates of both ACPA and RF conversion to seronegative status than patients treated with MTX alone. A higher proportion of patients converting to ACPA seronegative status receiving abatacept plus MTX achieved remission according to Disease Activity Score in 28 joints (C-reactive protein) or Clinical Disease Activity Index than patients who remained ACPA seropositive. Patients who converted to ACPA seronegative status treated with abatacept plus MTX had a greater cumulative probability of achieving sustained remission and less radiographic progression than those receiving MTX alone or patients in either treatment arm who remained ACPA seropositive.

Conclusions Compared with MTX alone, treatment with abatacept plus MTX was more likely to induce conversion to ACPA/RF seronegative status in patients with early, erosive RA. Conversion to ACPA seronegative status was associated with better clinical and radiographic outcomes.

INTRODUCTION

Rheumatoid arthritis (RA) is characterised by the production of autoantibodies, in particular rheumatoid factor (RF) and anti-citrullinated protein antibodies (ACPA)[1]. An estimated 50–70% of patients with RA present with detectable ACPA titres, which are mainly of the immunoglobulin (Ig)G isotype and directed against post-translationally modified proteins[1-3]. RF autoantibodies are primarily of the IgM isotype and directed against the Fc-portion of the IgG isotype[1]. RF and ACPA can be present without clinical symptoms for up to 10 years before the onset of RA[4-8], and as such make interesting early biomarkers for the disease. Both RF and ACPA are moderately correlated with markers of inflammation, although the correlation is greater for RF[9]. ACPA is particularly sensitive for diagnosis and is a better prognostic indicator than RF for more severe RA and more rapid disease progression[1,3]. In an early RA cohort, ACPA positivity was associated with a higher rate of joint destruction[10]. Hecht *et al.* demonstrated that both erosion number and size were highest in patients with concomitant ACPA and RF, and that their effects were additive[11]. On the other hand, the presence of RF compared with its absence is associated with higher disease activity in ACPA+ patients[12], in line with the amplifying role of RF[13]. In addition, RF- and ACPA-producing B cells are detectable at high levels in the synovial fluid of patients with RA, suggesting a direct contribution to synovial inflammation[14-17].

A recent report from Rombouts *et al.* provides evidence for a role of T cells in ACPA production. The authors reported that, unlike other autoantibodies or non-reactive IgG, ACPA IgG undergo N-linked glycosylation of the Fab variable domains[18]. The authors hypothesize that this glycosylation requires consensus sites not present in the germline Fab domain sequence, and that these sites are introduced by somatic hypermutation of the Ig variable region[18]. Somatic hypermutation occurs during the process of B-cell proliferation and differentiation that is regulated in part by activated T cells[3]. In addition, the strong association between ACPA and human leukocyte antigen class II genes suggests a role for antigen-specific CD4+ T cells in the immune response against citrullinated proteins[19].

Abatacept is a soluble fusion protein consisting of the extracellular domain of human cytotoxic T lymphocyte-associated antigen-4 (CTLA-4) linked to the modified Fc portion of human IgG1. Abatacept binds to CD80/CD86 on antigen-presenting cells (APCs), thereby blocking the interaction between CD80/CD86 and CD28 on T cells and inhibiting T cell co-stimulation[20,21]. In addition to peptide–major histocompatibility complex recognition between APCs and T cells, co-stimulation is required for (naive) T cells to become fully activated[1]. Thus, if co-stimulation is blocked, B cell differentiation into antibody-producing cells will likely be inhibited and antibody production impaired. Treatment with abatacept, through inhibition of T cell co-stimulation, might therefore be expected to impact on antibody production by B cells.

Abatacept is an effective treatment for both established[22,23] and early RA[24,25], and early treatment of RA has been shown to prevent disease progression and joint damage[24-27]. The

Abatacept trial to Gauge Remission and joint damage progression in methotrexate-naive patients with Early Erosive rheumatoid arthritis (AGREE) was a 2-year, phase III study with a 1-year, double-blind phase that assessed the efficacy, safety and tolerability of intravenous abatacept plus methotrexate (MTX) compared with placebo plus MTX, in MTX-naive patients with early erosive RA and poor prognostic indicators[28,29]. The primary results of the study demonstrated that treatment with abatacept plus MTX resulted in significantly greater and more sustained clinical and radiographic benefits than treatment with placebo plus MTX.

Since abatacept's mode of action includes inhibition of T cell co-stimulation, it was hypothesized that patients who converted to a seronegative status might have a better clinical response to abatacept treatment than those who remained seropositive. This post-hoc analysis of the AGREE study investigated the effects of abatacept in combination with MTX versus MTX alone on conversion to seronegative status in ACPA-seropositive and RF-seropositive patients, and the relationship between seroconversion and clinical response.

METHODS

Patient population and study design

This was a post hoc analysis performed using data from the previously published AGREE study (ClinicalTrials.gov identifier NCT00122382)[28,29]. Briefly, MTX-naive patients with early RA (≤2 years since diagnosis) who were positive for RF and/or ACPA antibodies and had evidence of erosion were randomised 1:1 to receive abatacept (~10 mg/kg intravenously according to weight range) plus MTX or placebo plus MTX (hereafter referred to as 'MTX alone') over a 12-month double-blind period followed by open-label abatacept plus MTX for an additional 12 months[28,29]. At baseline, all patients had high disease activity based on a tender joint count of ≥12, a swollen joint count of ≥10 and C-reactive protein (CRP) levels of ≥0.45 mg/dL.

Determination of autoantibody titres

Serum samples to assess levels of second-generation anti-cyclic citrullinated peptide-2 (a surrogate of ACPA) antibodies and RF were taken at screening and at 6 and 12 months of the double-blind period. Anti-cyclic citrullinated peptide-2 and RF antibody titres were determined by enzyme-linked immunosorbent assay (ELISA). The cut-off for ACPA positivity was 5 AU/mL and 15 IU/mL for RF positivity.

Outcome measures

ACPA and RF seroconversion was determined by comparing baseline antibody titres with titres at months 6 or 12 of the double-blind phase. All patients were positive for RF and/or ACPA at baseline. Those with antibody titres below the limit of detection by ELISA at months 6 or 12 were considered to have converted to a seronegative state.

Disease activity was measured using the Disease Activity Score in 28 joints (CRP) (DAS28 [CRP]) or the Clinical Disease Activity Index (CDAI). Remission was defined as DAS28 (CRP) <2.6 or CDAI ≤2.8. First remission was defined as the first visit at which a patient met the

requirements to achieve remission. Sustained first remission was defined as the first visit at which remission was reached and subsequently maintained for every visit up to month 12. First remission was determined after 6 and 12 months and sustained first remission was determined after 12 months of treatment.

Radiographs of the hands and feet were taken at screening, at 6 and 12 months and at the discontinuation visit. The Genant-modified Sharp scoring method was used to assess the mean change from baseline in total Sharp score (TSS), and erosion and joint space narrowing (JSN) scores at months 6 and 12.

Statistical analysis

In the original study, DAS28 (CRP)-defined remission was evaluated for the intent-to-treat population, with patients who discontinued considered to be non-responders. For the purpose of this report, analyses were based on patients with DAS28 (CRP) and CDAI data available at baseline and months 6 and 12. The proportions of patients achieving remission according to DAS28 (CRP) and CDAI were analysed as point estimates with 95% confidence intervals (CIs). Cumulative probability of time to achieve first remission and sustained first remission according to DAS28 (CRP)-defined and CDAI criteria were evaluated based on Kaplan–Meier estimates with 95% CIs. Patients who lost remission status were censored at the time of remission loss.

Mean changes from baseline in ACPA and RF titres were evaluated by analysis of covariance with treatment, baseline score and disease status as covariates. The adjusted mean change, treatment differences and corresponding 95% CIs were presented for months 6 and 12. In addition, the proportion of patients with conversion to ACPA and RF seronegative status at months 6 and 12 were analysed using point estimates with 95% CIs. The relationship between DAS28 (CRP) or CDAI remission and conversion to ACPA or RF seronegative status was investigated by determining the proportions (95% CIs) of patients in remission by seroconversion status at months 6 and 12, and between-group comparisons were made using the chi-square test. Mean changes from baseline in TSS, erosion and JSN scores were evaluated by analysis of covariance with treatment, baseline score and disease status as covariates. The adjusted mean change, treatment differences and corresponding 95% CIs were presented for months 6 and 12.

RESULTS

Patient population

In the original study, 509 patients were randomly assigned to receive abatacept plus MTX (n = 256) or MTX alone (n = 253)[22]. Of these, 459 patients completed year 1 and 433 completed year 2 [23]. Demographic data and baseline characteristics have been previously published[22,23]. Of the 434 patients who had ACPA status measures at baseline, month 6 and month 12, 21 (4.8%) were seronegative at month 6. Of the 461 patients who had RF status measures at baseline, month 6 and month 12, 61 (13.2%) were seronegative at month 6.

Table 1. Patient demographic data and baseline disease characteristics by conversion to ACPA and RF seronegative status at month 6

	Conversion to ACPA seronegative status		Persistent ACPA seropositive		Conversion to RF seronegative status		Persistent RF seropositive	
	Abatacept + MTX	MTX alone	Abatacept + MTX	MTX alone	Abatacept + MTX	MTX alone	Abatacept + MTX	MTX alone
	(n = 15)	(n = 6)	(n = 212)	(n = 202)	(n = 39)	(n = 22)	(n = 191)	(n = 209)
Age, years	50.7 (11.1)	61.2 (11.4)	49.8 (12.3)	48.8 (12.7)	51.6 (10.3)	49.5 (14.4)	49.6 (12.6)	49.7 (12.8)
Female, n (%)	13 (86.7)	6 (100)	157 (74.1)	159 (78.7)	29 (74.4)	18 (81.8)	145 (75.9)	170 (81.3)
Weight, kg	65.6 (17.0)	68.8 (16.6)	72.3 (17.8)	72.7 (17.9)	71.2 (17.2)	68.1 (16.1)	71.9 (18.3)	73.5 (18.1)
Race, White, n (%)	14 (93.3)	4 (66.7)	167 (78.8)	173 (85.6)	34 (87.2)	20 (90.9)	147 (77.0)	179 (85.6)
Region, n (%)								
N. America	2 (13.3)	0	40 (18.9)	27 (13.4)	9 (23.1)	3 (13.6)	32 (16.8)	34 (16.3)
S. America	5 (33.3)	0	83 (39.2)	87 (43.1)	7 (17.9)	9 (40.9)	88 (46.1)	88 (42.1)
Europe	7 (46.7)	4 (66.7)	72 (34.0)	75 (37.1)	20 (51.3)	8 (36.4)	56 (29.3)	74 (35.4)
ROW	1 (6.7)	2 (33.3)	17 (8.0)	13 (6.4)	3 (7.7)	2 (9.1)	15 (7.9)	13 (6.2)
Duration of RA, months	8.9 (8.8)	1.7 (1.5)	6.0 (7.4)	7.0 (7.1)	3.7 (5.0)	6.9 (8.0)	7.1 (8.0)	7.0 (7.1)
Tender joints	30.0 (16.2)	20.3 (6.9)	31.1 (14.9)	30.3 (13.7)	24.6 (14.3)	29.8 (15.0)	32.9 (15.1)	30.9 (14.0)
Swollen joints	23.2 (10.3)	15.8 (7.6)	22.9 (11.7)	22.4 (10.4)	20.9 (9.6)	20.4 (10.1)	23.7 (11.9)	22.4 (10.4)
Patient pain assessment	62.5 (25.5)	56.6 (27.4)	67.2 (22.2)	66.8 (22.5)	64.6 (24.9)	61.4 (22.3)	67.9 (22.4)	67.6 (22.8)
HAQ-DI	1.4 (0.7)	1.7 (0.6)	1.7 (0.7)	1.7 (0.7)	1.6 (0.5)	1.7 (0.6)	1.7 (0.7)	1.7 (0.7)
Patient global assessment, 100-mm VAS	61.7 (25.7)	50.3 (28.2)	66.3 (21.3)	64.3 (23.6)	67.5 (22.0)	61.5 (22.9)	65.4 (22.6)	63.7 (24.3)
Physician global assessment, 100-mm VAS	59.4 (16.3)	56.7 (17.4)	67.9 (18.2)	65.4 (19.1)	64.1 (18.5)	61.9 (16.0)	68.2 (18.3)	66.1 (19.4)
DAS28 (CRP)	6.2 (0.9)	5.9 (0.7)	6.3 (1.0)	6.3 (1.0)	6.1 (0.9)	6.0 (1.1)	6.4 (1.0)	6.3 (1.0)
DAS28 (ESR)	7.2 (0.6)	6.2 (0.7)	6.9 (1.0)	6.7 (1.1)	6.7 (0.8)	6.4 (1.3)	6.9 (1.0)	6.8 (1.1)
ESR, mm/h	44.4 (18.0)	55.5 (34.3)	49.5 (28.8)	49.8 (32.9)	48.5 (21.3)	41.2 (24.3)	49.4 (29.9)	51.1 (32.7)
CRP, mg/dL	2.4 (2.0)	4.7 (3.4)	3.3 (3.3)	3.8 (5.4)	3.0 (3.0)	2.6 (3.2)	3.2 (3.1)	3.8 (5.4)
Baseline RF positive, n (%)	14 (93.3)	6 (100)	204 (96.2)	197 (97.5)	39 (100)	22 (100)	191 (100)	209 (100)
Baseline ACPA positive, n (%)	15 (100)	6 (100)	212 (100)	202 (100)	34 (87.2)	15 (68.2)	179 (93.7)	185 (88.5)
Total Sharp score	7.1 (8.7)	15.4 (17.1)	7.7 (9.8)	6.7 (8.6)	6.6 (10.6)	5.7 (5.9)	7.6 (9.3)	6.5 (8.6)
JSN score	2.5 (4.6)	5.8 (9.7)	2.1 (4.1)	1.8 (3.9)	2.0 (4.8)	1.5 (2.5)	2.1 (3.9)	1.9 (4.1)
Erosion score	4.6 (5.0)	9.6 (8.1)	5.6 (6.3)	4.9 (5.5)	4.6 (6.2)	4.2 (3.9)	5.5 (6.1)	4.6 (5.2)

Data are mean (SD) unless stated otherwise. Conversion to ACPA or RF seronegative status at month 6 meant that patients who were ACPA or RF seropositive at baseline, respectively, became seronegative at month 6; persistent ACPA or RF seropositive meant that patients were ACPA or RF seropositive at both baseline and at month 6.

ACPA anti-citrullinated protein antibody, *CRP* C-reactive protein, *DAS28* Disease Activity Score in 28 joints, *ESR* erythrocyte sedimentation rate, *HAQ-DI* Health Assessment Questionnaire-Disability Index, *JSN* joint space narrowing, *MTX* methotrexate, *N. America* North America, *RA* rheumatoid arthritis, *RF* rheumatoid factor, *ROW* rest of world, *S. America* South America, *SD* standard deviation, *VAS* visual analogue scale

Patient demographic data and baseline disease characteristics by conversion to ACPA and RF seronegative status at month 6 are shown in Table 1. The baseline disease activity in the patients who seroconverted was DAS28-CRP 5.9 for the MTX treated patients compared to 6.2 in the Abatacept + MTX arm.

RF and ACPA titres following treatment with abatacept plus MTX or MTX alone

A decrease in autoantibody levels after 6 and 12 months, compared with baseline, was observed for all study groups. Mean ACPA and RF titres decreased from baseline following treatment with abatacept plus MTX and MTX alone (Figure 1). Whereas similar decreases in RF titres were observed in both treatment groups, treatment with abatacept plus MTX resulted in a larger decrease in ACPA titres versus MTX alone at both 6 and 12 months (the 95% CI of the estimate of difference did not cross 0; Figure 1).
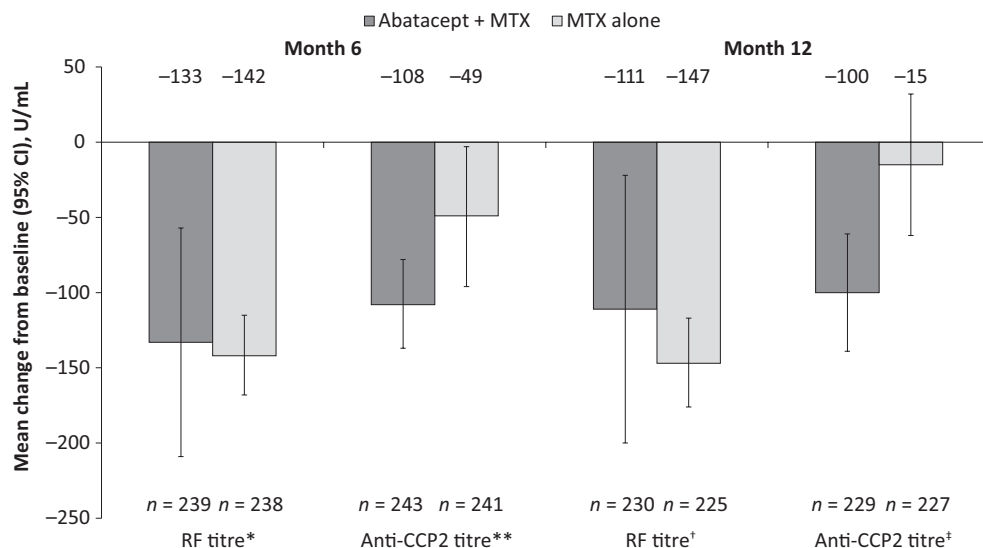

Figure 1. ACPA and RF titres in patients with early RA treated with abatacept + MTX compared with MTX alone. Antibody titres were determined by ELISA at baseline and month 6 and 12. Baseline to month 6 and baseline to month 12 were carried out as separate analyses. Baseline means (SD) for: *abatacept + MTX vs MTX alone were 305 (469) vs 273 (342); **abatacept + MTX vs placebo were 305 (534) vs 272 (514); †abatacept + MTX versus placebo were 297 (426) vs 272 (344); ‡abatacept + MTX versus placebo were 300 (537) vs 270 (524). *ACPA* anti-citrullinated protein antibody, *CI* confidence interval, *ELISA* enzyme-linked immunosorbent assay, *MTX* methotrexate, *RA* rheumatoid arthritis, *RF* rheumatoid factor, *SD* standard deviation

Conversion to RF and ACPA seronegative status following treatment with abatacept plus MTX or MTX alone

A numerically larger proportion of patients converted to become RF or ACPA seronegative in response to treatment with abatacept plus MTX versus MTX alone after 6 and 12 months of treatment. At 6 months, 17.0% (39/230) and 6.6% (15/227) of patients treated with abatacept plus MTX were RF and ACPA seronegative, respectively, compared with 9.5% (22/231) and 2.9% (6/208) of patients treated with MTX alone. At 12 months, 18.5% (41/222) and 7.1%

(15/212) of patients treated with abatacept plus MTX were RF and ACPA seronegative, respectively, compared with 14.6% (32/219) and 4.6% (9/198) of patients treated with MTX alone. The proportion of patients who converted to seronegative status was numerically higher in the abatacept plus MTX treatment group than in the MTX group. Estimated differences (95% CIs) between treatment groups for conversion to RF and ACPA seronegative status were, respectively, 7.4% (0.8–14.1) and 3.7% (–0.8 to 8.2) at 6 months, and 3.9% (–3.5 to 11.2) and 2.5% (–2.5 to 7.6) at 12 months; only the estimate of difference (95% CI) for RF seroconversion at month 6 did not cross 0 (Figure 2), indicating that abatacept plus MTX may have a particularly prominent effect on RF in the early treatment course.
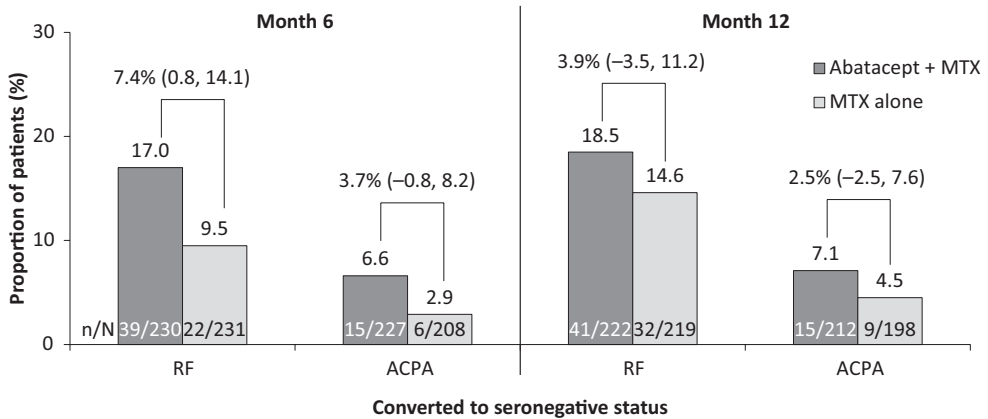

Figure 2. Conversion to ACPA and RF seronegative status in patients with early RA treated with abatacept + MTX compared with MTX alone. The proportion of patients with conversion to ACPA and RF seronegative status at months 6 and 12 and estimates of difference (95% CIs) between treatment groups are shown. Baseline to month 6 and baseline to month 12 were carried out as separate analyses. *ACPA* anti-citrullinated protein antibody, *CI* confidence interval, *ELISA* enzyme-linked immunosorbent assay, *MTX* methotrexate, *N* total number of patients in respective analysis, *n* number of patients that showed seroconversion, *RA* rheumatoid arthritis, *RF* rheumatoid factor

Clinical and radiographic responses by conversion to seronegative status

In the abatacept plus MTX arm, a higher proportion of patients who converted to ACPA seronegative status achieved DAS28 (CRP) and CDAI remission at 6 months compared with patients who were persistently ACPA seropositive (Figure 3); the estimate of difference (95% CI) between converters to seronegative status and those who were persistently ACPA seropositive did not cross 0 for DAS28 (CRP)-defined remission at month 6. The proportions (95% CIs) of patients who converted to ACPA seronegative status in the abatacept plus MTX arm and achieved DAS28 (CRP) and CDAI remission were 66.7% (42.8–90.5) and 46.7% (21.4–71.9) at 6 months, and 73.3% (51.0–95.7) and 46.7% (21.4–71.9) at 12 months, respectively. In comparison, the proportions (95% CIs) of patients who were persistently ACPA seropositive and achieved DAS28 (CRP) and CDAI remission were 32.6% (26.2–38.9) and 20.8% (15.3–26.2) at 6 months, and 48.7% (41.8–55.7) and 34.5% (27.9–41.2) at 12 months, respectively.

A higher proportion of patients treated with abatacept plus MTX achieved DAS28 (CRP) or CDAI remission at 6 and 12 months compared with patients treated with MTX alone, regardless of whether they converted to seronegative status or not. In the MTX alone arm, the proportions (95% CIs) of patients achieving DAS28 (CRP) and CDAI remission were 16.7% (0.0–46.5) and 16.7 (0.0–46.5) at 6 months, and 22.2% (0.0–49.4) and 11.1% (0.0–31.6) at 12 months, respectively, for patients who converted to ACPA seronegative status; and 21.8% (16.1–27.5) and 13.4% (8.7–18.1) at 6 months, and 31.8% (25.1–38.4) and 20.1% (14.4–25.8) at 12 months, respectively, for patients who were persistently ACPA seropositive.
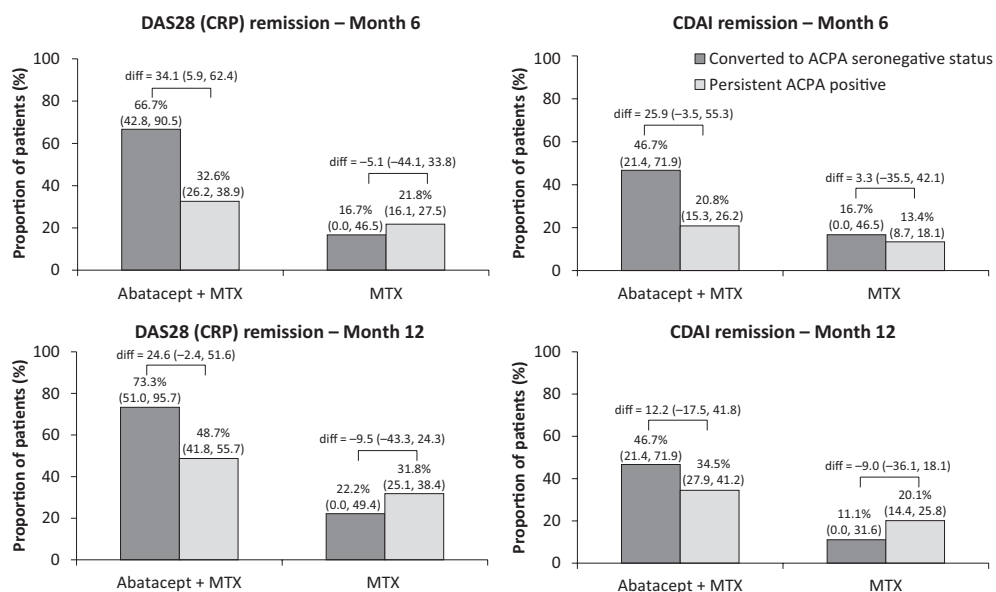

Figure 3. Percentage of patients achieving remission by conversion to ACPA seronegative status. Antibody titres were determined by ELISA at baseline and months 6 and 12. Baseline to month 6 and baseline to month 12 were carried out as separate analyses. *ACPA* anti-citrullinated protein antibody, *CDAI* Clinical Disease Activity Index, *CRP* C-reactive protein, *DAS28* Disease Activity Score in 28 joints, *ELISA* enzyme-linked immunosorbent assay, *MTX* methotrexate

In the abatacept plus MTX treatment arm, numerically, there was a higher cumulative probability of reaching sustained first DAS28 (CRP)-defined remission among patients who converted to seronegative status compared with those who remained ACPA seropositive (Figure 4). This difference was not observed among patients who received MTX alone. In patients who remained ACPA seropositive, there was a statistically significant benefit in the abatacept plus MTX group compared with MTX alone ($p = 0.001$; log-rank test). The proportion of patients who achieved sustained remission was consistently higher in the abatacept plus MTX treatment group versus MTX alone.

In both treatment groups, patients who underwent conversion to ACPA seronegative status showed less radiographic progression, as indicated by a smaller mean change from baseline

in Genant-modified TSS, erosion and JSN scores at both 6 and 12 months, than patients who were persistently ACPA seropositive (Figure 5). The estimate of difference (95% CI) between those who converted to seronegative status and those who remained ACPA seropositive did not cross 0 only for TSS and erosion score in the abatacept plus MTX group at month 12. Differences in TSS and erosions scores, but not JSN scores, between converters to ACPA seronegative status and patients who were persistently ACPA seropositive were larger among patients treated with abatacept plus MTX compared with those who received MTX alone.
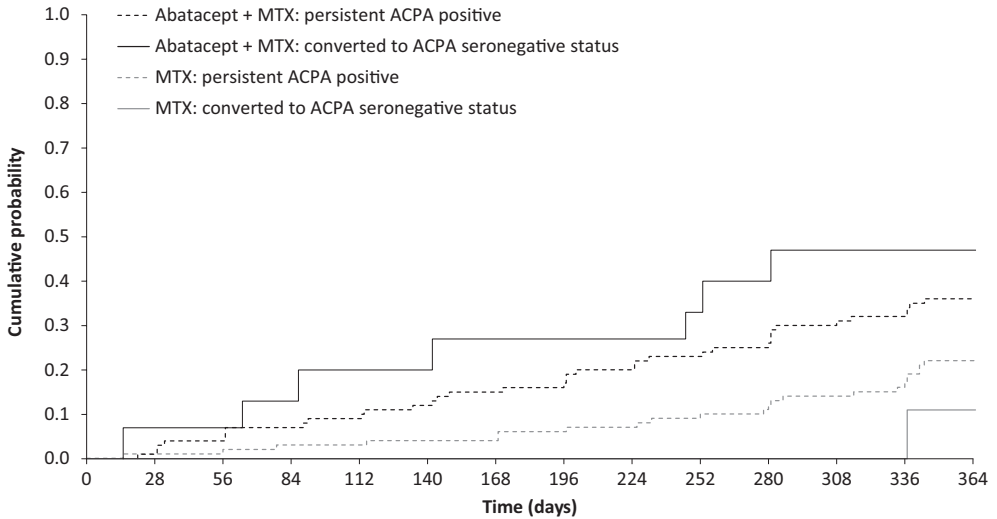

Figure 4. Cumulative probability of time to achieve first sustained DAS28 (CRP) remission by conversion to ACPA seronegative status. The cumulative probability of the time to achieve sustained first DAS28 (CRP) remission over 12 months in all patients treated with abatacept + MTX or MTX alone who underwent conversion to ACPA seronegative status compared with those who remained ACPA seropositive was evaluated based on estimated Kaplan–Meier curves with corresponding 95% CIs. In patients who remained ACPA seropositive, there was a statistically significant benefit in the abatacept plus MTX group compared with MTX alone ($p = 0.001$; log-rank test). There were no significant differences between the abatacept plus MTX versus MTX alone treatment groups in patients who underwent conversion to ACPA seronegative status, or within treatment groups between converters to ACPA seronegative status compared with those who remained ACPA seropositive. Antibody titres were determined by ELISA at baseline and months 6 and 12. Baseline to month 6 and baseline to month 12 were carried out as separate analyses. *ACPA* anti-citrullinated protein antibody, *CI* confidence interval, *CRP* C-reactive protein, *DAS28* Disease Activity Score in 28 joints, *ELISA* enzyme-linked immunosorbent assay, *MTX* methotrexate

DISCUSSION

In the AGREE study, patients with early, poor prognostic RA (erosions, highly active disease and seropositivity; 96.5% and 89.0% of patients were RF or ACPA seropositive), who were treated with abatacept plus MTX for 12 months achieved sustainable clinical, functional and radiographic benefits compared with patients treated with MTX alone[28-30]. The present posthoc analysis investigated the effect of abatacept in combination with MTX on RF and ACPA titres and the potential association between ACPA titres and clinical response. Combined

treatment with abatacept and MTX led to a decrease in both RF and ACPA titres over 6 and 12 months, and conversion to RF and ACPA seronegative status in 17.0–18.5% and 6.6–7.1% of patients, respectively. In those patients who converted to an autoantibody negative status
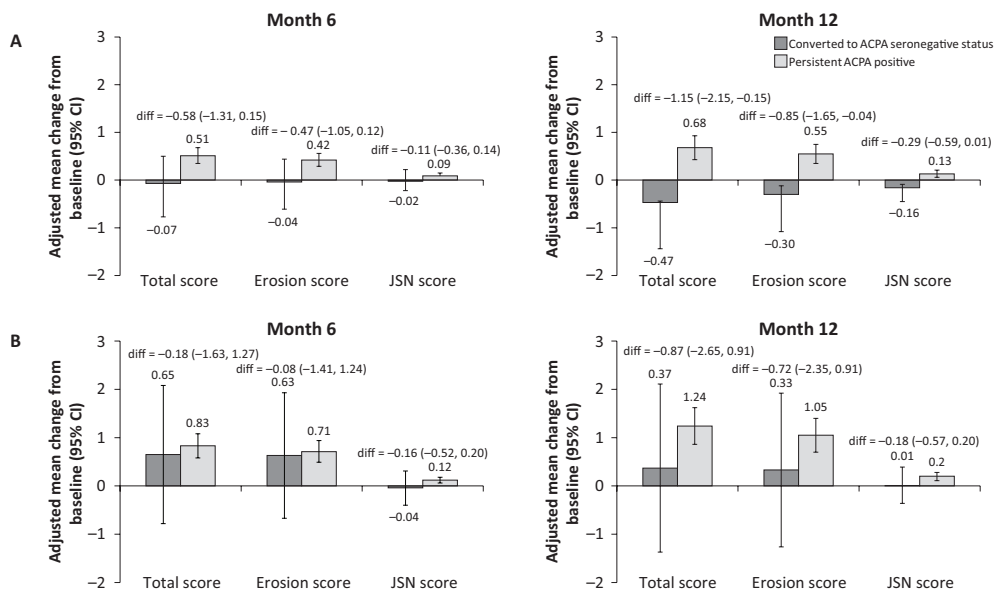

Figure 5. Radiographic outcomes in patients with early RA treated with (A) abatacept + MTX or (B) MTX alone by conversion to ACPA seronegative status. Antibody titres were determined by ELISA at baseline and months 6 and 12. Baseline to month 6 and baseline to month 12 were carried out as separate analyses. Error bars represent 95% CIs. *ACPA* anti-citrullinated protein antibody, *CI* confidence interval, *ELISA* enzyme-linked immunosorbent assay, *JSN* joint space narrowing, *MTX* methotrexate, *RA* rheumatoid arthritis, *TSS* total Sharp score

the remission rates were higher than in those patients who did not seroconvert.

Abatacept inhibits T cell co-stimulation by binding to CD80 and CD86 on APCs and blocking the binding of CD28 to CD80/86 [20]. B cells proliferate and differentiate into antibody-producing cells and switch from production of IgM to IgG antibodies in response to stimuli from activated CD4+ T cells, e.g. increased cytokine production[3]. Thus, abatacept has the potential to indirectly impact IgG isotype switching by inhibiting the co-stimulation and activation of T cells.

In the present study, after 6 and 12 months, a greater decrease in ACPA titres was observed with treatment with abatacept plus MTX compared with MTX alone, whereas mean decreases from baseline in RF titres were similar for the two treatment arms. However, in observational studies independent of the use of biological agents reductions in RF as well as ACPA levels have been observed and, indeed in line with the present study, more frequent RF seroconversion than ACPA seroconversion was observed. Reductions of both autoantibodies were linked to a reduction of disease activity and associated with reductions in disease activity[31]. RF autoantibodies are primarily of the IgM isotype whereas ACPA are primarily of

the IgG isotype[1]. B cells do not require T cell help to produce IgM isotype antibodies, whereas switching from IgM to IgG isotypes is a feature of B-cell somatic hypermutation, which occurs during proliferation and differentiation of B cells – in part regulated by activated T cells[3]. Thus, the difference in effect of abatacept plus MTX compared with MTX alone on RF versus ACPA titres might be explained by this difference in autoantibody isotype. In contrast, treatment with abatacept plus MTX led to higher rates of conversion to RF or ACPA seronegative status compared with treatment with MTX alone. Although abatacept inhibits T cell activation, it also exerts anti-inflammatory effects in a T cell independent way[32], potentially through direct effects on B cells[33] and macrophages[34].

Current treatment strategies for RA employ a targeted approach aimed at reaching remission or low disease activity[35,36]. The present analysis showed that in the abatacept plus MTX treatment arm the proportion of patients who achieved DAS28 (CRP)- or CDAI-defined remission was higher among those who converted to seronegative status than those who remained persistently ACPA seropositive. Furthermore, the cumulative probability of achieving sustained first remission according to DAS28 (CRP)-defined criteria was higher among patients who converted to ACPA seronegative status treated with abatacept plus MTX than in those who remained ACPA seropositive. The small proportion of patients who were converters to ACPA seronegative status showed less radiographic progression over 12 months than patients who remained ACPA seropositive, regardless of treatment.

These findings are in line with previous studies of abatacept in patients with early RA. In the ADJUST trial[25], patients with undifferentiated arthritis or very early RA treated with abatacept for 6 months had delayed disease progression and prolonged inhibition of radiographic progression after cessation of treatment versus placebo, with a decrease from baseline in RF and ACPA titres[25]. In the AVERT study[24], compared with patients treated with MTX alone, patients treated with abatacept plus MTX showed significantly higher rates of remission and a higher number of patients achieved sustained drug-free remission after withdrawal of all therapy, as well as reduced inflammation and structural damage progression as assessed by changes in MRI scores (synovitis, osteitis and bone erosions)[37]. Furthermore, in a post hoc analysis of the AVERT study (MTX-naïve patients with early RA and highly active and erosive disease; 100% and 95.2% of patients were ACPA and RF positive, respectively), a higher proportion of patients receiving abatacept plus MTX underwent conversion to ACPA seronegative status compared with those receiving MTX[38]. In addition, a numerically higher proportion of patients treated with abatacept plus MTX who became seronegative (ACPA IgM isotype) achieved clinical remission at 12 months compared with those who did not seroconvert, differences that were not seen for patients treated with MTX alone[38].

On the other hand, a post hoc analysis of the AMPLE trial suggested that, despite a similar clinical response over 2 years between the two treatment groups, only abatacept plus MTX produced a continuous decline in the median levels of most ACPAs beyond 1 year of treatment; an effect that was not sustained with adalimumab plus MTX[39].

In the abatacept plus MTX group, a link between conversion to seronegative status and remission/inhibition of structural damage was noticeable, while this link was less obvious in the MTX group. Taken together, these data demonstrate that abatacept is an effective treatment in patients with early RA and that, by modulating T-cell responses at very early stages of the disease, it might be possible to alter underlying autoimmune processes; i.e. slowing or halting disease progression with the potential for sustained drug-free remission.

There are limitations to post hoc analyses, which should be considered when interpreting the data presented here. The present post hoc analysis was a completers-only analysis, carried out on a subset of patients included in the original AGREE study who had complete data sets. The study was not designed or powered to detect differences between the treatment groups based on seroconversion status, thus statistical testing in this analysis should be interpreted with caution. Moreover there are no formal corrections for multiple testing. Finally, this post hoc analysis was carried out in a relatively small population; as such, only some of the findings reached 'significance', particularly in larger subgroups of patients. The findings would benefit from validation in a larger patient population.

In conclusion, the present post hoc analysis demonstrated that treatment with abatacept in combination with MTX led to a decrease in autoantibody titres, resulting in some patients undergoing conversion to RF and ACPA seronegative status. Conversion to ACPA seronegative status was associated with higher rates of remission, an increased likelihood of achieving sustained remission and less radiographic progression.

4

REFERENCES

1. Scott DL, Wolfe F, Huizinga TW. Rheumatoid arthritis. Lancet (London, England) 2010;376:1094-108.

2. Schellekens GA, de Jong BA, van den Hoogen FH, van de Putte LB, van Venrooij WJ. Citrulline is an essential constituent of antigenic determinants recognized by rheumatoid arthritis-specific autoantibodies. The Journal of clinical investigation 1998;101:273-81.

3. van Heemst J, van der Woude D, Huizinga TW, Toes RE. HLA and rheumatoid arthritis: how do they connect? Annals of medicine 2014;46:304-10.

4. Aho K, Heliovaara M, Maatela J, Tuomi T, Palosuo T. Rheumatoid factors antedating clinical rheumatoid arthritis. The Journal of rheumatology 1991;18:1282-4.

5. Aho K, von Essen R, Kurki P, Palosuo T, Heliovaara M. Antikeratin antibody and antiperinuclear factor as markers for subclinical rheumatoid disease process. The Journal of rheumatology 1993;20:1278-81.

6. Nielen MM, van Schaardenburg D, Reesink HW, et al. Specific autoantibodies precede the symptoms of rheumatoid arthritis: a study of serial measurements in blood donors. Arthritis and rheumatism 2004;50:380-6.

7. Rantapaa-Dahlqvist S, de Jong BA, Berglin E, et al. Antibodies against cyclic citrullinated peptide and IgA rheumatoid factor predict the development of rheumatoid arthritis. Arthritis and rheumatism 2003;48:2741-9.

8. van de Stadt LA, de Koning MH, van de Stadt RJ, et al. Development of the anti-citrullinated protein antibody repertoire prior to the onset of rheumatoid arthritis. Arthritis and rheumatism 2011;63:3226-33.

9. Ursum J, Bos WH, van de Stadt RJ, Dijkmans BA, van Schaardenburg D. Different properties of ACPA and IgM-RF derived from a large dataset: further evidence of two distinct autoantibody systems. Arthritis research & therapy 2009;11:R75.

10. van der Helm-van Mil AH, Verpoort KN, Breedveld FC, Toes RE, Huizinga TW. Antibodies to citrullinated proteins and differences in clinical progression of rheumatoid arthritis. Arthritis research & therapy 2005;7:R949-58.

11. Hecht C, Englbrecht M, Rech J, et al. Additive effect of anti-citrullinated protein antibodies and rheumatoid factor on bone erosions in patients with RA. Annals of the rheumatic diseases 2015;74:2151-6.

12. Aletaha D, Alasti F, Smolen JS. Rheumatoid factor, not antibodies against citrullinated proteins, is associated with baseline disease activity in rheumatoid arthritis clinical trials. Arthritis research & therapy 2015;17:229.

13. Laurent L, Anquetil F, Clavel C, et al. IgM rheumatoid factor amplifies the inflammatory response of macrophages induced by the rheumatoid arthritis-specific immune complexes containing anticitrullinated protein antibodies. Annals of the rheumatic diseases 2015;74:1425-31.

14. Amara K, Steen J, Murray F, et al. Monoclonal IgG antibodies generated from joint-derived B cells of RA patients have a strong bias toward citrullinated autoantigen recognition. The Journal of experimental medicine 2013;210:445-55.

15. Jasin HE. Autoantibody specificities of immune complexes sequestered in articular cartilage of patients with rheumatoid arthritis and osteoarthritis. Arthritis and rheumatism 1985;28:241-8.

16. Snir O, Widhe M, Hermansson M, et al. Antibodies to several citrullinated antigens are enriched in the joints of rheumatoid arthritis patients. Arthritis and rheumatism 2010;62:44-52.

17. Wernick RM, Lipsky PE, Marban-Arcos E, Maliakkal JJ, Edelbaum D, Ziff M. IgG and IgM rheumatoid factor synthesis in rheumatoid synovial membrane cell cultures. Arthritis and rheumatism 1985;28:742-52.

18.	Rombouts Y, Willemze A, van Beers JJ, et al. Extensive glycosylation of ACPA-IgG variable domains modulates binding to citrullinated antigens in rheumatoid arthritis. Annals of the rheumatic diseases 2016;75:578-85.

19.	Huizinga TW, Amos CI, van der Helm-van Mil AH, et al. Refining the complex rheumatoid arthritis phenotype based on specificity of the HLA-DRB1 shared epitope for antibodies to citrullinated proteins. Arthritis and rheumatism 2005;52:3433-8.

20.	Linsley PS, Nadler SG. The clinical utility of inhibiting CD28-mediated costimulation. Immunological reviews 2009;229:307-21.

21.	Moreland L, Bate G, Kirkpatrick P. Abatacept. Nature reviews Drug discovery 2006;5:185-6.

22.	Genovese MC, Becker JC, Schiff M, et al. Abatacept for rheumatoid arthritis refractory to tumor necrosis factor alpha inhibition. The New England journal of medicine 2005;353:1114-23.

23.	Kremer JM, Westhovens R, Leon M, et al. Treatment of rheumatoid arthritis by selective inhibition of T-cell activation with fusion protein CTLA4Ig. The New England journal of medicine 2003;349:1907-15.

24.	Emery P, Burmester GR, Bykerk VP, et al. Evaluating drug-free remission with abatacept in early rheumatoid arthritis: results from the phase 3b, multicentre, randomised, active-controlled AVERT study of 24 months, with a 12-month, double-blind treatment period. Annals of the rheumatic diseases 2015;74:19-26.

25.	Emery P, Durez P, Dougados M, et al. Impact of T-cell costimulation modulation in patients with undifferentiated inflammatory arthritis or very early rheumatoid arthritis: a clinical and imaging study of abatacept (the ADJUST trial). Annals of the rheumatic diseases 2010;69:510-6.

26.	Kremer JM, Peterfy C, Russell AS, et al. Longterm safety, efficacy, and inhibition of structural damage progression over 5 years of treatment with abatacept in patients with rheumatoid arthritis in the abatacept in inadequate responders to methotrexate trial. The Journal of rheumatology 2014;41:1077-87.

27.	Kremer JM, Russell AS, Emery P, et al. Long-term safety, efficacy and inhibition of radiographic progression with abatacept treatment in patients with rheumatoid arthritis and an inadequate response to methotrexate: 3-year results from the AIM trial. Annals of the rheumatic diseases 2011;70:1826-30.

28.	Bathon J, Robles M, Ximenes AC, et al. Sustained disease remission and inhibition of radiographic progression in methotrexate-naive patients with rheumatoid arthritis and poor prognostic factors treated with abatacept: 2-year outcomes. Annals of the rheumatic diseases 2011;70:1949-56.

29.	Westhovens R, Robles M, Ximenes AC, et al. Clinical efficacy and safety of abatacept in methotrexate-naive patients with early rheumatoid arthritis and poor prognostic factors. Annals of the rheumatic diseases 2009;68:1870-7.

30.	Smolen JS, Wollenhaupt J, Gomez-Reino JJ, et al. Attainment and characteristics of clinical remission according to the new ACR-EULAR criteria in abatacept-treated patients with early rheumatoid arthritis: new analyses from the Abatacept study to Gauge Remission and joint damage progression in methotrexate (MTX)-naive patients with Early Erosive rheumatoid arthritis (AGREE). Arthritis research & therapy 2015;17:157.

31.	Bohler C, Radner H, Smolen JS, Aletaha D. Serological changes in the course of traditional and biological disease modifying therapy of rheumatoid arthritis. Annals of the rheumatic diseases 2013;72:241-4.

32.	Jansen DT, el Bannoudi H, Arens R, et al. Abatacept decreases disease activity in a absence of CD4(+) T cells in a collagen-induced arthritis model. Arthritis research & therapy 2015;17:220.

33.	Rozanski CH, Arens R, Carlson LM, et al. Sustained antibody responses depend on

4

CD28 function in bone marrow-resident plasma cells. The Journal of experimental medicine 2011;208:1435-46.

34.   Bonelli M, Ferner E, Goschl L, et al. Abatacept (CTLA-4IG) treatment reduces the migratory capacity of monocytes in patients with rheumatoid arthritis. Arthritis and rheumatism 2013;65:599-607.

35.   Singh JA, Saag KG, Bridges SL, Jr., et al. 2015 American College of Rheumatology Guideline for the Treatment of Rheumatoid Arthritis. Arthritis & rheumatology (Hoboken, NJ) 2016;68:1-26.

36.   Smolen JS, Landewe R, Breedveld FC, et al. EULAR recommendations for the management of rheumatoid arthritis with synthetic and biological disease-modifying antirheumatic drugs: 2013 update. Annals of the rheumatic diseases 2014;73:492-509.

37.   Peterfy C, Burmester GR, Bykerk VP, et al. Sustained improvements in MRI outcomes with abatacept following the withdrawal of all treatments in patients with early, progressive rheumatoid arthritis. Annals of the rheumatic diseases 2016.

38.   Huizinga TWJ CS, Johnsen A, Zhu J, Furst DE, Bykerk VP. Effect of anti-cyclic citrullinated peptide 2 immunoglobulin M serostatus on efficacy outcomes following treatment with abatacept plus methotrexate in the AVERT trial. Ann Rheum Dis 2015;74(Suppl2).

39.   Connolly S MM, Schiff M, Weinblatt M, Fleischmann R, Robinson W. Modulation of the ACPA fine specificity in patients with RA treated with either abatacept or adalimumab in the AMPLE study. Ann Rheum Dis 2014;73 (Suppl 2).

4

PART III

CYTOKINE PRODUCING CD4+ T CELLS IN DISEASE AND HEALTH
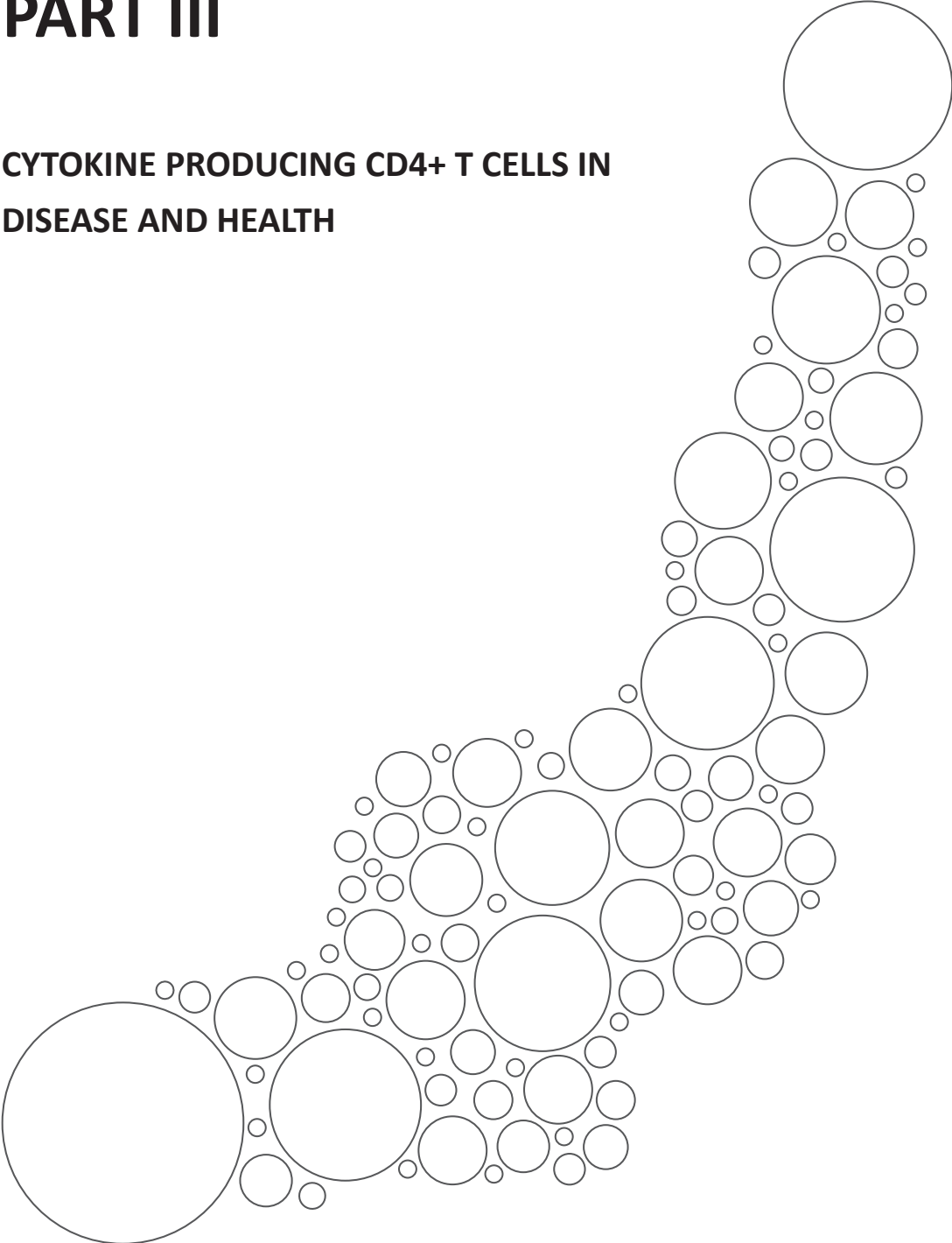
CHAPTER 5

IL-17-PRODUCING CD4+ T CELLS ARE INCREASED IN EARLY, ACTIVE AXIAL SPONDYLOARTHRITIS INCLUDING PATIENTS WITHOUT IMAGING ABNORMALITIES

Diahann T.S.L. Jansen, Marjolijn Hameetman, Jeroen van Bergen, Tom W.J. Huizinga, Désirée van der Heijde, René E.M. Toes & Floris A. van Gaalen
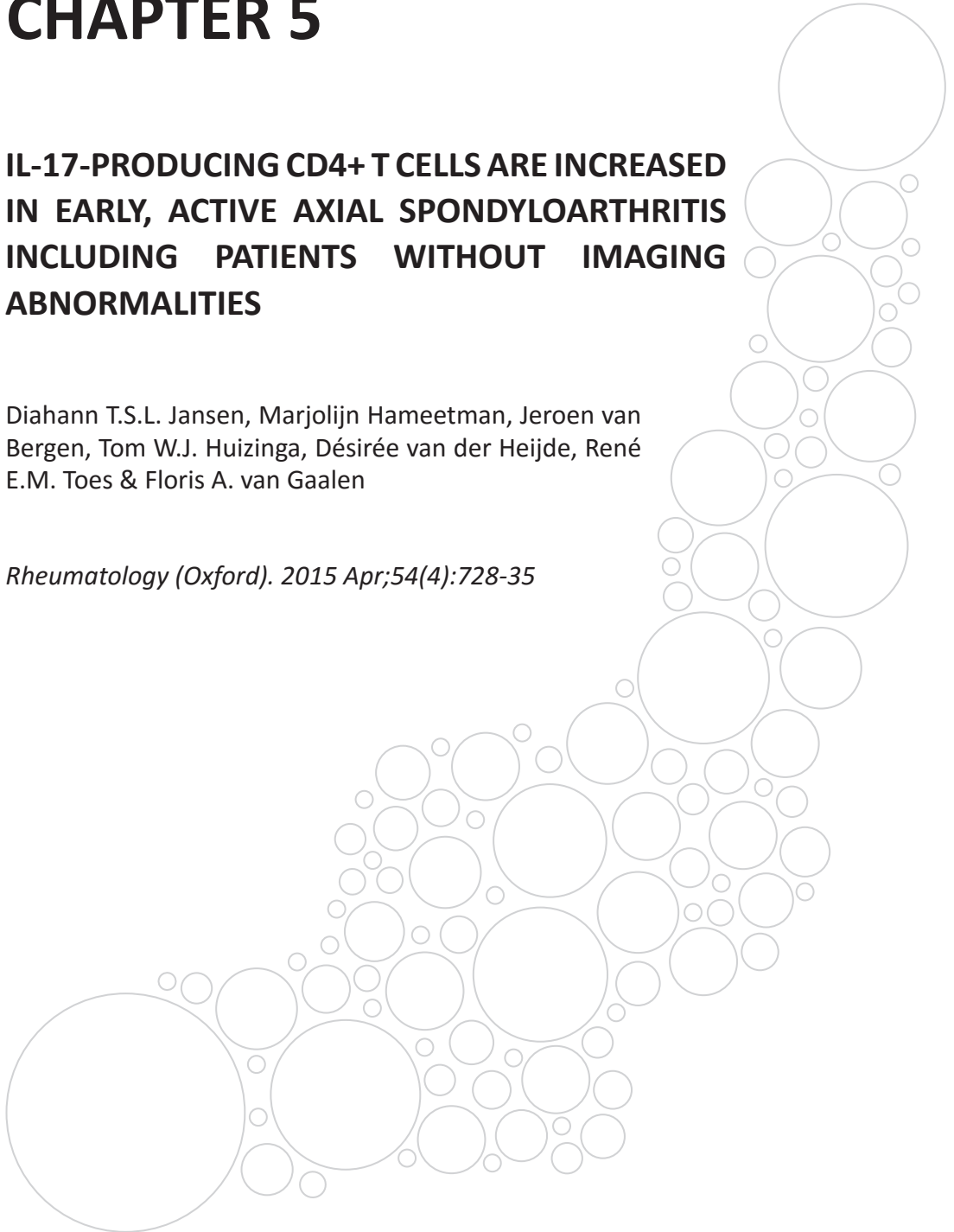
ABSTRACT

Introduction Increased numbers of IL-17-producing CD4+ T cells have been observed in ankylosing spondylitis. However, it is not known if these CD4+ T cells are already present in early disease or if this is a late disease phenomenon only. Therefore we aimed to investigate whether IL-17-producing CD4+ T cells are involved in early active axial spondyloarthritis including patients without imaging abnormalities, by determining the frequency and phenotype of IL-17-producing CD4+ T cells in these patients.

Methods Flow cytometry was used to analyse the cytokine production and surface marker expression of peripheral blood mononuclear cells from 31 patients suffering from early active HLA-B27-positive axial spondyloarthritis fulfilling the Assessment of SpondyloArthritis International Society (ASAS) criteria with or without MRI abnormalities and 21 healthy controls.

Results Patients with early active axial spondyloarthritis showed an increased percentage of IL-17-producing CD4+ T cells compared to the healthy controls (mean 1.1% *vs* 0.4% respectively, p=0.013). The percentage of IL-17-producing CD4+ T cells was equally increased in patients with and without MRI abnormalities (1.2% *vs* 1.1% respectively, p=0.81). These IL-17-producing CD4+ T cells expressed the αβ T-cell receptor but not the γδ T-cell receptor, exhibited a memory phenotype and expressed CD161, but only sporadically expressed killer cell immunoglobulin-like receptor 3DL2 (KIR3DL2).

Conclusion IL-17-producing CD4+ T cells are increased in patients with early active axial spondyloarthritis both with and without MRI abnormalities. This finding shows that the frequency of IL-17-producing CD4+ T cells is enhanced in the early stages of disease.

INTRODUCTION

Axial spondyloarthritis (SpA) is a common chronic disease involving the sacroiliac (SI) joints and the axial skeleton. The most well-known form of axial SpA is ankylosing spondylitis (AS) which is characterized by sacroiliitis on conventional radiographs. However, radiographs become positive for sacroiliitis at a rather late stage, as they detect only structural damage as a consequence of inflammation and not the inflammation itself. The term nonradiographic axial spondyloarthritis (nr-axSpA) has recently been introduced to identify patients with axial SpA without structural changes in the sacroiliac joints. The new Assessment of SpondyloArthritis International Society (ASAS) criteria were subsequently developed as classification criteria for axial SpA covering both radiographic axial SpA (AS) and nr-axSpA[1]. Patients with nr-axSpA can either show inflammation on MRI of the SI joints with one SpA feature (imaging arm) or be HLA-B27-positive with two additional SpA features (clinical arm).

SpA is an HLA-B27-associated inflammatory disease and several lines of evidence suggest that the pro-inflammatory cytokine interleukin 17-A (IL-17) is involved in the pathogenesis of AS. In animal models it has been described that IL-17-producing CD4+ T cells are expanded in SpA-prone HLA-B27 transgenic rats[2] and that IL-17-producing CD4+ T cells are increased in regional lymph nodes of male BXSB x NZB F1 mice that spontaneously develop seronegative ankylosing enthesitis in the ankle or tarsal joints[3]. In humans, an increase in the number of IL-17-producing CD4+ T cells in the blood of patients with AS compared with healthy controls has been reported[4-6]. However, other studies have not been able to reproduce these findings[7-9]. In addition, AS is associated with genetic polymorphisms of the IL-23 receptor with the susceptibility-conferring R381Q allele variant characterized by enhanced Th17 responses[10,11]. Finally, an anti-IL17A monoclonal antibody has shown promising results in the treatment of AS patients[12]. Irrespective of all the evidence for the involvement of IL-17 in the pathogenesis of AS, the underlying mechanism connecting HLA-B27 and IL-17 production is incompletely understood. Bowness *et al.* showed that HLA-B27 is capable of forming homodimers and that these homodimers are able to bind the killer cell immunoglobulin-like receptor 3DL2 (KIR3DL2)[13]. Furthermore, they showed that AS patients have increased levels of IL-17-producing CD4+ T cells that express KIR3DL2 and that binding of KIR3DL2 to HLA-B27 induces proliferation and production of IL-17 by these CD4+ T cells, potentially linking HLA-B27 to IL-17 production[14].

It is not known whether IL-17-producing CD4+ T cells play a role in disease initiation or maintenance. Furthermore, the expression of KIR3DL2 on IL-17-producing CD4+ T cells early in disease has not been examined. To investigate whether IL-17-producing CD4+ T cells are already involved at the onset of disease, we set out to determine the frequency and phenotype of IL-17-producing CD4+ T cells in early active axial SpA (axial SpA).

5

METHODS

Patients

Peripheral blood was obtained from patients visiting the outpatient clinic of the Leiden University Medical Center, Leiden, the Netherlands, classified with axial spondyloarthritis according to the ASAS criteria[1]. Fourteen patients had a negative MRI of the SI joints and 17 patients had a positive MRI with bone marrow oedema highly suggestive of sacroiliitis according to the ASAS definition. None of the MRI-negative patients had sacroiliitis on radiographs compared with 6 out of 17 patients with a positive MRI. All patients were HLA-B27-positive and on average had a high Ankylosing Spondylitis Disease Activity Score (ASDAS; Table 1). Median back pain duration was 16 months. The median number of SpA features in the MRI-negative patients was four (range three to six) and also four in MRI-positive patients (range two to six). Five patients used DMARDs because of an extra-axial manifestation; sulfasalazine was used in two patients for IBD and in two patients for peripheral arthritis. One patient used methotrexate for arthritis. Two patients used a TNF blocker (both adalimumab), one for IBD and one for psoriasis.

The average number of days between the MRI being performed and peripheral blood mononuclear cell (PBMC) isolation was 2.4 days (range 0-21). Written informed consent was obtained from all participating patients. The study has been reviewed and approved by the medical ethical committee of the Leiden University Medical Center.

Controls consisted of 21 healthy blood donors of which buffy coats were obtained from the blood bank (Sanquin, the Netherlands). Of these healthy controls, 12 individuals were HLA-B27 positive and 9 individuals were HLA-B27 negative to investigate the influence of HLA-B27 on the frequency of IL17-producing CD4+ T cells. Detailed patient and control characteristics are provided in Table 1.

Intracellular cytokine and surface staining

PBMCs were isolated from peripheral blood of buffy coats using Ficoll Paque gradient centrifugation (Leiden University Medical Center Pharmacy). Cells were stimulated with 50 ng/ml phorbol 12-myristate 13-acetate (PMA) (Sigma, St Louis, MO, USA) and 1 µg/ml ionomycin (Sigma) for 5 hours, in the presence of 5 µg/ml Brefeldin A (Sigma) during the final 4 hours of the incubation. After stimulation surface staining was performed using the following antibodies; CD3 PE-Cy7 (SK7), CD4 APC-Cy7 (RPA-T4), CD8 AlexaFluor 700 (RPA-T8), CD14 Pacific Blue (M5E2), CD28 FITC (CD28.2), CD45RO PE-CF594 (UCHL1), T cell receptor-αβ (TCRαβ) AlexaFluor 488 (WT31) and TCRγδ PE (B1) all purchased from BD Biosciences (San Jose, CA, USA), CD56 Brilliant Violet 605 (HCD56) and CD161 Brilliant Violet 421 (HP-3G10) purchased from Biolegend (San Diego, CA, USA) and KIR3DL2 PE (DX31) from the University of California San Francisco (San Francisco, CA, USA). Intracellular staining was performed using the Cytofix/Cytoperm Fixation/Permeabilization Solution Kit from BD Biosciences and IL-17A AlexaFluor 647 (eBio64CAP17; eBioscience, San Diego, CA, USA) and IFNγ PE (4S.B3; BD Biosciences). All samples were measured on a BD LSRFortessa cell analyser (BD Biosciences)

and analysed using BD FACSDIVA software (BD Biosciences) and FlowJo version 7.6.5 (FlowJo, Ashland, OR, USA).

Statistical analysis

All statistical analysis were performed using GraphPad Prism version 5 (GraphPad Software, La Jolla, CA, USA) including regression analysis. The different patient and control groups were compared using a Mann-Whitney test. p-values <0.05 were considered to be significant.

Table 1. Characteristics of patients with axial spondyloarthritis with and without imaging abnormalities and healthy controls

	MRI negative (n= 14)	MRI positive (n= 17)	Controls (n= 21)
Age median (range), years	29 (19-47)	30 (23-50)	47 (29-60)
Males, n (%)	5 (36)	14 (82)	12 (57)
Duration of back pain, median (range), months	17 (4-45)	16 (6-36)	n/a
Family history of SpA, n (%)	3 (21)	7 (41)	n/a
Inflammatory backpain, n (%)[a]	13 (93)	12 (71)	n/a
Heel pain, n (%)	3 (21)	3 (18)	n/a
Anterior uveitis, n (%)[b]	6 (43)	1 (6)	n/a
Arthritis, n (%)[b]	4 (29)	5 (29)	n/a
Dactylitis, n (%)[b]	1 (7)	2 (12)	n/a
Psoriasis, n (%)[b]	1 (7)	0 (0)	n/a
Inflammatory bowel disease, n (%)	2 (14)	0 (0)	n/a
HLA-B27 positive, n (%)	14 (100)	17 (100)	12 (57)
Elevated CRP or ESR, n (%)	3 (21)	9 (59)	n/a
Sacroiliitis on MRI, n (%)	0 (0)	17 (100)	n/a
Sacroiliitis on X-ray, n (%)	0 (0)	6 (36)	n/a
Current NSAID use, n (%)	9 (64)	14 (82)	n/a
Current DMARD use, n (%)	3 (21)	2 (12)	n/a
Current TNF-blocker use, n (%)	1 (7)	1 (6)	n/a
ASDAS-CRP, median (range)	3.1 (1.5-5.3)	3.0 (2.0-5.0)	n/a

[a]According to ASAS definition. [b]Physician observed. ASAS: Ankylosing SpondyloArthritis International Society; ASDAS-CRP: Ankylosing Spondylitis Disease Activity Score with CRP; n/a: not applicable.

RESULTS

Increased frequency of IL-17-producing CD4+ T cells in patients with axial SpA irrespective of imaging abnormalities

Flow cytometry was used to determine the intracellular expression of IL-17 by PBMCs from 31 patients with axial SpA and from 21 healthy controls after stimulation with PMA and ionomycin (patient and control characteristics are provided in Table 1). Patients with axial SpA exhibited a higher percentage of IL-17-producing CD4+ T cells compared with healthy controls (Figure 1A and 1B; mean 1.1% *vs* 0.4% in controls; p= 0.013). The percentage of IL-17-producing CD4+ T cells was equally increased in axial SpA patients with (n= 14) and without (n= 17) MRI abnormalities (mean 1.2% *vs* 1.1%, p= 0.81). Moreover, this increase was disease related and not HLA-B27 specific as the healthy controls positive (n= 12) and negative (n= 9) for HLA-B27 showed comparable percentages of IL-17-producing CD4+ T cells (mean 0.4% *vs* 0.3%, p= 0.45; Figure 1B). IL-17 production by CD8+ T cells was determined as well, however,
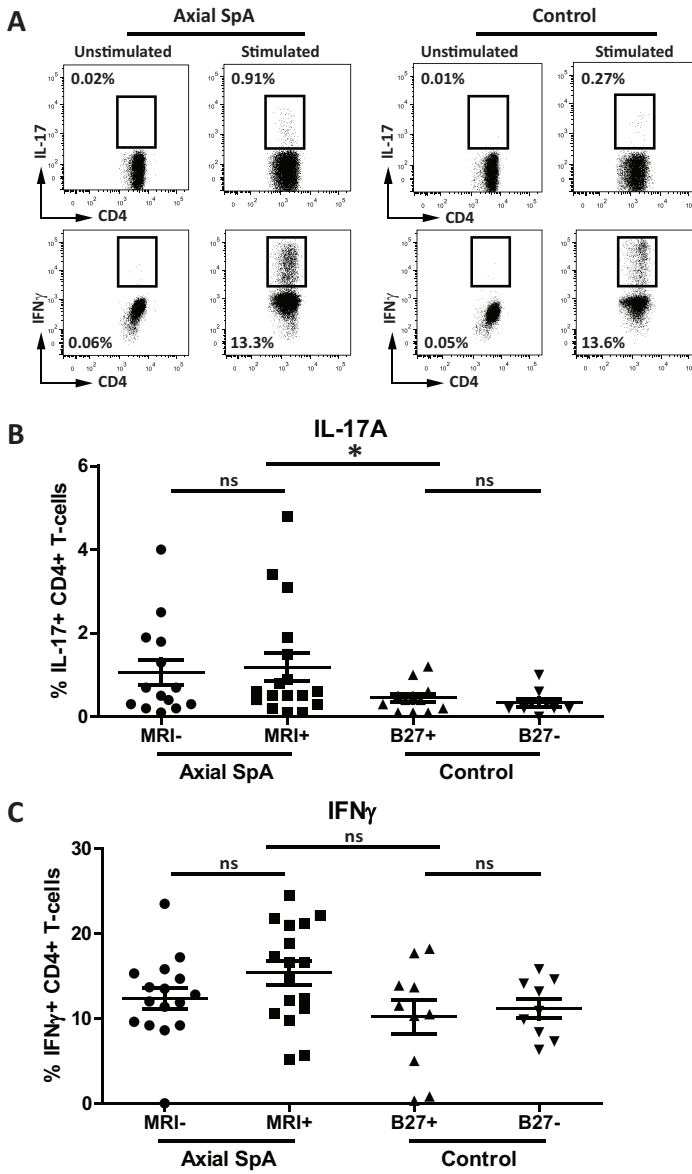
Figure 1. Increased percentage of IL-17-producing CD4+ T cells in patients with axial SpA irrespective of imaging abnormalities. PBMCs of 31 axial SpA patients and 21 healthy controls were stimulated with PMA and ionomycin for 5 hours and subsequently surface stained with CD3, CD4, CD8, CD14 and CD56 and intracellularly stained with IL-17A or IFNγ. The monocytes and natural killer cells were excluded by gating on the CD14- and CD56-negative cells and subsequently the T cells were selected by gating on CD3 and CD4 double-positive cells. Then the production of IL-17A and IFNγ by these CD4+ T cells was analysed. (A) Dot plots of a representative patient and control. (B) Overview of the IL-17-producing CD4+ T cells in axial SpA patients either with (MRI+; *n*= 17) or without (MRI-; *n*= 14) MRI abnormalities and healthy controls either positive (HLA-B27+; *n*= 12) or negative (HLA-B27-; *n*= 9) for HLA-B27. (C) Overview of the IFNγ-producing CD4+ T cells in axial SpA patients either with (MRI+) or without (MRI-) MRI abnormalities and healthy controls either positive (HLA-B27+) or negative (HLA-B27-) for HLA-B27. *$p < 0.05$. ns = not significant. PBMCs: peripheral blood mononuclear cells; PMA: phorbol 12-myristate 13-acetate.

IL-17+ CD8+ T cells were not detected in patients irrespective of imaging abnormalities nor in the healthy controls irrespective of their HLA-B27 status (data not shown). In addition to the intracellular expression of IL-17, the intracellular expression of IFNγ by CD4+ T cells was determined as well. The frequency of IFNγ-producing CD4+ T cells was higher in axial SpA patients compared with healthy controls, although no statistical significance was reached (mean 13.9% *vs* to 10.7%, *p*= 0.07; Figure 1C). Together, these data indicate an expansion of IL-17- and possibly IFNγ-producing CD4+ T cells in the PBMC fraction of axial SpA patients already early in the disease.

As controls were on average older than patients, we analysed whether the increased percentage of IL-17-producing CD4+ T cells in patients was correlated with age. In both patients and controls there was no correlation between age and the number of IL-17-producing CD4+ T cells as linear regression analysis correlating age versus percentage of IL-17-producing CD4+ T cells showed that the slope of the fitted line was not significantly different from zero (*p*= 0.64 for patients and *p*= 0.68 for controls; data not shown). Moreover, using the median age to dichotomize groups showed that the mean percentage of IL-17-producing CD4+ T cells was not significantly different between young or old patients compared with controls (mean 0.7% *vs* 1.5%, *p*= 0.15 and mean 0.3% *vs* 0.4%, *p*= 0.65, respectively; data not shown).

In addition, we investigated whether the presence of extra-axial manifestations or the use of DMARDs and biologicals in patients explained the finding. Both DMARD/biological use and a history of extra-axial manifestations was associated with a higher percentage of IL-17-producing CD4+ T cells compared with patients without (mean 1.9% *vs* 1.0% and mean 1.4 *vs* 1.0%, respectively), however, neither was significant (*p*= 0.17 and *p*= 0.98, respectively; data not shown). Of note, when the blood sampling for this study was performed, according to the clinical assessment of the treating physician, none of the patients with extra-axial manifestation had signs of activity of that manifestation except the one patient with psoriasis.

IL-17-producing CD4+ T cells in patients with axial SpA express TCRαβ and CD161 and exhibit a memory phenotype, but sporadically express KIR3DL2

IL-17 production by TCRαβ- and TCRγδ-positive CD4+ T cells in AS has been described[7,8]. Therefore the expression of TCRαβ and TCRγδ by the IL-17-producing CD4+ T cells of 11 axial SpA patients was evaluated using flow cytometry after stimulation with PMA and ionomycin. The IL-17-producing CD4+ T cells in patients with axial SpA did not express TCRγδ, but they did express TCRαβ (Figure 2A). To further characterize the IL-17-producing CD4+ T cells in axial SpA patients, the expression of CD161 was evaluated. CD161 is a marker of IL-17-producing T cells induced by RORC. Indeed, CD161 expression was observed on a large proportion of IL-17-producing CD4+ T cells. On average 50.8% of the IL-17-producing CD4+ T cells expressed CD161 in patients (Figure 2B). Since IL-17-producing CD4+ T cells are thought to reside within the memory pool, the memory status of the IL-17-producing CD4+ T cells was evaluated using the expression of CD28 and CD45RO. As expected, IL-17-producing CD4+ T

cells showed an expression pattern compatible with early memory (CD28+ CD45RO+) and memory phenotype (CD28- CD45RO+). On average 83.0% of the IL-17-producing CD4+ T cells were positive for CD28 and CD45RO and 10.8% of the IL-17-producing CD4+ T cells were CD28-CD45RO+ (Figure 2C).
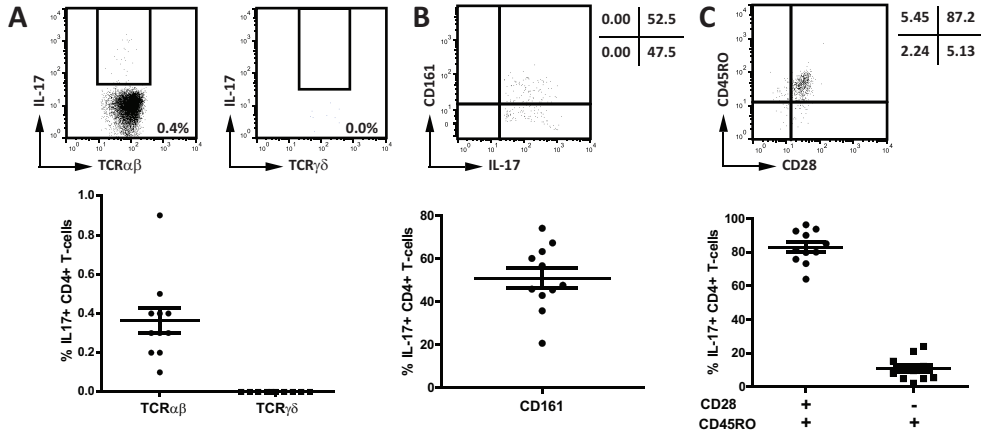

Figure 2. IL-17 is produced by TCRαβ-positive CD4+ T cells that exhibit a memory phenotype and show a heterogeneous expression of CD161. TCR expression of IL-17-producing CD4+ T cells of axial SpA patients was evaluated by determining the expression of TCRαβ and TCRγδ and subsequently the IL-17 production by these cells using flow cytometry. (A) Dot plots of a representative patient (top). Summary of 11 patients with each dot representing one patient (bottom). The expression of CD161 by IL-17-producing CD4+ T cells was also determined by flow cytometry. (B) Dot plot of a representative donor (top). Cells were gated on CD3+CD4+ IL17+ T cells and their IL-17 production (*x*-axis) and CD161 expression (*y*-axis) is depicted. A summary of 11 patients is depicted in the bottom graph. (C) Memory phenotype of the IL-17-producing CD4+ T cells. The cells were gated on CD3+CD4+ T cells positive for IL-17 and subsequently the memory phenotype was determined by different combinations of expression of CD28 and CD45RO. CD28+CD45RO- cells were considered to be naïve T cells, CD28+CD45RO+ cells were considered to be early memory T cells, CD28-CD45RO- cells were considered to be memory T cells and CD28-CD45RO- cells were considered to be late memory cells. Representative dot plot of CD45RO and CD28 expression by IL-17-producing CD4+ T cells (top). Summary of 11 patients is depicted in the bottom graph.

HLA-B27 has been described to bind to KIR3DL2 expressed by CD4+ T cells in AS patients, thereby stimulating IL-17 production[14]. Therefore, the expression of KIR3DL2 on the IL-17-producing CD4+ T cells of patients with axial SpA was determined by flow cytometry. Expression of KIR3DL2 was detected on a small percentage of CD4+ T cells, on average 0.8% of the CD4+ T cells expressed KIR3DL2 (Figure 3A and 3B). Of these KIR3DL2+ CD4+ T cells, on average 2% produced IL-17 after stimulation. Thus, although a relative increase in IL-17-producing cells was observed within the KIR3DL2+ CD4+ T cells versus the total CD4+ T cell population (i.e. 2% *vs* 1.2%), only 0.02% of CD4+ T cells were double positive for IL-17 and KIR3DL2 (Figure 3C) as a result of the relative infrequency of KIR3DL2+ CD4+ T cells in peripheral blood. The expression of other KIRs was also evaluated using an antibody that recognizes KIR2DL2, KIR2DL3 and KIR2DS2 (KIR2DL2/3). Expression of KIR2DL2/3 was

detected on average on 0.1% of the CD4+ T cells (Figure 3D and 3E). Unexpectedly, a relative large fraction of these cells produced IL-17 as, on average 11.9% of the KIR2DL2/3+ CD4+ T cells stained positive for IL-17. Nonetheless, KIR2DL2/3 is expressed by a minority of CD4+ T cells, as only 0.01% of the total CD4+ T cells were IL-17 and KIR2DL2/3 positive (Figure 3F).
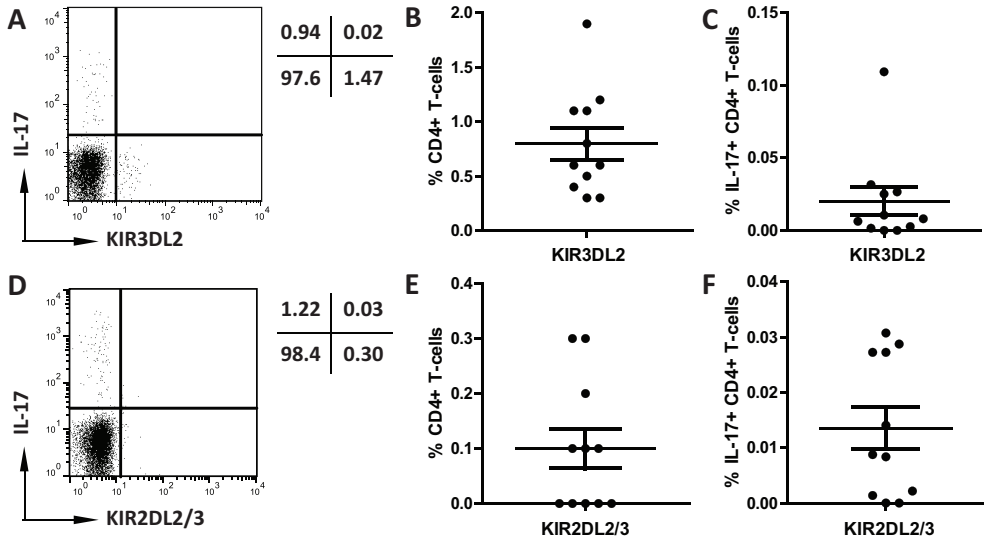

Figure 3. A small minority of IL-17-producing CD4+ T cells express KIRs. Killer cell immunoglobulin-like receptor (KIR) expression of IL-17-producing CD4+ T cells of patients with axial SpA was analysed using FACS. Cells were gated on CD3+CD4+ T cells and subsequently KIR and IL-17 expression was determined. Representative dot plots of IL-17 and KIR expression are depicted: (A) KIR3DL2 and (D) KIR2DL2/3. Summary of expression of (B) KIR3DL2 and (E) KIR2DL2/3 on CD4+ T cells of 11 patients. (C) and (F) represent the percentage of double-positive CD4+ T cells; either (C) IL-17 and KIR3DL2 or (F) IL-17 and KIR2DL2/3 double-positive cells.

5

DISCUSSION

Increased levels of IL-17-producing CD4+ T cells have been described in patients with AS with long disease duration and in animal models for SpA[2,4-6,15]. Whether this T cell population is already present in early disease is not known. Therefore, patients with axial SpA with short disease duration were tested for IL-17-producing CD4+ T cells and compared with healthy controls either positive or negative for HLA-B27. Patients with axial SpA showed an increased percentage of IL-17-producing CD4+ T cells compared with healthy controls. The percentage of IL-17-producing CD4+ T cells was similar in patients with and without MRI abnormalities. This increased percentage of IL-17-producing CD4+ T cells was disease related and not HLA-B27 specific as the healthy controls positive and negative for HLA-B27 exhibited comparable percentages of IL-17 producing CD4+ T cells. The IL-17-producing CD4+ T cells expressed TCRαβ and CD161 and exhibited a memory phenotype consistent with previous reports[4,5,8].

In contrast to our results, Appel et al.[9] reported no increase of IL-17-producing CD4+ T cells

in peripheral blood in SpA patients. Furthermore, a recent published study performed in Spain reported a decreased percentage of Th17 cells in patients with non-radiographic axial SpA compared with healthy controls[8]. Selection of patients could explain these differences. Compared with our patients, the Spanish patients had on average low disease activity based on the BASDAI, only a few patients had increased CRP and the number of SpA features was low[8]. In addition, despite a relatively short disease duration with a median back pain duration of only 16 months, already 6 out of 17 patients (36%) with a positive MRI showed signs of sacroiliitis on radiographs in our study. There are also technical differences, as the Spanish study used different isolation and stimulation of the cells and in particular a much longer stimulation of cells with PMA and ionomycin for 16 hours. Collectively, these data suggest that IL-17-producing CD4+ T cells are elevated only in active disease, which would limit the potential diagnostic use of measuring IL-17-producing CD4+ T cells in the peripheral blood of axial SpA patients. Moreover, increased levels of IL-17-producing CD4+ T cells have also been reported in rheumatoid arthritis[4,16-21] and in most reports the levels correlated with disease activity, demonstrating that this is not a disease-specific finding, but a general inflammation-related phenomenon. On the other hand, IL-17-producing CD4+ T cells were elevated irrespective of the presence of MRI abnormalities, making our results relevant to patients fulfilling both the imaging and the clinical arm of the ASAS classification criteria.

Our results were obtained from the peripheral blood compartment. However, the site of interest is the primary site of inflammation and the frequency of IL-17-producing cells in this compartment could be different from the peripheral blood compartment[9,22]. Biopsies of the affected target tissue in the spine are difficult to obtain in patients suffering from SpA which represents a clear limitation of the current study.

SpA is strongly associated with HLA-B27 and several hypotheses have been proposed to explain the role of HLA-B27 in the disease pathology[23]. One of these hypotheses proposes that HLA-B27 heavy chains can form homodimers that are able to bind KIR3DL2[13,24]. KIRs are typically expressed by natural killer (NK) cells, however, a subset of CD4+ T cells has been found to express KIR3DL2[25] consistent with our findings. CD4+ KIR3DL2+ T cells have been reported to be increased in AS patients and reportedly proliferate and produce IL-17 upon binding to HLA-B27 homodimers[14]. We found expression of KIR3DL2 by IL-17-producing CD4+ T cells in only a small minority of cells. This indicates that an interaction between KIR3DL2 and HLA-B27 is not required for induction and expansion of IL-17-producing CD4+ T cells in early disease. In addition, the higher frequency of KIR3DL2+ CD4+ T cells reported in later stages of disease suggests that these KIR3DL2+ CD4+ T cells expand as the disease becomes more chronic and since our patients suffered from active disease argues against a role in disease initiation. Nonetheless, given the relatively low frequency of KIR3DL2+ CD4+ T cells in peripheral blood, it would be interesting to investigate the absolute number of IL-17-producing KIR3DL2+ CD4+ T cells in peripheral blood in patients with established disease. Likewise, it would be interesting to study whether IL-17-production is confined to the

KIR3DL2+ CD4+ T cell pool or whether other KIR-expressing T cells, as surrogates for T cells with an activated/memory phenotype, are also more often IL-17 positive, as suggested by the data presented in the current article.

In summary, we report an increased frequency of IL-17-producing CD4+ T cells in axial SpA patients compared with healthy controls irrespective of MRI abnormalities. These results demonstrate that the frequency of IL-17-producing CD4+ T cells is enhanced in the early stages of disease.

5

REFERENCES

1. Rudwaleit M, van der Heijde D, Landewe R, et al. The development of Assessment of SpondyloArthritis international Society classification criteria for axial spondyloarthritis (part II): validation and final selection. Ann Rheum Dis 2009;68:777-83.

2. Glatigny S, Fert I, Blaton MA, et al. Proinflammatory Th17 cells are expanded and induced by dendritic cells in spondylarthritis-prone HLA-B27-transgenic rats. Arthritis Rheum 2012;64:110-20.

3. Abe Y, Ohtsuji M, Ohtsuji N, et al. Ankylosing enthesitis associated with up-regulated IFN-gamma and IL-17 production in (BXSB x NZB) F(1) male mice: a new mouse model. Mod Rheumatol 2009;19:316-22.

4. Shen H, Goodall JC, Hill Gaston JS. Frequency and phenotype of peripheral blood Th17 cells in ankylosing spondylitis and rheumatoid arthritis. Arthritis Rheum 2009;60:1647-56.

5. Jandus C, Bioley G, Rivals JP, Dudler J, Speiser D, Romero P. Increased numbers of circulating polyfunctional Th17 memory cells in patients with seronegative spondylarthritides. Arthritis Rheum 2008;58:2307-17.

6. Xueyi L, Lina C, Zhenbiao W, Qing H, Qiang L, Zhu P. Levels of circulating Th17 cells and regulatory T cells in ankylosing spondylitis patients with an inadequate response to anti-TNF-alpha therapy. J Clin Immunol 2013;33:151-61.

7. Kenna TJ, Davidson SI, Duan R, et al. Enrichment of circulating interleukin-17-secreting interleukin-23 receptor-positive gamma/delta T cells in patients with active ankylosing spondylitis. Arthritis Rheum 2012;64:1420-9.

8. Bautista-Caro MB, Arroyo-Villa I, Castillo-Gallego C, et al. Decreased Th17 and Th1 cells in the peripheral blood of patients with early non-radiographic axial spondyloarthritis: a marker of disease activity in HLA-B27(+) patients. Rheumatology (Oxford) 2013;52:352-62.

9. Appel H, Maier R, Wu P, et al. Analysis of IL-17(+) cells in facet joints of patients with spondyloarthritis suggests that the innate immune pathway might be of greater relevance than the Th17-mediated adaptive immune response. Arthritis Res Ther 2011;13:R95.

10. Di MP, Di CA, Laggner U, et al. The IL23R R381Q gene variant protects against immune-mediated diseases by impairing IL-23-induced Th17 effector response in humans. PLoS One 2011;6:e17160.

11. Sarin R, Wu X, Abraham C. Inflammatory disease protective R381Q IL23 receptor polymorphism results in decreased primary CD4+ and CD8+ human T-cell functional responses. Proc Natl Acad Sci U S A 2011;108:9560-5.

12. Baeten D, Baraliakos X, Braun J, et al. Anti-interleukin-17A monoclonal antibody secukinumab in treatment of ankylosing spondylitis: a randomised, double-blind, placebo-controlled trial. Lancet 2013;382:1705-13.

13. Kollnberger S, Bird L, Sun MY, et al. Cell-surface expression and immune receptor recognition of HLA-B27 homodimers. Arthritis Rheum 2002;46:2972-82.

14. Bowness P, Ridley A, Shaw J, et al. Th17 cells expressing KIR3DL2+ and responsive to HLA-B27 homodimers are increased in ankylosing spondylitis. J Immunol 2011;186:2672-80.

15. Ebihara S, Ono M. Inhibition of IL-17 by Antibody Administration Improves Onset of Tarsal Ankylosis In a Murine Model. Arthritis and Rheumatism 2011;63:S528-S.

16. Miao J, Geng J, Zhang K, et al. Frequencies of circulating IL-17-producing CD4+CD161+ T cells and CD4+CD161+ T cells correlate with disease activity in rheumatoid arthritis. Mod Rheumatol 2013.

17. Gullick NJ, Abozaid HS, Jayaraj DM, et al. Enhanced and persistent levels of interleukin (IL)-17(+) CD4(+) T cells and serum IL-17 in patients with early inflammatory arthritis. Clin Exp Immunol 2013;174:292-301.

18.	Chen DY, Chen YM, Chen HH, Hsieh CW, Lin CC, Lan JL. Increasing levels of circulating Th17 cells and interleukin-17 in rheumatoid arthritis patients with an inadequate response to anti-TNF-alpha therapy. Arthritis Res Ther 2011;13:R126.

19.	Leipe J, Grunke M, Dechant C, et al. Role of Th17 cells in human autoimmune arthritis. Arthritis Rheum 2010;62:2876-85.

20.	Alzabin S, Abraham SM, Taher TE, et al. Incomplete response of inflammatory arthritis to TNFalpha blockade is associated with the Th17 pathway. Ann Rheum Dis 2012;71:1741-8.

21.	Arroyo-Villa I, Bautista-Caro MB, Balsa A, et al. Frequency of Th17 CD4+ T cells in early rheumatoid arthritis: a marker of anti-CCP seropositivity. PLoS One 2012;7:e42189.

22.	Noordenbos T, Yeremenko N, Gofita I, et al. Interleukin-17-positive mast cells contribute to synovial inflammation in spondylarthritis. Arthritis Rheum 2012;64:99-109.

23.	Dougados M, Baeten D. Spondyloarthritis. Lancet 2011;377:2127-37.

24.	Kollnberger S, Chan A, Sun MY, et al. Interaction of HLA-B27 homodimers with KIR3DL1 and KIR3DL2, unlike HLA-B27 heterotrimers, is independent of the sequence of bound peptide. Eur J Immunol 2007;37:1313-22.

25.	van BJ, Thompson A, van der Slik A, Ottenhoff TH, Gussekloo J, Koning F. Phenotypic and functional characterization of CD4 T cells expressing killer Ig-like receptors. J Immunol 2004;173:6719-26.

5

CHAPTER 6

INTERLEUKIN 27 IS EXPRESSED BY CD4+ T CELLS

Diahann T.S.L. Jansen, Marieke Bax, Aleida M. Bakker, Martine Baarse & René E.M. Toes
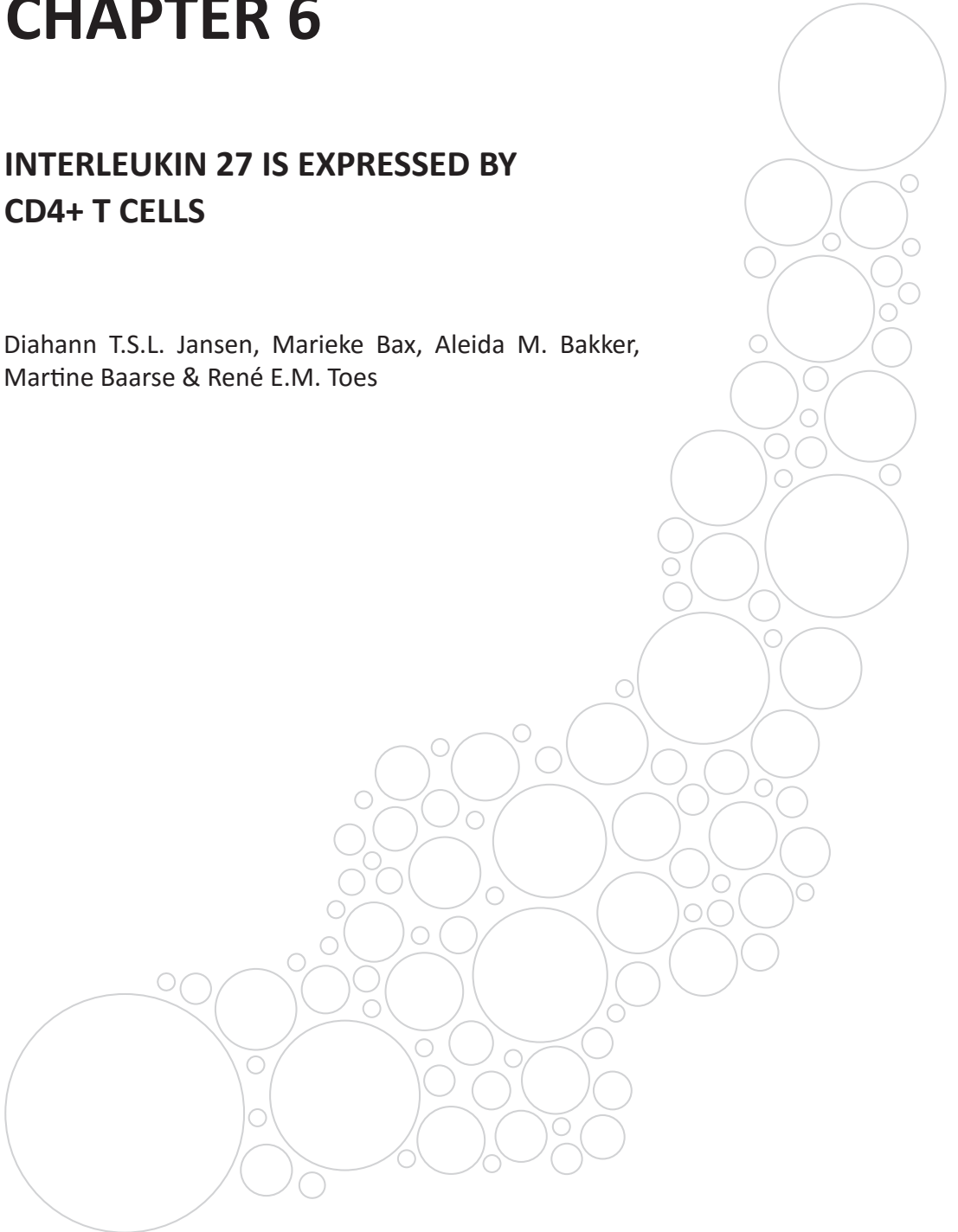
ABSTRACT

Introduction IL-27 is a cytokine belonging to the IL-12 cytokine family. It is composed of the subunits p28 and Epstein-Barr virus-induced gene 3 (EBI3) and is mainly produced by macrophages and dendritic cells. IL-27 was initially described as a Th1 promoting factor as it facilitates differentiation of naive CD4+ T cells into Th1 cells. However, conversion of activated T cells towards Tr1-like cells and suppression of Th2 and Th17 differentiation have been described as well.

Methods Considering the interesting capabilities of IL-27, we investigated whether also T cells are able to produce IL-27 in humans.

Results Intracellular staining of PBMCs for IL-27 showed that in addition to monocytes, CD4+ T cells expressed IL-27 upon stimulation with anti-CD3 and anti-CD28, while CD8+ T cells did not. Blocking of the staining with the IL-27 cytokine indicated that the staining was specific for IL-27. To investigate the CD4+ T cells in more detail we isolated the cells via different isolation methods. mRNA data showed almost no IL-27 p28 mRNA (specific subunit of IL-27) without stimulation, while a strong increase in mRNA levels was observed after stimulation with anti-CD3 and anti-CD28 indicating that IL-27 is produced by CD4+ T cells upon stimulation. Intracellular FACS staining of the isolated CD4+ T cells showed IL-27 positive CD4+ T cells after stimulation. However, we observed IL-27 positive CD4+ T cells without stimulation of the cells as well.

Conclusions Our data indicates that CD4+ T cells are capable of expressing IL-27 after activation. Since IL-27 is implicated in a variety of inflammatory diseases, CD4+ T cells could be an interesting source of this cytokine and potential biomarker or therapeutic target.

INTRODUCTION

IL-27 is part of the IL-12 cytokine family and is a heterodimeric cytokine composed of p28 (IL-27 p28) and Epstein-Barr virus-induced gene 3 (EBI3), mainly produced by activated antigen presenting cells[1-6]. The receptor of IL-27 consists of gp130 (also part of the receptor of the IL-6 family cytokines) and WSX-1 (the alpha subunit of the IL-27R complex) and activates STAT1 and/or STAT3[5]. As a result of the STAT 1 activation, IL-27 was initially described to promote Th1 differentiation, since STAT 1 activation leads to the induction and activation of T-bet, which induces the expression of IL-12Rβ2 making naïve CD4+ T-cells reactive to IL-12 stimulation for IFNγ production[1,5,7-9]. However, IL-27 has also been described to suppress IL-23 mediated Th17 differentiation and IL-4 mediated Th2 differentiation and therefore IL-27 has immunosuppressive effects as well[10-12]. In addition, IL-27 has been described to act on activated or differentiated helper T-cells by converting them into IL-10 producing Tr1-like cells[13,14].

Since IL-27 possesses pro- and anti-inflammatory effects, its therapeutic potential has been investigated in several animal models for immune-related disorders. The pro-inflammatory properties of IL-27 could be applied to augment anti-tumor responses[15], while the anti-inflammatory effects are interesting in inflammatory/autoimmune diseases. Local administration of IL-27 into the ankles of mice with collagen induced arthritis (CIA) ameliorated inflammation and bone erosion in addition to reduction of serum and joint IL-17 levels[16]. In a separate study, recombinant IL-27 was intraperitoneally administered to CIA mice resulting in reduced incidence and number of arthritic paws[17].

Considering the interesting properties of IL-27, we investigated whether, in addition to antigen presenting cells, T cells can produce IL-27 in humans.

METHODS

Isolation of cells

Peripheral mononuclear cells were isolated from buffy coats obtained from healthy volunteers (Sanquin Bloodbank, Leiden, the Netherlands) using Ficoll Paque density gradient centrifugation (Leiden University Medical Center Pharmacy, Leiden, the Netherlands). Subsequently, CD4+ T cells were either positively (Dynabeads FlowComp Human CD4, Invitrogen, California, USA) or negatively (CD4 Human Isolation Kit II, Miltenyi Biotec, Germany) isolated using magnetic separation.

Flowcytrometric analysis of IL-27 expression

Total PBMCs or isolated CD4+ T cells were stimulated with 5 ug/ml anti-CD3 (clone OKT3, eBioscience, California, USA) and 1 ug/ml anti-CD28 (Sanquin, The Netherlands) overnight and incubated with 10 ug/ml Brefeldin A (Sigma, St Louis, USA) for the last 4 hours. After stimulation, staining for dead cells (Fixation and dead cell discrimination kit, Miltenyi Biotec) and surface markers were performed using the following antibodies; CD3 Alexa Fluor 700 (UCHT1), CD4 PE-Cy7 (SK3), CD8 PerCP (SK1), CD14 Pacific Blue (M5E2) all purchased from

BD Biosciences (San Jose, California, USA). Intracellular staining for IL-27 was performed using the Cytofix/Cytoperm Fixation/Permeabilization Solution Kit from BD Biosciences and the anti-IL27 PE or APC antibody (307426) from R&D Systems (Minnesota, USA). In addition to IL-27, intracellular staining for several other cytokines was performed using the following antibodies; IL-4 (MP4-25D2), IL-10 (JES3-9D7), IFNγ (4S.B3), TNFα (MAb11) (all from BD Biosciences), IL-22 (142928) from R&D Systems and IL-6 (MQ2-13A5) and IL-17A (eBio064DEC017) from eBioscience. All samples were measured on a BD LSRFortessa cell analyser (BD Biosciences) and analyzed using BD FACSDIVA software (BD Biosciences) and FlowJo version 7.6.5 (FlowJo, Ashland, USA).

mRNA expression of IL27 p28

Isolated CD4+ T cells were stimulated with anti-CD3 and anti-CD28 or left unstimulated as control overnight. Subsequently, RNA was isolated using the RNAEasy kit (Qiagen, Germany) according to the supplier's protocol and converted to cDNA with SuperscriptIII (Invitrogen, USA). QPCR for the unique chain of IL-27, IL27p28, was performed and GAPDH was used as housekeeping gene to normalize the expression.

RESULTS

IL-27 is expressed by CD4+ T cells

To investigate whether human T cells are capable of producing IL-27, PBMCs were stained with different surface markers to discriminate CD4+ and CD8+ T cells and monocytes in combination with intracellular IL-27 staining using flow cytometry. The PBMCs were stimulated with anti-CD3 and anti-CD28 overnight and after stimulation IL-27 expression was detected by monocytes as expected (Figure 1A). Gating on the CD8+ T cells revealed a very low percentage of IL-27 positive CD8+ T cells (Figure 1B). However, IL-27 expression was detected in CD4+ T cells. Even in the unstimulated PBMCs, a small percentage of CD4+ T cells was positive for IL-27, but after stimulation a considerable percentage of the CD4+ T cells stained positive with the anti-IL-27 antibody (Figure 1C).

Since IL-27 has been described to have several effects on T cells, but not to be produced by CD4+ T cells in healthy humans, we blocked the anti-IL-27 antibody with recombinant IL-27 to confirm that the antibody binds specifically to IL-27. As IL-35 shares a subunit with IL-27 (EBI3), we also blocked the anti-IL-27 antibody with recombinant IL-35. The IL-27 positive signal provided by the anti-IL-27 antibody was completely abolished when 100 pg/ml or higher concentrations of IL-27 was added to the staining (Figure 1D and 1E). Addition of recombinant IL-35 did not abrogate the IL-27 positive signal indicating that the anti-IL-27 antibody specifically binds to IL-27 and not to the related IL-35.

Together, these results indicate that human CD4+ T cells can express IL-27.

Isolated CD4+ T cells expressed IL-27 p28 mRNA

To further investigate and confirm the IL-27 expression by CD4+ T cells, CD4+ T cells were
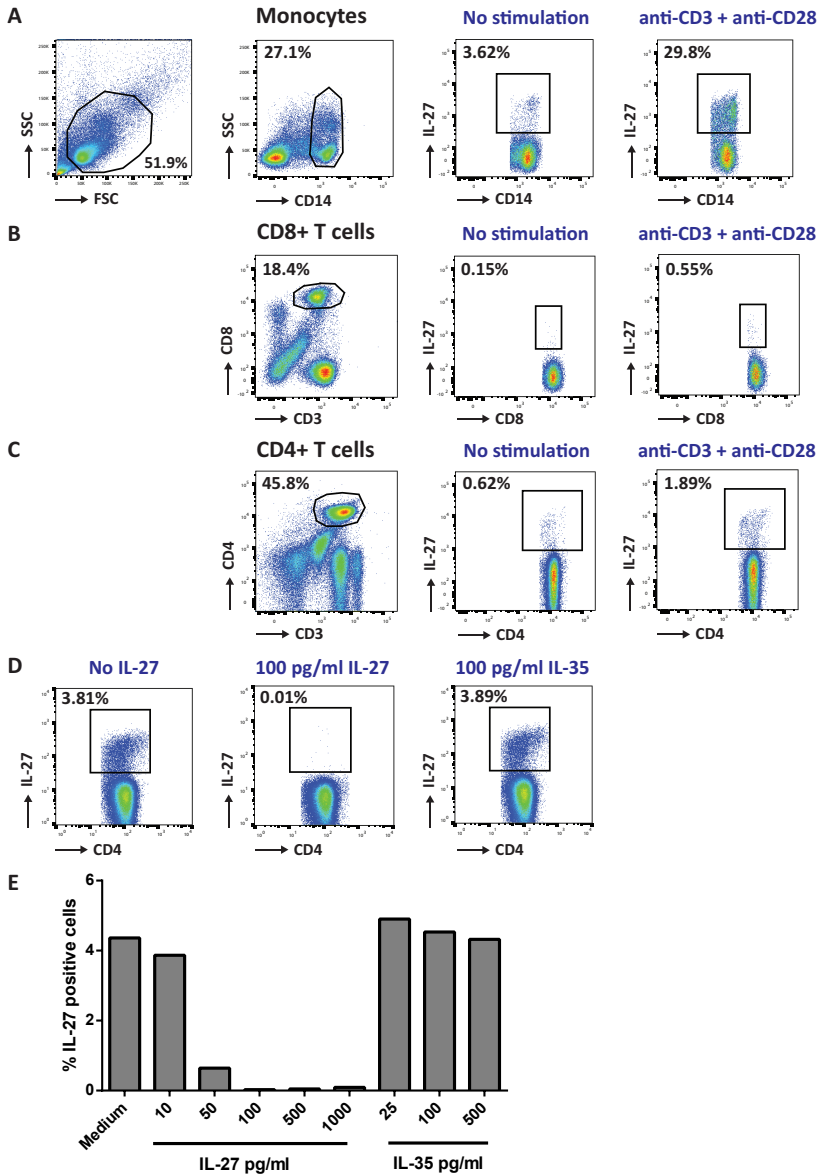
Figure 1. IL-27 is expressed by CD4+ T cells. PBMCs were stimulated overnight with anti-CD3 and anti-CD28 and stained for flowcytometric analysis with surface markers to identify, CD4+ T cells, CD8+ T cells and monocytes and intracellular to detect IL-27 expression. (A) Monocytes were identified by their CD14 expression and dot plots represent the gating strategy for monocytes and the IL-27 expression with and without anti-CD3 and anti-CD28 stimulation. (B) Cells double positive for CD3 and CD8 were identified as CD8+ T cells and dot plots depict the gating strategy and IL-27 expression of CD8+ T cells with and without stimulation with anti-CD3 and anti-CD28. (C) CD4+ T cells were identified by double positivity for CD3 and CD4. The dot plots display IL-27 positive CD4+ T cells with and without overnight stimulation with anti-CD3 and anti-CD28. (D) Dot plots showing IL-27 positive CD4+ T cells after stimulation with anti-CD3 and anti-CD28 with no recombinant IL-27 added (left), with 100 pg/ml IL-27 added (middle) or with 100 pg/ml recombinant IL-35 added (right). (E) Summary of the percentage of IL-27-positive CD4+ T cells in the different blocking conditions.

isolated using magnetic separation techniques and their IL-27 expression was again determined using flow cytometry (Figure 2A). CD4+ T cells were isolated using positive magnetic separation as well as negative magnetic separation. Both isolation procedures were utilized for confirmatory purposes. The purity of the cell populations was typically between 96% and 99%.
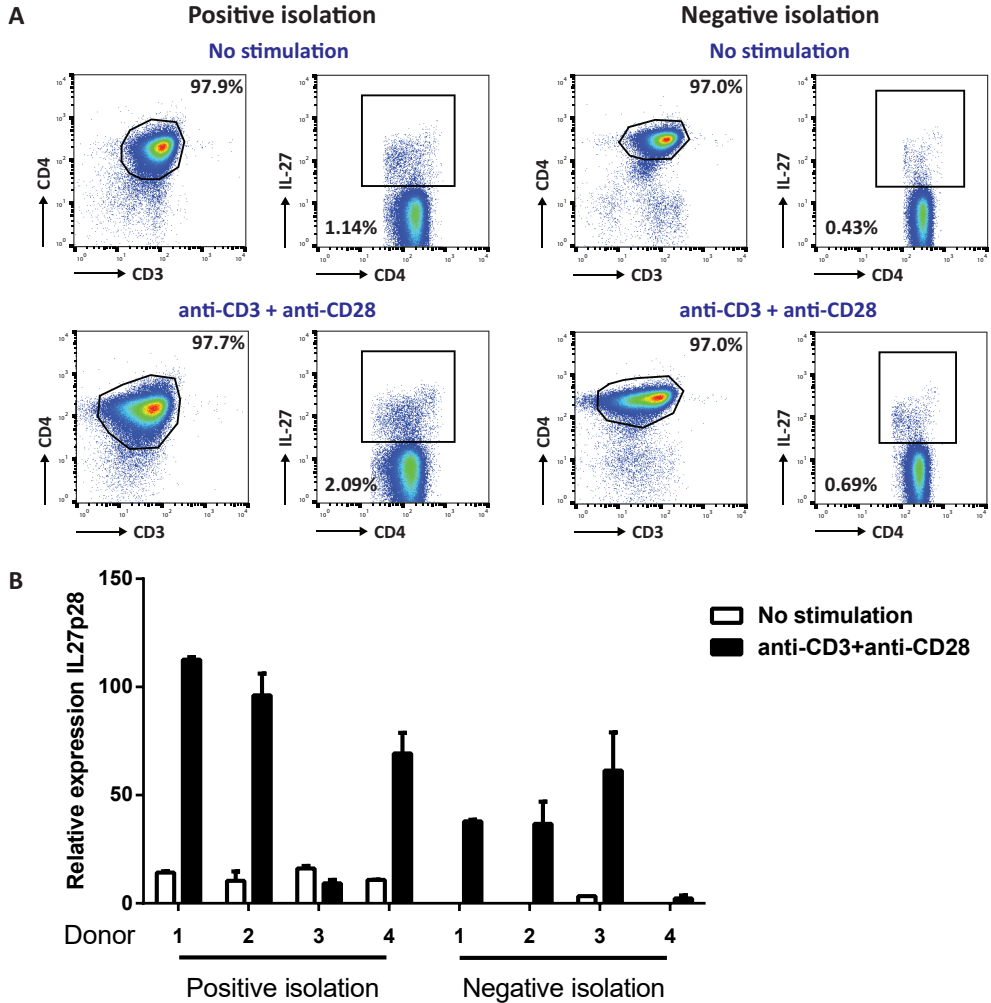
Figure 2. Isolated CD4+ T cells expressed IL27 protein and IL27 p28 mRNA. CD4+ T cells were isolated using positive or negative magnetic separation and stimulated overnight with anti-CD3 and anti-CD28 to analyze protein and mRNA expression of IL-27. (A) Flowcytometric analysis of the intracellular expression of IL-27 by positively (left) or negatively (right) isolated CD4+ T cells with (bottom) and without (top) stimulation. Percentage CD3+CD4+ T cells depicted is calculated from the total living cell population. The percentage IL27+CD4+ T cells is calculated from the CD3+CD4+ T cell population. (B) Isolated total CD4+ T cells populations were stimulated overnight with anti-CD3 and anti-CD28 and mRNA expression of the unique chain of IL-27, IL27 p28, was determined by qPCR. Relative expression to housekeeping gene GAPDH is depicted of four different donors.

To confirm the IL-27 expression by CD4+ T cells, we next performed mRNA expression analysis. Expression of the unique subunit of IL-27, IL27 p28, was analyzed by qPCR in CD4+ T cells isolated by either positive or negative magnetic separation. Intriguingly, high IL27 p28 expression was detected in the CD4+ T cells stimulated with anti-CD3 and anti-CD28, while the unstimulated CD4+ T cells showed low or no expression of IL27 p28 (Figure 2B). These results indicate that IL27 p28 mRNA expression is induced by activation of the CD4+ T cells.

IL27-positive CD4+ T cells did not express other T-helper subset cytokines
Over the years, several T helper subsets have been described producing their own signature cytokines[18]. To determine whether the IL-27 expressing CD4+ T cells are a part of one of these T helper subsets staining for IL-27 was combined with either T helper 1 cytokines IFNγ and TNFα, T helper 2 cytokine IL-4, T helper 17 cytokines IL-17, IL-6 and IL-22 and regulatory T cell cytokine IL-10 (Figure 3). IL-27-positive CD4+ T cells did not co-express one of these signature T helper subset cytokines, indicating that IL-27 positive CD4+ T cells are separate from one of the previously described T helper subsets.
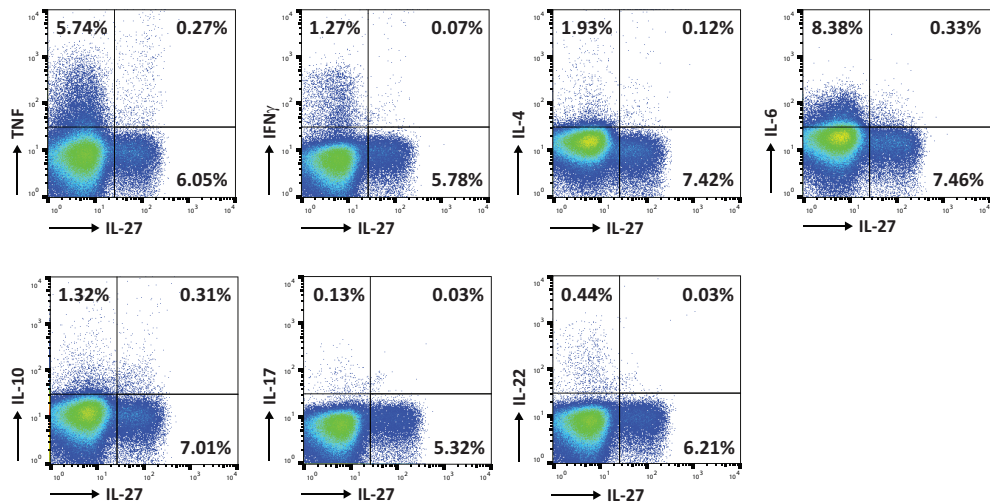
Figure 3. IL-27-positive CD4+ T cells did not express other T helper subset cytokines. CD4+ T cells were intracellular stained for the expression of IL-27 and several other known T helper subset cytokines after stimulation with anti-CD3 and anti-CD28. Dot plots show CD3+ CD4+ double positive cells and their expression of IL-27 in combination with either, TNFα, IFNγ, IL-4, IL-6, IL-10, IL-17 or IL-22.

DISCUSSION
IL-27 is an interesting cytokine as it has been described to possess pro- and anti-inflammatory properties[1]. It is produced by antigen presenting cells and has well described effects on CD4+ T cells. Our results indicate that IL-27 not only has an effect on CD4+ T cells, but that CD4+ T cells can also produce it in non-inflammatory conditions. After stimulation with anti-CD3 and anti-CD28, IL-27 production could be detected using flow cytometry and mRNA expression

analysis. Interestingly, the IL-27 producing CD4+ T cells did not produce any of the signature cytokines identifying the different T helper subsets indicating that they are not part of the well-defined T helper subsets.

Production of IL-27 by CD4+ T cells has been described before in pleural effusions of tuberculosis patients[19,20]. However, Yang *et al.* described very high percentages of IL-27-positive CD4+ T cells. On average 46.8% of the CD4+ T cells produced IL-27, which is not comparable to our results. This difference could be explained by the difference in diseased pleural effusion and healthy peripheral blood. In a subsequent study[20], the same group reported that the IL-27 producing CD4+ T cells are memory T cells separated from Th2, Th17 and Th22 cells based on their cytokine secretion and transcription factor profile which corresponds to our data. Recently, Kimura *et al.* reported IL-27 positive CD4+ T cells in a malaria parasite infection mouse model[21]. They also described IL-27-positive CD4+ T cells to be distinct from Th1 or regulatory Tr1 cells, in line with our data.

To verify the observation that CD4+ T cells produced IL-27 when stimulating PBMCs with anti-CD3 and anti-CD28, CD4+ T cells were isolated using positive magnetic selection. Intriguingly, unstimulated isolated CD4+ T cells already showed IL-27 positive cells. In unstimulated PBMCs a small percentage of the CD4+ T cells were positive for IL-27, however, a significant increase was observed after stimulation. To exclude the possibility that positive selection pre-activated the CD4+ T cells, negative isolation was performed as well. As observed for positively sorted cells, unstimulated negatively isolated CD4+ T cells showed IL-27 positivity as well. This is in contrast to the mRNA expression data, which indicate that unstimulated CD4+ T cells, either positively or negatively isolated, do not express IL-27, while there is a good expression of IL27p28 after stimulation. Future studies are required to clarify this apparent discrepancy.

The finding that CD4+ T cells are capable of producing IL-27 themselves is very interesting, however, the function and further characterization of these T cells would be the topic for future studies. It would be interesting to investigate the transcription factors expressed by these cells as their cytokine profile indicated that they most likely are not part of the already well-described T helper subsets. Since IL-27 has been reported to have beneficial effects in mouse models for rheumatoid arthritis[16,17], it would be interesting to enumerate and phenotype IL-27 positive CD4+ T cells in patients compared to healthy controls and potentially identifying a new biomarker. In addition, increased levels of IL-27 in synovial fluid of rheumatoid arthritis patients has been reported[22] and a polymorphism of IL27p28 has been described to be associated with severity of the disease[23] making IL-27 an interesting target for therapy.

In conclusion, CD4+ T cells are capable of producing IL-27 after activation via the T cell receptor making them a source of IL-27 and potential biomarker or therapeutic target.

REFERENCES

1.   Hunter CA. New IL-12-family members: IL-23 and IL-27, cytokines with divergent functions. Nature reviews Immunology 2005;5:521-31.

2.   Hunter CA, Kastelein R. Interleukin-27: balancing protective and pathological immunity. Immunity 2012;37:960-9.

3.   Kastelein RA, Hunter CA, Cua DJ. Discovery and biology of IL-23 and IL-27: related but functionally distinct regulators of inflammation. Annual review of immunology 2007;25:221-42.

4.   Yoshida H, Hunter CA. The immunobiology of interleukin-27. Annual review of immunology 2015;33:417-43.

5.   Yoshida H, Miyazaki Y. Regulation of immune responses by interleukin-27. Immunological reviews 2008;226:234-47.

6.   Batten M, Ghilardi N. The biology and therapeutic potential of interleukin 27. Journal of molecular medicine (Berlin, Germany) 2007;85:661-72.

7.   Takeda A, Hamano S, Yamanaka A, et al. Cutting edge: role of IL-27/WSX-1 signaling for induction of T-bet through activation of STAT1 during initial Th1 commitment. Journal of immunology (Baltimore, Md : 1950) 2003;170:4886-90.

8.   Pflanz S, Hibbert L, Mattson J, et al. WSX-1 and glycoprotein 130 constitute a signal-transducing receptor for IL-27. Journal of immunology (Baltimore, Md : 1950) 2004;172:2225-31.

9.   Pflanz S, Timans JC, Cheung J, et al. IL-27, a heterodimeric cytokine composed of EBI3 and p28 protein, induces proliferation of naive CD4+ T cells. Immunity 2002;16:779-90.

10.   Stumhofer JS, Laurence A, Wilson EH, et al. Interleukin 27 negatively regulates the development of interleukin 17-producing T helper cells during chronic inflammation of the central nervous system. Nature immunology 2006;7:937-45.

11.   Batten M, Li J, Yi S, et al. Interleukin 27 limits autoimmune encephalomyelitis by suppressing the development of interleukin 17-producing T cells. Nature immunology 2006;7:929-36.

12.   Yoshimura T, Takeda A, Hamano S, et al. Two-sided roles of IL-27: induction of Th1 differentiation on naive CD4+ T cells versus suppression of proinflammatory cytokine production including IL-23-induced IL-17 on activated CD4+ T cells partially through STAT3-dependent mechanism. Journal of immunology (Baltimore, Md : 1950) 2006;177:5377-85.

13.   Fitzgerald DC, Zhang GX, El-Behi M, et al. Suppression of autoimmune inflammation of the central nervous system by interleukin 10 secreted by interleukin 27-stimulated T cells. Nature immunology 2007;8:1372-9.

14.   Awasthi A, Carrier Y, Peron JP, et al. A dominant function for interleukin 27 in generating interleukin 10-producing anti-inflammatory T cells. Nature immunology 2007;8:1380-9.

15.   Hisada M, Kamiya S, Fujita K, et al. Potent antitumor activity of interleukin-27. Cancer research 2004;64:1152-6.

16.   Pickens SR, Chamberlain ND, Volin MV, et al. Local expression of interleukin-27 ameliorates collagen-induced arthritis. Arthritis and rheumatism 2011;63:2289-98.

17.   Niedbala W, Cai B, Wei X, et al. Interleukin 27 attenuates collagen-induced arthritis. Annals of the rheumatic diseases 2008;67:1474-9.

18.   Zhu J, Yamane H, Paul WE. Differentiation of effector CD4 T cell populations (*). Annual review of immunology 2010;28:445-89.

19.   Yang WB, Liang QL, Ye ZJ, et al. Cell origins and diagnostic accuracy of interleukin 27 in pleural effusions. PloS one 2012;7:e40450.

20.   Xia H, Ye ZJ, Zhou Q, et al. IL-27 and IL-27-producing CD4+ T cells in human tuberculous pleural effusion. Tuberculosis (Edinburgh, Scotland) 2014;94:579-88.

6

21.   Kimura D, Miyakoda M, Kimura K, et al. Interleukin-27-Producing CD4(+) T Cells Regulate Protective Immunity during Malaria Parasite Infection. Immunity 2016;44:672-82.

22.   Tanida S, Yoshitomi H, Ishikawa M, et al. IL-27-producing CD14(+) cells infiltrate inflamed joints of rheumatoid arthritis and regulate inflammation and chemotactic migration. Cytokine 2011;55:237-44.

23.   Paradowska-Gorycka A, Raszkiewicz B, Jurkowska M, et al. Association of single nucleotide polymorphisms in the IL27 gene with rheumatoid arthritis. Scandinavian journal of immunology 2014;80:298-305.

6

CHAPTER 7

SUMMARIZING DISCUSSION
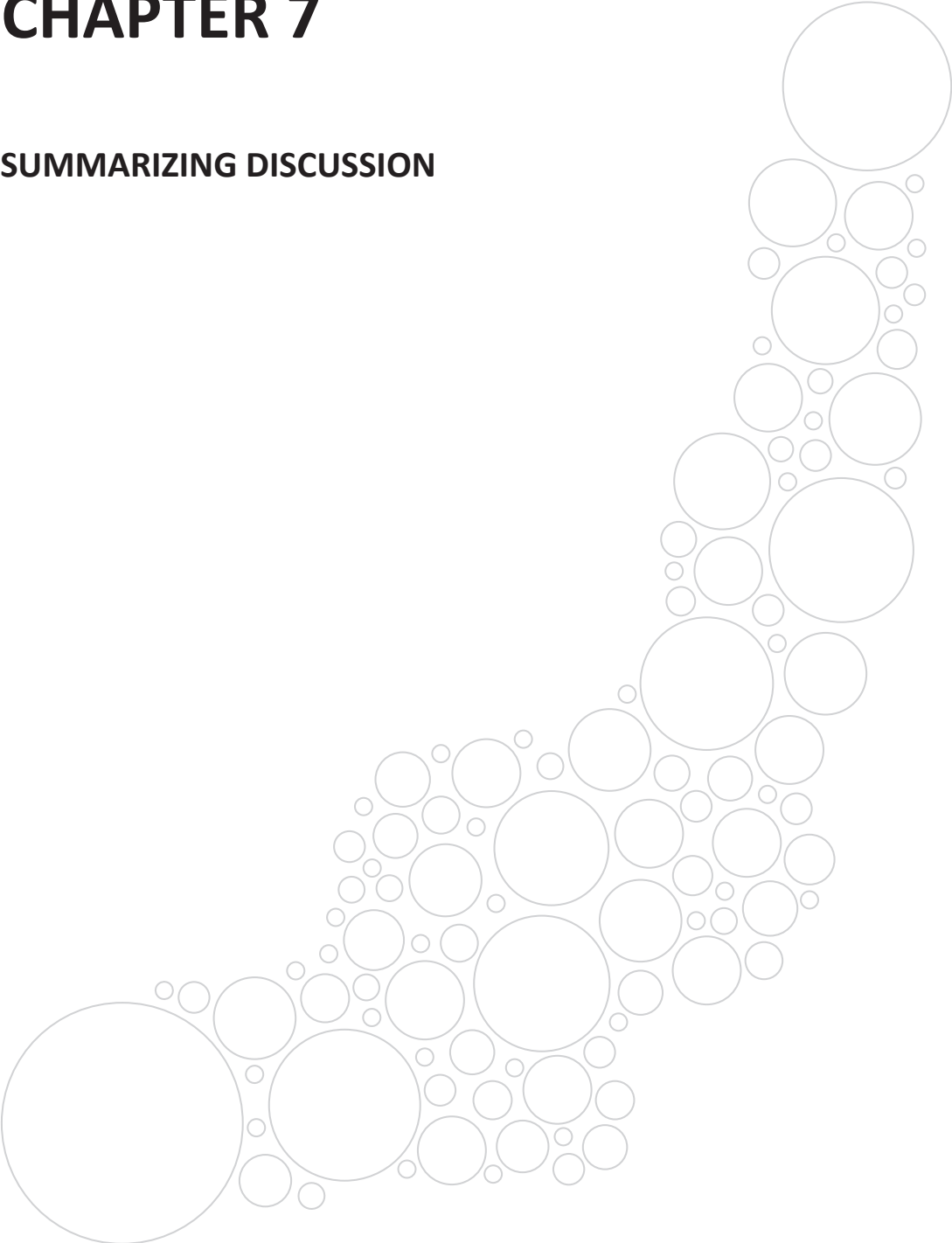
THE ADAPTIVE IMMUNE SYSTEM

The adaptive immune system protects the human body from invading pathogens by providing a highly specific immune response facilitated by T and B cells and by generating memory, which results in a fast and specific response upon a second infection with the same pathogen. To provide protection against a wide variety of pathogens, T and B cells can recognize a wide variety of antigens. This widespread recognition of antigens is achieved by random gene rearrangements in the T and B cell receptors. To ensure these random gene rearrangements do not generate self-antigen reactive cells, T and B cells are selected by their recognition pattern before they are allowed to enter the periphery[1]. However, this selection is not absolute and self-reactive T and B cells can escape to the periphery causing autoimmune disease like RA. This thesis focused on the role of the adaptive immune system in the development, treatment and diagnosis of rheumatic disorders.

PART I MOLECULAR BASIS FOR THE HLA-RA ASSOCIATION

In the first part of this thesis we focused on the longstanding association between the HLA locus and RA. ACPA autoantibodies separate RA patients into two distinct disease subsets, ACPA-positive and APCA-negative RA[2]. These two patient subsets differ in disease progression and risk of radiographic damage, but also in the associated HLA class II haplotypes[3-5]. In **Chapter 2**, we focused on ACPA-positive RA and the association with HLA-DRB1*0401, one of the shared epitope molecules which predisposes to APCA-positive RA and their linked HLA-DQ molecules as well as the protective HLA-DRB1*1301 allele. The molecular basis for this association is incompletely understood. Studies have shown that the association could be explained by the difference in binding and presentation of arthritogenic peptides as the residues responsible for the association are located in the antigen binding groove of the HLA-molecule[6,7]. We identified a new autoantigen, vinculin, recognized by ACPA from RA patients and by CD4+ T cells from HLA-DRB1*1301-negative individuals. We focused on a specific epitope of vinculin containing the amino acid sequence DERAA, which is also present in the HLA-DRB1*1301 molecule and in a large number of pathogens. Intriguingly, this vinculin-DERAA epitope and pathogen-derived DERAA-epitopes are only presented by the HLA-DQ molecules that are linked to the RA predisposing HLA-DR molecules and not by the HLA-DR molecules itself, indicating that also HLA-DQ molecules could explain the HLA-RA association. We further investigated the CD4+ T cells that recognize DERAA-epitopes and identified pathogen-derived DERAA epitope specific CD4+ T cells in addition to vinculin-DERAA specific CD4+ T cells in HLA-DRB1*1301 negative individuals. We identified epitopes from three gut-residing bacteria (*Campylobacter coli, Lactobacillus curvatus* and *Lactobacillus sakei*) to be recognized by the same TCR as the vinculin-DERAA self-epitope. These data are important as they show that a single TCR can crossreact between both DERAA-sequences from pathogens and self-protein vinculin. This molecular mimicry or crossreactivity between pathogen-derived and self-protein-derived epitopes provides an explanation for the presence of activated self-reactive CD4+ T cells directed to vinculin. These activated self-reactive CD4+ T cells can

7

provide help to B cells to produce ACPAs, which subsequently leads to the maturation of the ACPA response and acceleration of the autoimmune response[8-10]. This reaction will be absent in HLA-DRB1*1301 individuals, since the HLA-DRB1*1301-derived DERAA peptide will be presented in the thymus, which will lead to tolerization of the DERAA-reactive T cell response, the absence of help to B cells and protection against the development of an autoimmune response. These data provide an explanation how self-reactive T cell responses are induced and how the predisposing and protective HLA-alleles are involved in shaping such responses. In **Chapter 2**, we only focused on the protective effect of HLA-DRB1*1301, however, the DERAA sequence can be found in other protective HLA-DRB1 alleles (*0402, *1102, *1103) as well, but their low frequency in Caucasian populations impede functional studies[11]. Intriguingly, processing of these alleles generates a similar HLA-DERAA epitope suggesting that these alleles could protect through the same pathway as HLA-DRB1*1301[12]. Additional studies are required to further delineate the protective effect of HLA-DRB1*1301 and the potential use as therapeutic strategy.

The presence of activated self-reactive CD4+ T cells through molecular mimicry indicates a break of T cell tolerance and a role for CD4+ T cells in the development of RA by shaping the B cell response to citrullinated proteins. This is in line with previous evidence for a role for T cells in the ACPA response, including the observation that ACPAs contain all IgG subtypes, that ACPAs show extensive somatic hypermutation and that shared epitope alleles influence ACPA levels and fine specificity[13-15]. However, T cells most probably do not contribute to the initial break of B cell tolerance. The presence of ACPA can be detected up to ten years before disease onset and at that point the ACPA titers are low with restricted peptide reactivity[16-18]. A recent study using over 12,000 twins showed that environmental and stochastic factors are more important in the development of ACPA than the shared epitope alleles since the HLA-alleles predisposing for ACPA-positive RA, do not predispose to ACPA in healthy subjects[19]. Likewise, a study in a large cohort of healthy controls showed that almost 2% of this healthy cohort was positive for ACPA and that shared epitope status did not correlate with ACPA positivity[20]. This suggests that a 'first hit' is responsible for the loss of B cell tolerance to citrullinated self-proteins and the development of ACPA. A 'second hit' is subsequently required to progress from ACPA positivity to ACPA-positive RA. This second hit most likely involves help from T cells to B cells and subsequent maturation of the ACPA response[21,22]. The trigger of the 'second hit' is not known, however, it is conceivable that infection with a pathogen leads to activation of pathogen-directed T cell responses that crossreact with self-antigens resulting in activation of self-reactive B cells and expansion of the ACPA response. Since the shared epitope alleles are mainly associated with progression from ACPA positivity to ACPA-positive RA, protection from the development of self-reactive CD4+ T cells by HLA-DRB1*1301 is suggested to protect from the 'second hit'. Indeed, a recent study has shown that the protective HLA-DR13-alleles do not protect against formation of ACPA, but rather to ACPA-positive disease[23]. The time between the 'first hit' and the 'second hit' might provide a

window for therapy to prevent the development of ACPA-positive RA. Inhibiting the pathogens triggering crossreactivity, targeting DERAA-directed T cells or exploring the protective HLA-DR1*1301 effect could potentially be an effective therapeutic strategy to prevent progression from ACPA-positivity to ACPA-positive RA.

PART II THE MODE OF ACTION OF THE BIOLOGICAL ABATACEPT

The goal of current treatment strategies for RA is to treat to remission. Most RA patients cannot be cured from their disease, however, the development of biological DMARDs has made a tremendous contribution in controlling inflammation and disease progression. When RA patients respond well to their therapy, sustained low disease activity or remission can be achieved and in some cases even drug-free remission is accomplished[24]. Remission can be achieved by different biological DMARDs that target a specific pathway in the immune response. One of these biological DMARDs is Abatacept, a fusion protein of human CTLA-4 and the Fc region of human IgG1. Abatacept is thought to block costimulation of T cells by inhibiting binding of CD28 on the T cells to CD80 or CD86 on the APC as CTLA-4 binds to CD80 and CD86 with a higher affinity than CD28 (Figure 1)[25-27]. In the AMPLE study Abatacept was head-to-head compared to the TNF inhibitor Adalimumab in patients on a stable background of methotrexate. This study showed similar efficacy based on clinical, functional and radiographic outcomes[28]. Interestingly, TNF inhibitors are thought to have a rapid mode of action as they directly inhibit inflammation by blocking TNF, whereas Abatacept is thought to have a slow mode of action as the effect of costimulation blockade does not become apparent directly. Consequently, similar efficacy of Adalimumab and Abatacept indicates a different mode of action of Abatacept in addition to inhibition of costimulation. In **Chapter 3**, we investigated whether the mode of action of Abatacept depends solely on its ability to inhibit T cell activation. We showed that Abatacept is still effective in the absence of CD4+ T cells in a mouse model of arthritis, indicating that Abatacept has another mode of action in addition to costimulation blockade. Further studies are required to specify this different mode of action, however, a wide range of possible targets of Abatacept have been described. Since we observed a decrease in serum antibody titers after Abatacept treatment and a decrease in antibody titers in the supernatant of *ex vivo* cultured spleen and bone marrow cells from mice treated with Abatacept and depleted of CD4+ T cells, Abatacept could have a direct effect on B cells. This observation is in line with the report of Rozanski *et al.* showing that CD28 serves as a survival signal for long lived plasma cells. Loss of CD28 or its ligands CD80 and CD86 caused significant loss of long lived plasma cells resulting in decreased antibody titers[29]. As Abatacept prevents the binding of CD28 to CD80 and CD86, this survival signal could be abrogated leading to loss of long lived plasma cells and consequently a decrease in antibody titers corresponding with our observations presented in **Chapter 3**. Likewise, it has been reported that elevated expression of activation induced cytidine deaminase (AID) in recirculating follicular CD86+ B cells and increased germinal center activity are associated with the production of autoantibodies in the BXD2 mouse model of autoimmune disease[30].

7

Treatment with CTLA-4-Ig (Abatacept) resulted in normalization of AID expression in the B-cells and suppression of IgG autoantibodies, which could explain the decrease in IgG titers we observed after Abatacept treatment in the absence of CD4+ T cells.

The CD4+ T cell-independent effect could also be explained by the induction of nitric oxide synthase (NOS) or indoleamine 2,3-dioxygenase (IDO) by APCs[31-33]. In an allergic airway inflammation model, CTLA-4-Ig was described to suppress inflammation in CD28/BLTA-double deficient mice and this suppression could be reversed by treatment with a NOS inhibitor. In addition, CTLA-4-Ig treatment was ineffective in NOS2-deficient mice indicating that the suppressive effect of CTLA-4-Ig on inflammation is mediated by NO[31]. IDO is an enzyme that degrades the essential amino acid tryptophan resulting in local depletion of tryptophan[34]. This depletion is sensed by neighbouring T cells inducing GCN2 kinase expression leading to cell arrest and thereby inhibition of T cell proliferation and inhibition of the expansion of the immune response[35-39]. In addition to the suppressing effect on proliferating effector T cells, IDO expressing dendritic cells are able to promote the activation of regulatory T cells and the differentiation of naïve T cells to regulatory T cells[34,40,41]. Ligation of CD80 and CD86 by CTLA-4 induces IDO activity in dendritic cells and as CTLA-4-Ig binds to CD80/86, it is capable of IDO induction potentially explaining the inflammation suppressing effects of Abatacept[32,33].

In addition to effects on T-cells, IDO has been described to affect other cell types as well. A recent study reported on IDO expression by osteoclast precursors after CTLA-4-Ig challenge. In this study it was shown that CTLA-4-Ig could induce apoptosis and a reduction in frequency of osteoclast precursors and osteoclastogenesis[42]. In RA patients treated with Abatacept, a reduction in the frequency of osteoclast precursors was described after treatment, indicating that Abatacept could reduce the number of osteoclast precursors and therefore the number of osteoclasts. This could explain the reduction in bone erosion after Abatacept treatment in RA patients. Together, these and other studies describing the promotion of bone formation by CTLA-4-Ig, point to the anti-erosive effects of Abatacept independent of its role on T cells[43]. Likewise, Abatacept has also been described to have a direct effect on monocytes and macrophages. For example, Bonelli *et al.* reported a decreased expression of adhesion molecules and a reduction in endothelial adhesion and transendothelial migratory capacity of monocytes after Abatacept treatment in RA patients[44]. Decreased cytokine production and reduction of the inflammatory reaction by macrophages have been reported as a result of Abatacept treatment as well, which could account for the beneficial effect in the treatment of RA[45-48].

Abatacept could exert its effectiveness through all the pathways and targets explained above and summarized in Figure 1. The different observed clinical effects do suggest the use of multiple modes of action. The direct anti-inflammatory effects on monocytes and macrophages could account for the rapid effects that are observed through similar efficacy compared to TNF-inhibitor Adalimumab[28]. Moreover, the effects on the T and B cells as part of the adaptive immune could explain the observed achieved remission after Abatacept

treatment as the underlying autoimmune response is targeted and inhibited[49,50]. All these different modes of action make Abatacept an interesting treatment option for early RA.

In **Chapter 4**, we reported that Abatacept treatment in early RA could induce conversion from being autoantibody positive to being autoantibody negative and that this conversion was associated with remission. This is in line with previous reports on the AGREE study, in which high remission rates and less radiographic damage were described[49,50]. Two other studies evaluating the effect of Abatacept in early RA (ADJUST and AVERT) reported robust efficacy as well, and in some cases even drug-free remission was achieved[51,52]. In conclusion, Abatacept is an effective treatment for RA[53,54]. This widespread effectiveness might be explained by the different modes of action Abatacept can exert (Figure 1) making Abatacept (in combination with methotrexate) an effective drug that can be used when synthetic DMARDs fail to control RA.
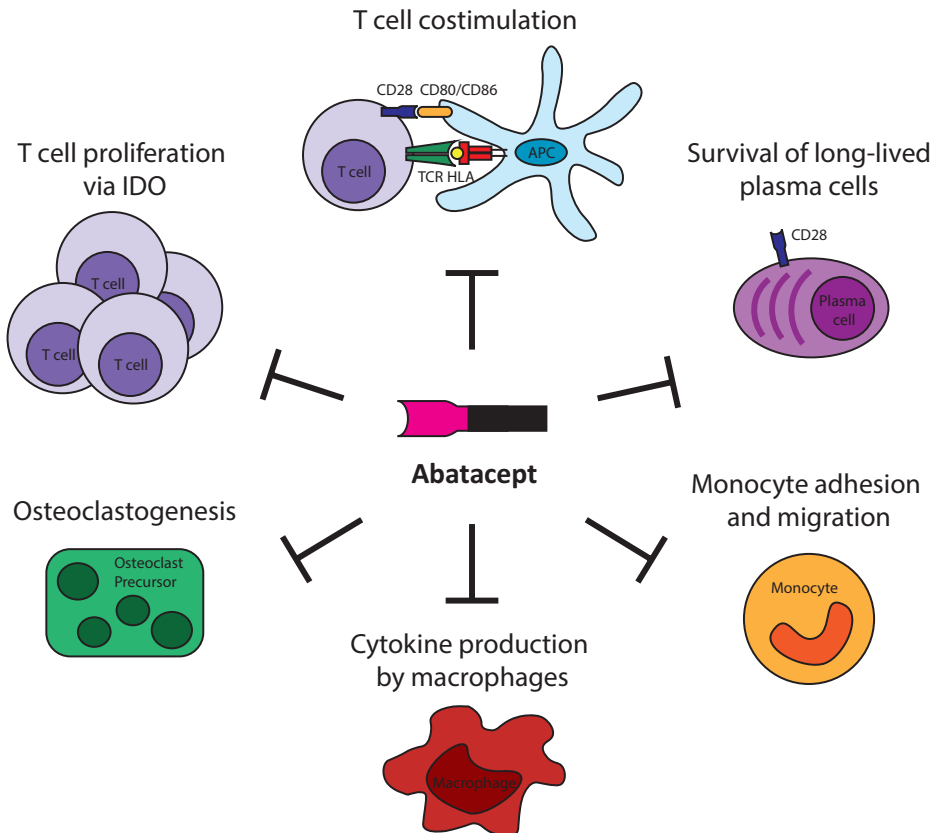

Figure 1. Possible modes of action of Abatacept. Abatacept is thought to block costimulation of T cells by inhibiting the binding of CD28 to CD80/CD86. In addition, several other mechanisms have been described as well. Abatacept could block survival of long-lived plasma cells as CD28 serves as a survival signal for these cells. Abatacept is also capable of decreasing the expression of adhesion molecules on monocytes and therefore their migration capacity. Abatacept has been described to reduce the cytokine production and inflammatory response of macrophages. Inhibition of osteoclastogenesis after Abatacept treatment has been described as well. Abatacept can also induce IDO production, which inhibits the proliferation of T cells by degrading the essential amino acid tryptophan.

PART III CYTOKINE PRODUCING CD4+ T CELLS IN DISEASE AND HEALTH

Advances in understanding the pathogenesis of RA have led to the development of new therapeutics with improved outcomes. However, current conventional and biologic DMARD-based therapies are not successful in reaching remission in all rheumatic disease patients and early diagnosis is still challenging. Not every patient responds to methotrexate or TNF inhibitors and a change in treatment strategy to another biologic DMARD is consequently required to control the inflammation[55]. However, it takes a few months to evaluate whether a DMARD is effective in a patient and if the DMARD is not effective the inflammation has the chance to progress causing more damage. Therefore, it is important to be able to determine which patients are going to respond to a specific therapeutic and which patients are not. Biomarkers could be a helpful tool in determining diagnosis and predict response to therapy. Cells of the adaptive immune system, such as CD4+ T cells, could be a good candidate to function as biomarker. CD4+ T cells can be divided in several subsets based on their function and cytokine production as discussed in Chapter 1 [56,57]. In **Chapter 5** and **6**, we have attempted to determine whether certain CD4+ T cell subsets are specifically increased in disease and can function to identify patients in an early stage of disease. In **Chapter 6**, we focused on IL-27-positive CD4+ T cells and in **Chapter 5** we were interested in IL-17-producing CD4+ T cells. Early diagnosis of ankylosing spondylitis is important as current diagnosis is based on structural damage on radiographs, however, this bone formation is irreversible and a sign of advanced disease. The anti-IL-17A monoclonal antibody, secukinumab, has shown promising results in the treatment of ankylosing[58,59]. Therefore, we investigated whether IL-17-producing CD4+ T cells were already increased in patients with early, active spondyloarthritis to potentially use this population as a diagnostic biomarker. Despite the observed increase in IL-17-producing CD4+ T cells in early spondyloarthritis patients compared to healthy controls, the potential to use this population as biomarker was limited, as the population appeared to be increased only in active disease. Since increased levels of IL-17-producing CD4+ T cells are also detected in RA patients[60-62], this increased population is not disease-specific, but rather a general inflammation-related phenomenon.

Autoantigen-specific CD4+ T cells are potentially a more suitable biomarker as they represent a disease-specific cell population. They can be identified using peptide-HLA multimers, which also allows for phenotypic and single-cell analysis[63,64]. Autoantigen-specific CD4+ T cells have been identified in RA patients as well as in healthy controls. However, in RA patients these cells exhibit a proinflammatory phenotype, while they appear to be regulatory in healthy controls[7,65,66]. Therefore, phenotypic analysis should be combined with the peptide-HLA multimers to be implemented as a disease specific biomarker. Current strategies to treat RA that are under development are focused on antigen-specific tolerance induction leaving the anti-pathogen and anti-tumor responses unimpaired. These strategies include administration of low or escalating doses of relevant antigenic peptides, exposure of tolerogenic dendritic cells to relevant peptides and strategies targeting dendritic cells[22,67]. However, the diversity

of autoantigens in RA makes the choice of antigen for immunotherapy challenging. Nonetheless, it is important to develop tools to monitor the effects of immunotherapy on the number, phenotype and function of antigen-specific T and B cells in conjunction with the development of the immunotherapies itself. Peptide-HLA multimers have great potential utility for the enumeration and phenotypic analysis of autoantigen-specific CD4+ T cells in response to therapy. They could also be employed as a selection tool to predict response to antigen-specific therapy by identification of the specific CD4+ T cell response against the antigen used in the antigen-specific therapy. Moreover, the use of peptide-HLA multimers in RA patients, healthy controls and their first degree relatives could also provide more details on the pathogenesis of RA. Good biomarkers will be very helpful in early diagnosis, predicting response to therapy and therefore treatment choice and monitoring response to therapy and the cells of the adaptive immune system are potentially good candidates to serve as biomarkers. However, more research is required to identify these disease specific biomarkers and their involvement in the disease development.

In conclusion, the adaptive immune system plays a very important role in the development of RA as crossreactive CD4+ T cells are involved in the autoreactive inflammatory response helping B cells to develop into autoantibody producing cells leading to the maturation of the ACPA response and ACPA-positive RA. Targeting the adaptive immune response with Abatacept helps to reduce inflammation and disease severity by possibly targeting several players in the adaptive immune system and potentially the innate immune system as well. Given that not every therapy is effective in every patient, monitoring progression and response to therapy would be very helpful and could be established using selective parts of the adaptive immune system. The data presented in this thesis indicate that the adaptive immune system is an important player in the development, therapy and diagnosis of arthritis with important implications for the development of future therapeutic strategies.

7

REFERENCES

1.   Parham P. The Immune System. New York: Garland Science; 2005.

2.   van der Helm-van Mil AH, Huizinga TW. Advances in the genetics of rheumatoid arthritis point to subclassification into distinct disease subsets. Arthritis research & therapy 2008;10:205.

3.   van der Helm-van Mil AH, Verpoort KN, Breedveld FC, Toes RE, Huizinga TW. Antibodies to citrullinated proteins and differences in clinical progression of rheumatoid arthritis. Arthritis research & therapy 2005;7:R949-58.

4.   Verpoort KN, van Gaalen FA, van der Helm-van Mil AH, et al. Association of HLA-DR3 with anti-cyclic citrullinated peptide antibody-negative rheumatoid arthritis. Arthritis Rheum 2005;52:3058-62.

5.   Huizinga TW, Amos CI, van der Helm-van Mil AH, et al. Refining the complex rheumatoid arthritis phenotype based on specificity of the HLA-DRB1 shared epitope for antibodies to citrullinated proteins. Arthritis and rheumatism 2005;52:3433-8.

6.   Hill JA, Southwood S, Sette A, Jevnikar AM, Bell DA, Cairns E. Cutting edge: the conversion of arginine to citrulline allows for a high-affinity peptide interaction with the rheumatoid arthritis-associated HLA-DRB1*0401 MHC class II molecule. Journal of immunology (Baltimore, Md : 1950) 2003;171:538-41.

7.   Scally SW, Petersen J, Law SC, et al. A molecular basis for the association of the HLA-DRB1 locus, citrullination, and rheumatoid arthritis. The Journal of experimental medicine 2013;210:2569-82.

8.   Wucherpfennig KW, Strominger JL. Molecular mimicry in T cell-mediated autoimmunity: viral peptides activate human T cell clones specific for myelin basic protein. Cell 1995;80:695-705.

9.   Enouz S, Carrie L, Merkler D, Bevan MJ, Zehn D. Autoreactive T cells bypass negative selection and respond to self-antigen stimulation during infection. The Journal of experimental medicine 2012;209:1769-79.

10.   Sewell AK. Why must T cells be cross-reactive? Nat Rev Immunol 2012;12:669-77.

11.   van der Helm-van Mil AH, Huizinga TW, Schreuder GM, Breedveld FC, de Vries RR, Toes RE. An independent role of protective HLA class II alleles in rheumatoid arthritis severity and susceptibility. Arthritis Rheum 2005;52:2637-44.

12.   Snijders A, Elferink DG, Geluk A, et al. An HLA-DRB1-derived peptide associated with protection against rheumatoid arthritis is naturally processed by human APCs. Journal of immunology (Baltimore, Md : 1950) 2001;166:4987-93.

13.   Verpoort KN, Jol-van der Zijde CM, Papendrecht-van der Voort EA, et al. Isotype distribution of anti-cyclic citrullinated peptide antibodies in undifferentiated arthritis and rheumatoid arthritis reflects an ongoing immune response. Arthritis Rheum 2006;54:3799-808.

14.   Amara K, Steen J, Murray F, et al. Monoclonal IgG antibodies generated from joint-derived B cells of RA patients have a strong bias toward citrullinated autoantigen recognition. The Journal of experimental medicine 2013;210:445-55.

15.   Verpoort KN, Cheung K, Ioan-Facsinay A, et al. Fine specificity of the anti-citrullinated protein antibody response is influenced by the shared epitope alleles. Arthritis Rheum 2007;56:3949-52.

16.   van de Stadt LA, de Koning MH, van de Stadt RJ, et al. Development of the anti-citrullinated protein antibody repertoire prior to the onset of rheumatoid arthritis. Arthritis and rheumatism 2011;63:3226-33.

17.   Rantapaa-Dahlqvist S, de Jong BA, Berglin E, et al. Antibodies against cyclic citrullinated peptide and IgA rheumatoid factor predict the development of rheumatoid arthritis. Arthritis and rheumatism 2003;48:2741-9.

18.   Nielen MM, van Schaardenburg D, Reesink HW, et al. Specific autoantibodies

precede the symptoms of rheumatoid arthritis: a study of serial measurements in blood donors. Arthritis and rheumatism 2004;50:380-6.

19. Hensvold AH, Magnusson PK, Joshua V, et al. Environmental and genetic factors in the development of anticitrullinated protein antibodies (ACPAs) and ACPA-positive rheumatoid arthritis: an epidemiological investigation in twins. Annals of the rheumatic diseases 2015;74:375-80.

20. Terao C, Ohmura K, Ikari K, et al. Effects of smoking and shared epitope on the production of anti-citrullinated peptide antibody in a Japanese adult population. Arthritis care & research 2014;66:1818-27.

21. Willemze A, Trouw LA, Toes RE, Huizinga TW. The influence of ACPA status and characteristics on the course of RA. Nature reviews Rheumatology 2012;8:144-52.

22. Koning F, Thomas R, Rossjohn J, Toes RE. Coeliac disease and rheumatoid arthritis: similar mechanisms, different antigens. Nature reviews Rheumatology 2015;11:450-61.

23. van Heemst J, Hensvold AH, Jiang X, et al. Protective effect of HLA-DRB1*13 alleles during specific phases in the development of ACPA-positive RA. Annals of the rheumatic diseases 2015.

24. Nagy G, van Vollenhoven RF. Sustained biologic-free and drug-free remission in rheumatoid arthritis, where are we now? Arthritis research & therapy 2015;17:181.

25. Linsley PS, Nadler SG. The clinical utility of inhibiting CD28-mediated costimulation. Immunological reviews 2009;229:307-21.

26. Moreland L, Bate G, Kirkpatrick P. Abatacept. Nat Rev Drug Discov 2006;5:185-6.

27. Emery P. The therapeutic potential of costimulatory blockade with CTLA4Ig in rheumatoid arthritis. Expert opinion on investigational drugs 2003;12:673-81.

28. Schiff M, Weinblatt ME, Valente R, et al. Head-to-head comparison of subcutaneous abatacept versus adalimumab for rheumatoid arthritis: two-year efficacy and safety findings from AMPLE trial. Annals of the rheumatic diseases 2014;73:86-94.

29. Rozanski CH, Arens R, Carlson LM, et al. Sustained antibody responses depend on CD28 function in bone marrow-resident plasma cells. The Journal of experimental medicine 2011;208:1435-46.

30. Hsu HC, Wu Y, Yang P, et al. Overexpression of activation-induced cytidine deaminase in B cells is associated with production of highly pathogenic autoantibodies. Journal of immunology (Baltimore, Md : 1950) 2007;178:5357-65.

31. Deppong CM, Parulekar A, Boomer JS, Bricker TL, Green JM. CTLA4-Ig inhibits allergic airway inflammation by a novel CD28-independent, nitric oxide synthase-dependent mechanism. European journal of immunology 2010;40:1985-94.

32. Grohmann U, Orabona C, Fallarino F, et al. CTLA-4-Ig regulates tryptophan catabolism in vivo. Nature immunology 2002;3:1097-101.

33. Munn DH, Sharma MD, Mellor AL. Ligation of B7-1/B7-2 by human CD4+ T cells triggers indoleamine 2,3-dioxygenase activity in dendritic cells. Journal of immunology (Baltimore, Md : 1950) 2004;172:4100-10.

34. Mellor AL, Munn DH. IDO expression by dendritic cells: tolerance and tryptophan catabolism. Nat Rev Immunol 2004;4:762-74.

35. Munn DH, Sharma MD, Baban B, et al. GCN2 kinase in T cells mediates proliferative arrest and anergy induction in response to indoleamine 2,3-dioxygenase. Immunity 2005;22:633-42.

36. Lee GK, Park HJ, Macleod M, Chandler P, Munn DH, Mellor AL. Tryptophan deprivation sensitizes activated T cells to apoptosis prior to cell division. Immunology 2002;107:452-60.

37. Mellor AL, Keskin DB, Johnson T, Chandler P, Munn DH. Cells expressing indoleamine 2,3-dioxygenase inhibit T cell responses. Journal of immunology (Baltimore, Md : 1950) 2002;168:3771-6.

7

38.   Mellor AL, Baban B, Chandler P, et al. Cutting edge: induced indoleamine 2,3 dioxygenase expression in dendritic cell subsets suppresses T cell clonal expansion. Journal of immunology (Baltimore, Md : 1950) 2003;171:1652-5.

39.   Terness P, Bauer TM, Rose L, et al. Inhibition of allogeneic T cell proliferation by indoleamine 2,3-dioxygenase-expressing dendritic cells: mediation of suppression by tryptophan metabolites. The Journal of experimental medicine 2002;196:447-57.

40.   Sharma MD, Baban B, Chandler P, et al. Plasmacytoid dendritic cells from mouse tumor-draining lymph nodes directly activate mature Tregs via indoleamine 2,3-dioxygenase. The Journal of clinical investigation 2007;117:2570-82.

41.   Chen W, Liang X, Peterson AJ, Munn DH, Blazar BR. The indoleamine 2,3-dioxygenase pathway is essential for human plasmacytoid dendritic cell-induced adaptive T regulatory cell generation. Journal of immunology (Baltimore, Md : 1950) 2008;181:5396-404.

42.   Bozec A, Zaiss MM, Kagwiria R, et al. T cell costimulation molecules CD80/86 inhibit osteoclast differentiation by inducing the IDO/tryptophan pathway. Science translational medicine 2014;6:235ra60.

43.   Axmann R, Herman S, Zaiss M, et al. CTLA-4 directly inhibits osteoclast formation. Annals of the rheumatic diseases 2008;67:1603-9.

44.   Bonelli M, Ferner E, Goschl L, et al. Abatacept (CTLA-4IG) treatment reduces the migratory capacity of monocytes in patients with rheumatoid arthritis. Arthritis and rheumatism 2013;65:599-607.

45.   Brizzolara R, Soldano S, Montagna P, et al. [CTLA4-Ig interferes and downregulates the proinflammatory activities of rheumatoid synovial macrophages in monoculture]. Reumatismo 2011;63:80-5.

46.   Cutolo M, Paolino S, Pizzorni C, et al. Effects of combined treatments with CTLA4-IG (abatacept), dexamethasone and methotrexate on cultured human macrophages. Clinical and experimental rheumatology 2016.

47.   Cutolo M, Soldano S, Contini P, et al. Intracellular NF-kB-decrease and IKBalpha increase in human macrophages following CTLA4-Ig treatment. Clinical and experimental rheumatology 2013;31:943-6.

48.   Cutolo M, Soldano S, Montagna P, et al. CTLA4-Ig interacts with cultured synovial macrophages from rheumatoid arthritis patients and downregulates cytokine production. Arthritis research & therapy 2009;11:R176.

49.   Bathon J, Robles M, Ximenes AC, et al. Sustained disease remission and inhibition of radiographic progression in methotrexate-naive patients with rheumatoid arthritis and poor prognostic factors treated with abatacept: 2-year outcomes. Annals of the rheumatic diseases 2011;70:1949-56.

50.   Smolen JS, Wollenhaupt J, Gomez-Reino JJ, et al. Attainment and characteristics of clinical remission according to the new ACR-EULAR criteria in abatacept-treated patients with early rheumatoid arthritis: new analyses from the Abatacept study to Gauge Remission and joint damage progression in methotrexate (MTX)-naive patients with Early Erosive rheumatoid arthritis (AGREE). Arthritis research & therapy 2015;17:157.

51.   Emery P, Burmester GR, Bykerk VP, et al. Evaluating drug-free remission with abatacept in early rheumatoid arthritis: results from the phase 3b, multicentre, randomised, active-controlled AVERT study of 24 months, with a 12-month, double-blind treatment period. Annals of the rheumatic diseases 2015;74:19-26.

52.   Emery P, Durez P, Dougados M, et al. Impact of T-cell costimulation modulation in patients with undifferentiated inflammatory arthritis or very early rheumatoid arthritis: a clinical and imaging study of abatacept (the ADJUST trial). Annals of the rheumatic diseases 2010;69:510-6.

53.　　Kremer JM, Westhovens R, Leon M, et al. Treatment of rheumatoid arthritis by selective inhibition of T-cell activation with fusion protein CTLA4Ig. The New England journal of medicine 2003;349:1907-15.

54.　　Genovese MC, Becker JC, Schiff M, et al. Abatacept for rheumatoid arthritis refractory to tumor necrosis factor alpha inhibition. The New England journal of medicine 2005;353:1114-23.

55.　　Klareskog L, Catrina AI, Paget S. Rheumatoid arthritis. Lancet (London, England) 2009;373:659-72.

56.　　Zhu J, Paul WE. CD4 T cells: fates, functions, and faults. Blood 2008;112:1557-69.

57.　　Zhu J, Yamane H, Paul WE. Differentiation of effector CD4 T cell populations (*). Annual review of immunology 2010;28:445-89.

58.　　Baeten D, Baraliakos X, Braun J, et al. Anti-interleukin-17A monoclonal antibody secukinumab in treatment of ankylosing spondylitis: a randomised, double-blind, placebo-controlled trial. Lancet (London, England) 2013;382:1705-13.

59.　　Baeten D, Sieper J, Braun J, et al. Secukinumab, an Interleukin-17A Inhibitor, in Ankylosing Spondylitis. The New England journal of medicine 2015;373:2534-48.

60.　　Miao J, Geng J, Zhang K, et al. Frequencies of circulating IL-17-producing CD4+CD161+ T cells and CD4+CD161+ T cells correlate with disease activity in rheumatoid arthritis. Modern rheumatology / the Japan Rheumatism Association 2014;24:265-570.

61.　　Gullick NJ, Abozaid HS, Jayaraj DM, et al. Enhanced and persistent levels of interleukin (IL)-17(+) CD4(+) T cells and serum IL-17 in patients with early inflammatory arthritis. Clinical and experimental immunology 2013;174:292-301.

62.　　Leipe J, Grunke M, Dechant C, et al. Role of Th17 cells in human autoimmune arthritis. Arthritis Rheum 2010;62:2876-85.

63.　　Law SC, Benham H, Reid HH, Rossjohn J, Thomas R. Identification of self-antigen-specific T cells reflecting loss of tolerance in autoimmune disease underpins preventative immunotherapeutic strategies in rheumatoid arthritis. Rheumatic diseases clinics of North America 2014;40:735-52.

64.　　Wooldridge L, Lissina A, Cole DK, van den Berg HA, Price DA, Sewell AK. Tricks with tetramers: how to get the most from multimeric peptide-MHC. Immunology 2009;126:147-64.

65.　　Snir O, Rieck M, Gebe JA, et al. Identification and functional characterization of T cells reactive to citrullinated vimentin in HLA-DRB1*0401-positive humanized mice and rheumatoid arthritis patients. Arthritis Rheum 2011;63:2873-83.

66.　　James EA, Rieck M, Pieper J, et al. Citrulline-specific Th1 cells are increased in rheumatoid arthritis and their frequency is influenced by disease duration and therapy. Arthritis & rheumatology (Hoboken, NJ) 2014;66:1712-22.

67.　　Thomas R. Dendritic cells as targets or therapeutics in rheumatic autoimmune disease. Current opinion in rheumatology 2014;26:211-8.

7

ADDENDUM

NEDERLANDSE SAMENVATTING
CURRICULUM VITAE
LIST OF PUBLICATIONS
DANKWOORD
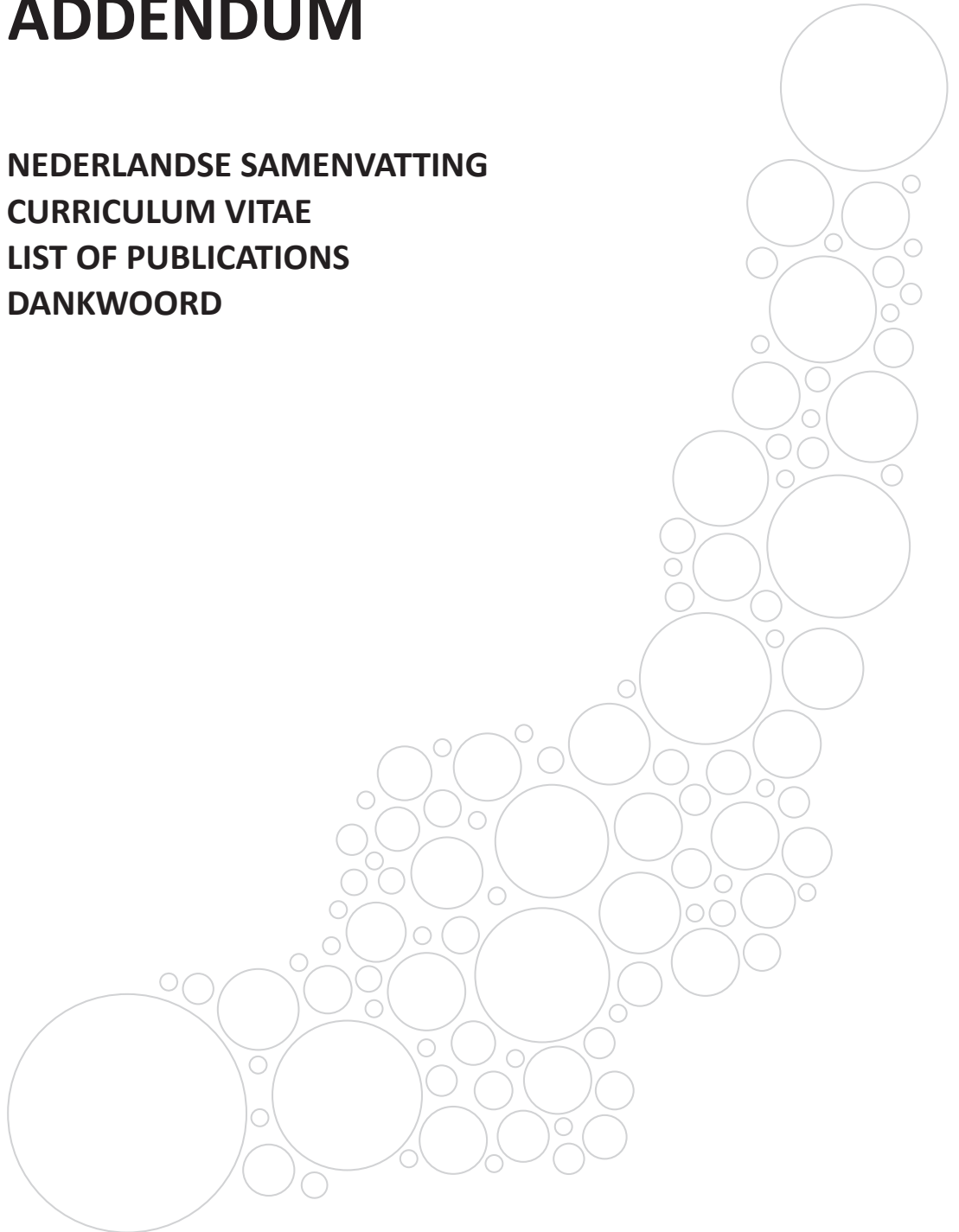
NEDERLANDSE SAMENVATTING

Het immuunsysteem

Het immuunsysteem beschermt het menselijk lichaam tegen ziekteverwekkers zoals bacteriën, virussen, schimmels en parasieten. Het bestaat uit twee delen om deze bescherming te waarborgen: het aangeboren en het verworven immuunsysteem. Het aangeboren immuunsysteem is de eerste lijn van bescherming tegen een indringer, die ziekte veroorzaakt, en reageert snel, maar is niet specifiek voor de ziekteverwekker die op dat moment het lichaam aanvalt. Het verworven immuunsysteem reageert langzamer, maar is zeer specifiek. Dit systeem onthoudt hoe het bij een aanval moet reageren en zorgt voor een snelle en specifieke immuunreactie tijdens een tweede infectie met dezelfde ziekteverwekker. Deze specifieke afweerreactie wordt uitgevoerd door T- en B-cellen die via hun T- en B-cel receptor een grote variëteit aan ziekteverwekkers kunnen herkennen en opruimen. Om te voorkomen dat deze T- en B-cellen reageren tegen lichaamseigen eiwitten, moeten ze een strenge selectie ondergaan voordat ze de bloedcirculatie in mogen. Echter, deze selectie is niet altijd perfect waardoor T- en B-cellen die lichaamseigen eiwitten herkennen, kunnen ontsnappen en een auto-immuunziekte zoals reumatoïde artritis (RA) kunnen veroorzaken.

Reumatoïde artritis

RA is een systemische ontstekingsziekte die gekenmerkt wordt door ontsteking van de gewrichten wat leidt tot afbraak van kraakbeen en bot. Van de wereldbevolking is 0,5-1% aangedaan en de prevalentie is hoger naarmate de leeftijd stijgt. Een van de kenmerken van RA is de aanwezigheid van autoantilichamen, zoals reumafactor en anti-citrulline antilichamen (ACPA). Deze autoantilichamen worden gemaakt door B-cellen en herkennen lichaamseigen eiwitten in plaats van ziekteverwekkers. ACPA kan gedetecteerd worden in 50 tot 70% van de RA patiënten en is zeer specifiek voor RA. Daarom wordt de aanwezigheid van ACPA en reumafactor gebruikt in de criteria voor de diagnose van RA. ACPA kan tot 10 jaar voordat klinische symptomen ontwikkelen, gevonden worden in het serum van patiënten. Daarnaast hebben ACPA-positieve patiënten ernstigere gewrichtsafbraak en ziekteprogressie dan ACPA-negatieve patiënten, waardoor ACPA-status gebruikt kan worden als een voorspellende biomarker. Meerdere risicofactoren voor de ontwikkeling van RA zijn over de jaren heen geïdentificeerd. Zowel omgevingsfactoren, zoals roken, als genetische risicofactoren zijn beschreven. De grootste genetische risicofactor voor ACPA-positieve RA is de HLA klasse II locus. HLA-moleculen zijn verantwoordelijk voor de presentatie van eiwitfragmenten (peptiden) van ziekteverwekkers aan T-cellen. Herkenning van het HLA-peptide complex resulteert vervolgens in de activatie van de T-cel en de bijbehorende effectormechanismen. De genen die coderen voor de HLA-moleculen zijn verschillend tussen individuen. Deze verschillen bevinden zich vooral in het deel van het HLA klasse II molecuul dat betrokken is bij het presenteren van peptiden, waardoor verschillende HLA-moleculen verschillende peptiden kunnen presenteren. Dit verschil in peptide-repertoire is mogelijk de verklaring

&

waarom bepaalde HLA klasse II moleculen beschermen tegen de ontwikkeling van een ziekte en andere HLA-moleculen leiden tot een hoger risico.

De oorzaak van RA is onbekend, maar studies naar de drijfveren van de ontstekingsreactie hebben geleid tot de ontwikkeling van therapieën die de kwaliteit van leven van RA patiënten zeer hebben verbeterd. Deze therapieën zijn gericht op het verminderen van de ontstekingsreactie en hebben daardoor moleculen of cellen van het immuunsysteem als doelwit.

Dit proefschrift bestudeert de rol van het verworven immuunsysteem in de ontwikkeling, behandeling en diagnose van reumatische aandoeningen.

Onderzoek beschreven in dit proefschrift

Het eerste deel van dit proefschrift beschrijft de associatie tussen de HLA klasse II locus en RA. Het is al vele jaren bekend dat bepaalde varianten van het HLA klasse II molecuul geassocieerd zijn met een hogere kans op het ontwikkelen van ACPA-positieve RA, zoals HLA-DRB1*04, en dat andere varianten geassocieerd zijn met bescherming, zoals HLA-DRB1*13. Echter, de moleculaire basis van deze associatie is onbekend. **Hoofdstuk 2** beschrijft de studies naar de bijdrage van de HLA klasse II moleculen die leiden tot hoger risico, en de HLA klasse II moleculen die beschermen tegen de ontwikkeling van RA, aan de associatie tussen HLA en RA onderzocht. We hebben een nieuw (lichaamseigen) autoantigen geïdentificeerd, genaamd vinculine, dat herkend wordt door ACPA en CD4+ T-cellen in individuen die HLA klasse II moleculen dragen, die leiden tot een hogere kans op de ontwikkeling van RA. De kern van de sequentie van het vinculine peptide, dat herkend wordt door de CD4+ T-cellen die vinculine herkennen, bevat 5 opeenvolgende aminozuren, die in dezelfde volgorde voorkomen in vele ziekteverwekkers en het beschermende HLA klasse II molecuul HLA-DRB1*13. Deze vinculine-specifieke CD4+ T-cellen kunnen ook reageren op peptiden afgeleid van ziekteverwerkers, ook wel kruisreactie genoemd. Deze cellen herkennen dus zowel ziekteverwekkers als het lichaamseigen vinculine. Echter, deze kruisreagerende CD4+ T-cellen konden we niet detecteren in individuen die het beschermende HLA-DRB1*13 molecuul dragen. Dit resultaat toont aan dat het peptide afgeleid van het beschermende HLA molecuul tolerantie induceert in deze individuen wat het beschermende effect van HLA-DRB1*13 verklaart. Doordat deze individuen geen CD4+ T-cellen hebben die kunnen reageren op vinculine, zal er geen afweerreactie tegen het lichaamseigen vinculine gestart worden en zullen er geen vinculine-herkennende ACPAs geproduceerd worden, wat vervolgens tot de ontwikkeling van RA kan leiden. Deze resultaten impliceren dat CD4+ T cellen die ziekteverwekkers herkennen en vervolgens ook lichaamseigen eiwitten kunnen herkennen, betrokken zijn bij de associatie tussen HLA en RA en een moleculaire basis voor de bijdrage van beschermende en predisponerende HLA moleculen leveren.

Het tweede deel van dit proefschrift beschrijft het geneesmiddel Abatacept. Abatacept is een fusie-eiwit bestaande uit CTLA-4 en het constante deel van de antilichaamvorm

immunoglobuline G1 (IgG1). Het veronderstelde werkingsmechanisme is dat Abatacept de costimulatie van T-cellen blokkeert door te binden aan CD80 en CD86 op antigen-presenterende cellen. T-cellen hebben naast herkenning van het HLA-peptide complex extra signalen nodig voor activatie. Een van deze signalen is de binding van CD28 op de T-cel aan CD80 of CD86 op de antigen-presenterende cel. Doordat CTLA4 aan CD80 en CD86 bindt, kan CD28 niet meer binden, en zal de T-cel niet geactiveerd worden en geen ontsteking kunnen veroorzaken. In **hoofdstuk 3** zijn de studies beschreven die aantonen dat Abatacept ook nog een ander werkingsmechanisme heeft. Door gebruik te maken van een muismodel voor artritis, het collageen geïnduceerde artritis model, hebben we kunnen aantonen dat Abatacept nog steeds effectief is in de afwezigheid van CD4+ T-cellen. Deze bevinding impliceert dat Abatacept nog een ander werkingsmechanisme heeft aangezien het niet het blokkeren van costimulatie van CD4+ T-cellen kan zijn, omdat deze niet aanwezig waren in het gebruikte model. In **hoofdstuk 4** is het effect van Abatacept in een cohort van patiënten met vroege RA (AGREE studie) onderzocht. We beschrijven dat behandeling met Abatacept in combinatie met methotrexaat ervoor kan zorgen dat patiënten die positief zijn voor autoantilichamen, autoantilichaam negatief worden. Deze conversie van positief naar negatief voor autoantilichamen is vervolgens geassocieerd met remissie, een staat van vermindering van ziekteverschijnselen, en met minder radiografische progressie.

Dit deel van het proefschrift laat zien dat Abatacept een effectieve behandeling is voor RA met verschillende werkingsmechanismen.

In deel drie van dit proefschrift staat het gebruik van het verworven immuunsysteem als biomarker voor vroege diagnose centraal. In **hoofdstuk 5** is onderzocht of IL-17-producerende CD4+ T-cellen potentieel gebruikt kunnen worden als biomarker voor vroege diagnose van ankyloserende spondylitis (AS). Vroege diagnose van deze ziekte is belangrijk aangezien de huidige diagnose gesteld wordt op basis van structurele schade zichtbaar op röntgenfoto's. Echter, deze botformatie is onomkeerbaar en een teken van vergevorderde ziekte. Een van de effectormechanismen van CD4+ T-cellen is het produceren van signaalstoffen, ook wel cytokinen genoemd. Een van deze cytokinen is interleukine 17, ook wel IL-17 genoemd. Het geneesmiddel secukinumab vangt IL-17 weg en toont veelbelovende resultaten als behandeling voor AS. Dit toont aan dat IL-17 betrokken is bij het ziekteproces in AS en daarom hebben we onderzocht of IL-17-producerende CD4+ T-cellen al verhoogd zijn in patiënten met vroege AS. Ondanks dat het percentage IL-17-producerende CD4+ T-cellen hoger was in vroege AS patiënten in vergelijking met gezonde controles, is deze populatie cellen geen geschikte biomarker aangezien het percentage alleen hoger was in patiënten met actieve ziekte. Aangezien een verhoogd percentage IL-17-producerende CD4+ T-cellen ook gevonden wordt in RA patiënten, is het verhoogde percentage niet specifiek voor AS, maar een algemeen ontstekings-gerelateerd verschijnsel.

Hoofdstuk 6 beschrijft de studies naar een ander cytokine, genaamd interleukine 27 (IL-

27). IL-27 is beschreven als een cytokine met zowel pro- als anti-inflammatoire effecten en wordt geproduceerd door antigen-presenterende cellen. In dit hoofdstuk laten we zien dat CD4+ T-cellen ook IL-27 kunnen produceren in gezonde individuen. Behandeling met IL-27 in muismodellen voor artritis heeft gunstige effecten op de ziekte. Het is dus interessant om IL-27 producerende CD4+ T-cellen te onderzoeken in RA patiënten en potentieel een nieuwe biomarker te identificeren. Hiernaast zijn verhoogde IL-27 levels in ontstekingsvocht in RA patiënten beschreven en is een variant van het IL-27 gen geassocieerd met de ernst van de ziekte, wat IL-27 een interessant doel voor de ontwikkeling van nieuwe behandelstrategieën maakt.

Conclusie

Dit proefschrift beschrijft dat het verworven immuunsysteem een belangrijke rol speelt in de ontwikkeling van RA aangezien kruisreactieve CD4+ T-cellen betrokken zijn bij de autoreactieve ontstekingsreactie door hulp te geven aan B-cellen die vervolgens autoantilichamen (ACPA) gaan produceren, wat leidt tot ACPA-positieve RA. Het aanpakken van het verworven immuunsysteem via de behandeling met Abatacept vermindert de ontsteking en ziekteactiviteit doordat het zich richt op meerdere spelers van het verworven immuunsysteem en wellicht ook het aangeboren immuunsysteem. Aangezien niet elke behandeling aanslaat in iedere patiënt, is het monitoren van de respons op de behandeling belangrijk. Dit kan bereikt worden door specifieke delen van het verworven immuunsysteem te gebruiken. De resultaten beschreven in dit proefschrift tonen aan dat het verworven immuunsysteem belangrijk is in de ontwikkeling, behandeling en diagnose van artritis en hebben belangrijke implicaties voor de ontwikkeling van toekomstige behandelstrategieën.

&

CURRICULUM VITAE

Diahann Talia Satirah Ludovica Jansen werd geboren op 6 mei 1986 in Rotterdam. In 2004 slaagde zij voor het gymnasium aan het Coornhert Gymnasium te Gouda, waarna zij Biomedische Wetenschappen is gaan studeren aan de Universiteit Leiden. Tijdens haar bachelor deed ze onderzoek op de afdeling Reumatologie in het Leids Universitair Medisch Centrum onder leiding van dr. Andreea Ioan-Facsinay en Prof. dr. René Toes.

Na het behalen van haar bachelor diploma in 2007 heeft Diahann zich een jaar ingezet voor de studenten Geneeskunde en Biomedische Wetenschappen aan de Universiteit Leiden als fulltime bestuurslid Onderwijs Biomedische Wetenschappen van de studievereniging Medische Faculteit der Leidse Studenten (M.F.L.S.). Tijdens haar master Biomedical Sciences heeft ze stage gelopen bij de afdeling Klinische Genetica in het Leids Universitair Medisch Centrum onder supervisie van Prof. dr. Cees Harteveld en dr. Marion Phylipsen. Hiernaast heeft ze twee vakken gevolgd aan het Karolinska Institutet in Stockholm, Zweden. Haar masteropleiding heeft ze vervolgens afgerond met een stage in de groep van Prof. dr. Bart Roep onder begeleiding van dr. Fleur Kleijwegt in het Leids Universitair Medisch Centrum. Aansluitend is ze haar promotieonderzoek begonnen is op de afdeling Reumatologie onder begeleiding van Prof. dr. René Toes en Prof. dr. Tom Huizinga in 2011. De resultaten van dit onderzoek zijn beschreven in dit proefschrift.

Diahann vervolgt op dit moment haar werk naar de invloed van het adaptieve immuunsysteem in reumatoïde artritis als postdoc in de groep van Prof. dr. Ranjeny Thomas aan het University of Queensland Diamantina Institute in Brisbane, Australië.

&

LIST OF PUBLICATIONS

Lude Franke*, Hanane el Bannoudi*, **Diahann T.S.L. Jansen**, Klaas Kok, *et al.*
Association analysis of copy numbers of FC-gamma-receptors for rheumatoid arthritis and other immune-mediated phenotypes. *Eur J Hum Genet. 2016 Feb;24(2):263-70*

Diahann T.S.L. Jansen*, Hanane el Bannoudi*, Ramon Arens, Kim L.L. Habets, *et al.*
Abatacept decreases disease activity in the absence of CD4+ T-cells in the collagen induced arthritis model. *Arthritis Res Ther. 2015 Aug 20;17:220*

Diahann T.S.L. Jansen*, Jurgen van Heemst*, Antonis K. Moustakas, Marieke Bax, *et al.*
Cross-reactivity to vinculin and microbes provides a molecular basis for HLA-based protection against rheumatoid arthritis. *Nat Commun. 2015 May 5;6:6681*

Diahann T.S.L. Jansen, Marjolijn Hameetman, Jeroen van Bergen, Tom W.J. Huizinga, *et al.*
IL-17 producing CD4+ T-cells are increased in early, active axial spondyloarthritis including patients without imaging abnormalities. *Rheumatology (Oxford). 2015 Apr;54(4):728-35*

Jeroen N. Stoop, Bi-Sheng Liu, Jing Shi, **Diahann T.S.L. Jansen**, *et al.*
Antibodies specific for carbamylated proteins precede the onset of clinical symptoms in mice with collagen induced arthritis. *PloS One. 2014 Jul;9(7):e102163*

Fleur S. Kleijwegt, **Diahann T.S.L. Jansen**, Josefine Teeler, Antoinette M. Joosten, *et al.*
Tolerogenic dendritic cells impede priming of naïve CD8(+) T cells and deplete memory CD8(+) T cells. *Eur J Immunol. 2013 Jan;43(1):85-92*

Marion Phylipsen, Supawadee Yamsri, Emmely E. Treffers, **Diahann T.S.L. Jansen**, *et al.*
Non-invasive prenatal diagnosis of beta-thalassemia and sickle-cell disease using pyrophosphorolysis-activated polymerization and melting curve analysis. *Prenat Diagn. 2012 Jun;32(6):578-87*

*Authors contributed equally

&

DANKWOORD

Mijn periode als PhD student is niet alleen een periode geweest waarin in mijzelf heb ontwikkeld als onderzoeker, maar is een belangrijke periode in vele aspecten van mijn leven geweest, waar veel mensen aan hebben bijgedragen, die ik graag wil bedanken.

Allereerst wil ik mijn promotoren, prof.dr. René Toes en prof.dr. Tom Huizinga, bedanken voor hun begeleiding en vertrouwen. Beste René, bedankt voor de fijne DERAA-meetingen, die vaak begonnen met interessante weetjes, maar vooral een goede uitwisseling van kennis waren waardoor ik na afloop vol inspiratie weer verder ging met mijn projecten. Ik heb nog elke dag profijt van de kritische blik, die je mij hebt geleerd. Beste Tom, jouw enthousiasme en passie voor wetenschap zijn erg aanstekelijk en werken inspirerend. Bedankt voor je klinische en statistische analyse kennis.

Verder wil ik iedereen binnen de afdeling Reumatologie bedanken voor de aangename sfeer en het plezier dat ik heb gehad tijdens mijn promotietijd. Aangezien ik het grootste deel van mijn tijd in het lab heb besteed, wil ik graag alle analisten bedanken. Marjolijn voor het SpA project, Aleida voor het PCR werk voor het IL-27 hoofdstuk, Martine voor het DERAA project en de muizen, Ellen voor de muizen en FACS kennis en Gerrie, Nivine, Linda, Joris, Joanneke, Annemarie en Stefan voor de altijd goede sfeer in het lab. Verder wil ik iedereen die geholpen heeft bij mijn grote offersessies bedanken. Jeroen in het bijzonder voor vrijwel alles wat ik weet van muizen en arthritis muismodellen. Iedereen van C5 voor de loopjes naar de koffie- (en voor mij thee-) automaat en de gezellige gesprekken: Inge, Jolien, Hanane, Jing, Parawee, Jurgen, Priscilla, Daniël, Rosanne, Anja, Ayla, Hilde, Tobias, Lise, Jaqueline, Joost, Rosalie, Marije, Myrthe, Sanne, Hester, Hendy, Marieke, Kim en Yoann. Bouchra, bedankt voor je bijdrage als student aan een interessant project dat helaas geen onderdeel van dit proefschrift is geworden. Floris, bedankt voor je begeleiding van het SpA project. Andreea, Leendert, Uli, Fina en Diane bedankt voor jullie input en soms lastige vragen tijdens werkbesprekingen. Iedereen van 'beneden' op het stafcentrum, in het bijzonder Hughine, voor al je hulp rondom mijn boekje en verdediging en natuurlijk ook Joyce en Nancy. En niet te vergeten mijn borrelcommissiegenootjes, waar ik onvergetelijke themaborrels voor de afdeling mee heb georganiseerd.

Promoveren is hard werken, maar je hebt ook ontspanning nodig en daar wil ik graag mijn vrienden en familie voor bedanken. Mijn studievrienden Samantha, Alex, Leonie, Michelle, Leonie, Michael, Ilse, Maartje, Kay, Marieke en Kattria. Kat, ook al wonen we al jaren niet meer in hetzelfde land, we weten elkaar toch altijd weer te vinden en dan gaat het altijd ook even over science en onze projecten. De rest van de Luxers, oud-huisgenoten, bestuursgenoten en vriendinnen van de middelbare school.

Mijn ouders en zusjes, bedankt voor jullie onvoorwaardelijke steun en liefde. Ik kan altijd op jullie rekenen en ik waardeer onze sterke zussenband. Hans, Lies, Sofie en Freek, jullie ook bedankt voor jullie steun en advies.

Tot slot wil ik jou bedanken, Adriaan. Bedankt voor alle liefde en steun die je mij over de

&

jaren hebt gegeven en voor alles wat je hebt gedaan om het voor mij mogelijk te maken mijn boekje te schrijven. Helemaal toen we in Australië zaten en ik zat te typen in plaats van het land met jou te verkennen. Australië is tot nu toe ons meest uitdagende avontuur en alvast bedankt voor alle avonturen die nog in onze toekomst liggen.